

## Support Information

### $\alpha$ -alkylidene $\delta$ -lactones inhibit quorum sensing phenotypes in *Chromobacterium* strain CV026 showing interaction within the CviR receptor

Fernanda Favero<sup>1,2</sup>, Terezinha A. Tolentino<sup>1</sup>, Vinicius Fernandes<sup>3</sup>, Werner Treptow<sup>3 $\alpha$</sup> , Alex L. Pereira<sup>2 $\S$</sup> , Angelo H.L. Machado<sup>1\*</sup>.

1: Instituto de Química, Universidade de Brasília, Campus Universitário Darcy Ribeiro, Asa Norte, Brasília, DF, 70910-900, Brazil

2: Campus of Ceilândia, University of Brasília, Centro Metropolitano, Conjunto A, Ceilândia Sul, Brasília, DF, 72220-275, Brazil

3: Laboratório de Biologia Teórica e Computacional, Departamento de Biologia Celular, Universidade de Brasília, Campus Universitário Darcy Ribeiro, Asa Norte, Brasília, DF, 70910-900, Brazil

Corresponding authors. \*Angelo H. L. Machado - E-mail: nagelo@unb.br

$\S$  Alex L. Pereira - E-mail: alexpereira@unb.br

$\alpha$  Werner Treptow - E-mail: treptow@unb.br

## Content:

### 1. Schemes and figures: Page 5–19

Schemes S1. Synthesis of chlorolactone ( <b>20</b> ).
<b>Scheme S2.</b> Violacein quantification assay.
<b>Figure S1.</b> Violacein quantification assay for <b>10E</b> .
<b>Figure S2.</b> Violacein quantification assay for <b>10Z</b> .
<b>Figure S3.</b> Violacein quantification assay for <b>11E</b> .
<b>Figure S4.</b> Violacein quantification assay for <b>11Z</b> .
<b>Figure S5.</b> Violacein quantification assay for <b>12E</b> .
<b>Figure S6.</b> Violacein quantification assay for <b>12Z</b> .
<b>Figure S7.</b> Violacein quantification assay for <b>13E</b> .
<b>Figure S8.</b> Violacein quantification assay for <b>13Z</b> .
<b>Figure S9.</b> Violacein quantification assay for <b>14E</b> .
<b>Figure S10.</b> Violacein quantification assay for <b>15E</b> .
<b>Figure S11.</b> Violacein quantification assay for <b>16E</b> .
<b>Figure S12.</b> Violacein quantification assay for <b>17E</b> .
<b>Figure S13.</b> Violacein quantification assay for <b>18E</b> .
<b>Figure S14.</b> Violacein quantification assay for <b>19E</b> .
<b>Figure S15.</b> Violacein quantification assay for <b>20</b> .
<b>Figure S16.</b> Ligand binding domain for <b>2/CviR</b> .
<b>Figure S17.</b> Ligand binding domain for <b>20/CviR</b> .
<b>Figure S18.</b> Overlap of <b>2</b> with <b>10E</b> , and ligand binding domain for <b>10E/CviR</b> , respectively.
<b>Figure S19.</b> Overlap of <b>2</b> with <b>10Z</b> , and ligand binding domain for <b>10Z/CviR</b> , respectively.
<b>Figure S20.</b> Overlap of <b>2</b> with <b>11E</b> , and ligand binding domain for <b>11E/CviR</b> , respectively.
<b>Figure S21.</b> Overlap of <b>2</b> with <b>11Z</b> , and ligand binding domain for <b>11Z/CviR</b> , respectively.
<b>Figure S22.</b> Overlap of <b>2</b> with <b>12E</b> , and ligand binding domain for <b>12E/CviR</b> , respectively.
<b>Figure S23.</b> Overlap of <b>2</b> with <b>12E</b> , and ligand binding domain for <b>12E/CviR</b> , respectively.
<b>Figure S24.</b> Overlap of <b>2</b> with <b>13E</b> , and ligand binding domain for <b>13E/CviR</b> , respectively.
<b>Figure S25.</b> Overlap of <b>2</b> with <b>13Z</b> , and ligand binding domain for <b>13E/CviR</b> , respectively.
<b>Figure S26.</b> Overlap of <b>2</b> with <b>14E</b> , and ligand binding domain for <b>14E/CviR</b> , respectively.
<b>Figure S27.</b> Overlap of <b>2</b> with <b>15E</b> , and ligand binding domain for <b>15E/CviR</b> , respectively.
<b>Figure S28.</b> Overlap of <b>2</b> with <b>16E</b> , and ligand binding domain for <b>16E/CviR</b> , respectively.
<b>Figure S29.</b> Overlap of <b>2</b> with <b>17E</b> , and ligand binding domain for <b>17E/CviR</b> , respectively.
<b>Figure S30.</b> Overlap of <b>2</b> with <b>18E</b> , and ligand binding domain for <b>18E/CviR</b> , respectively.
<b>Figure S31.</b> Overlap of <b>2</b> with <b>19E</b> , and ligand binding domain for <b>19E/CviR</b> , respectively.
<b>Figure S32.</b> (A): Chemical structure of <b>21</b> ; B: CviR (PDB ID: 3PQ5) complex with <b>21</b> (blue), in yellow is shown HHL to exemplify the LBD.; (C): LBD complex with <b>21</b> (blue), in yellow is shown HHL ( <b>2</b> ) to exemplify the LBD.

**2. NMR spectra of 1–25.** Page 20–69

S2.1. $^1\text{H}$ NMR spectrum of <b>8 (E/Z) R = Methyl</b> in $\text{CDCl}_3$ .	S2.2. $^{13}\text{C}$ NMR spectrum of <b>8 (E/Z) R = Methyl</b> in $\text{CDCl}_3$ .
S2.3. $^1\text{H}$ NMR spectrum of <b>8 (E/Z) R = Ethyl</b> in $\text{CDCl}_3$ .	S2.4. $^{13}\text{C}$ NMR spectrum of <b>8 (E/Z) R = Ethyl</b> in $\text{CDCl}_3$ .
S2.5. $^1\text{H}$ NMR spectrum of <b>8 (E/Z) R = n-Hexyl</b> in $\text{CDCl}_3$ .	S2.6. $^{13}\text{C}$ NMR spectrum of <b>8 (E/Z) R = n-Hexyl</b> in $\text{CDCl}_3$ .
S2.7. $^1\text{H}$ NMR spectrum of <b>8 (E/Z) R = n-Heptyl</b> in $\text{CDCl}_3$ .	S2.8. $^{13}\text{C}$ NMR spectrum of <b>8 (E/Z) R = n-Heptyl</b> in $\text{CDCl}_3$ .
S2.9. $^1\text{H}$ NMR spectrum of <b>8 (E/Z) R = iso-Propyl</b> in $\text{CDCl}_3$ .	S2.10. $^{13}\text{C}$ NMR spectrum of <b>8 (E/Z) R = iso-Propyl</b> in $\text{CDCl}_3$ .
S2.11. $^1\text{H}$ NMR spectrum of <b>8 (E) R = Phenyl</b> in $\text{CDCl}_3$ .	S2.12. $^{13}\text{C}$ NMR spectrum of <b>8 (E) R = Phenyl</b> in $\text{CDCl}_3$ .
S2.13. $^1\text{H}$ NMR spectrum of <b>8 (E) R = 4-Cl-Phenyl</b> in $\text{CDCl}_3$ .	S2.14. $^{13}\text{C}$ NMR spectrum of <b>8 (E) R = 4-Cl-Phenyl</b> in $\text{CDCl}_3$ .
S2.15. $^1\text{H}$ NMR spectrum of <b>8 (E) R = 4-Br-Phenyl</b> in $\text{CDCl}_3$	S2.16. $^{13}\text{C}$ NMR spectrum of <b>8 (E) R = 4-Br-Phenyl</b> in $\text{CDCl}_3$ .
S2.17. $^1\text{H}$ NMR spectrum of <b>8 (E) R = 3,4-methylenedioxypyhenyl</b> in $\text{CDCl}_3$ .	S2.18. $^{13}\text{C}$ NMR spectrum of <b>8 (E) R = 3,4-methylenedioxypyhenyl</b> in $\text{CDCl}_3$ .
S2.19. $^1\text{H}$ NMR spectrum of <b>8 (E) R = 4-NO<sub>2</sub>-Phenyl</b> in $\text{CDCl}_3$ .	S2.20. $^{13}\text{C}$ NMR spectrum of <b>8 (E) R = 4-NO<sub>2</sub>-Phenyl</b> in $\text{CDCl}_3$ .
S2.21. $^1\text{H}$ NMR spectrum of <b>10E</b> in $\text{CDCl}_3$ .	S2.22. $^{13}\text{C}$ NMR spectrum of <b>10E</b> in $\text{CDCl}_3$ .
S2.23. $^1\text{H}$ NMR spectrum of <b>10Z</b> in $\text{CDCl}_3$ .	S2.24. $^{13}\text{C}$ NMR spectrum of <b>10Z</b> in $\text{CDCl}_3$ .
S2.25. $^1\text{H}$ NMR spectrum of <b>11E</b> in $\text{CDCl}_3$ .	S2.26. $^{13}\text{C}$ NMR spectrum of <b>11E</b> in $\text{CDCl}_3$ .
S2.27. $^1\text{H}$ NMR spectrum of <b>11Z</b> in $\text{CDCl}_3$	S2.28. $^{13}\text{C}$ NMR spectrum of <b>11Z</b> in $\text{CDCl}_3$ .
S2.29. $^1\text{H}$ NMR spectrum of <b>12E</b> in $\text{CDCl}_3$ .	S2.30. $^{13}\text{C}$ NMR spectrum of <b>12E</b> in $\text{CDCl}_3$ .
S2.31. $^1\text{H}$ NMR spectrum of <b>12Z</b> in $\text{CDCl}_3$ .	S2.32. $^{13}\text{C}$ NMR spectrum of <b>12Z</b> in $\text{CDCl}_3$ .
S2.33. $^1\text{H}$ NMR spectrum of <b>13E</b> in $\text{CDCl}_3$	S2.34. $^{13}\text{C}$ NMR spectrum of <b>13E</b> in $\text{CDCl}_3$ .
S2.35. $^1\text{H}$ NMR spectrum of <b>13Z</b> in $\text{CDCl}_3$ .	S2.36. $^{13}\text{C}$ NMR spectrum of <b>13Z</b> in $\text{CDCl}_3$ .
S2.37. $^1\text{H}$ NMR spectrum of <b>14E</b> in $\text{CDCl}_3$ .	S2.38. $^{13}\text{C}$ NMR spectrum of <b>14E</b> in $\text{CDCl}_3$ .
S2.39. $^1\text{H}$ NMR spectrum of <b>15E</b> in $\text{CDCl}_3$ .	S2.40. $^{13}\text{C}$ NMR spectrum of <b>15E</b> in $\text{CDCl}_3$ .
S2.41. $^1\text{H}$ NMR spectrum of <b>16E</b> in $\text{CDCl}_3$ .	S2.42. $^{13}\text{C}$ NMR spectrum of <b>16E</b> in $\text{CDCl}_3$ .
S2.43. $^1\text{H}$ NMR spectrum of <b>17E</b> in $\text{CDCl}_3$ .	S2.44. $^{13}\text{C}$ NMR spectrum of <b>17E</b> in $\text{CDCl}_3$ .
S2.45. $^1\text{H}$ NMR spectrum of <b>18E</b> in $\text{CDCl}_3$ .	S2.46. $^{13}\text{C}$ NMR spectrum of <b>18E</b> in $\text{CDCl}_3$ .
S2.47. $^1\text{H}$ NMR spectrum of <b>19E</b> in $\text{CDCl}_3$ .	S2.48. $^{13}\text{C}$ NMR spectrum of <b>19E</b> in $\text{CDCl}_3$ .
S2.49. $^1\text{H}$ NMR spectrum of <b>20</b> in $\text{CDCl}_3$ .	S2.50. $^{13}\text{C}$ NMR spectrum of <b>20</b> in $\text{CDCl}_3$ .

**3. IR spectra of compounds 10 - 20.**

Page 70–77

S3.1. IR (ATR) spectrum of <b>10E</b> .	S3.2. IR (ATR) spectrum of <b>10Z</b> .
S3.3. IR (ATR) spectrum of <b>11E</b> .	S3.4. IR (ATR) spectrum of <b>11Z</b> .
S3.5. IR (ATR) spectrum of <b>12E</b> .	S3.6. IR (ATR) spectrum of <b>12Z</b> .
S3.7. IR (ATR) spectrum of <b>13E</b> .	S3.8. IR (ATR) spectrum of <b>13Z</b> .

<b>S3.9.</b> IR (ATR) spectrum of <b>14E</b> .	<b>S3.10.</b> IR (ATR) spectrum of <b>15E</b> .
<b>S3.11.</b> IR (ATR) spectrum of <b>16E</b> .	<b>S3.12.</b> IR (ATR) spectrum of <b>17E</b> .
<b>S3.13.</b> IR (ATR) spectrum of <b>18E</b>	<b>S3.14.</b> IR (ATR) spectrum of <b>19E</b> .
<b>S3.15.</b> IR (ATR) spectrum of <b>20</b> .	

**4. HRMS spectra of compounds **10 – 19**.**

Page 78–91

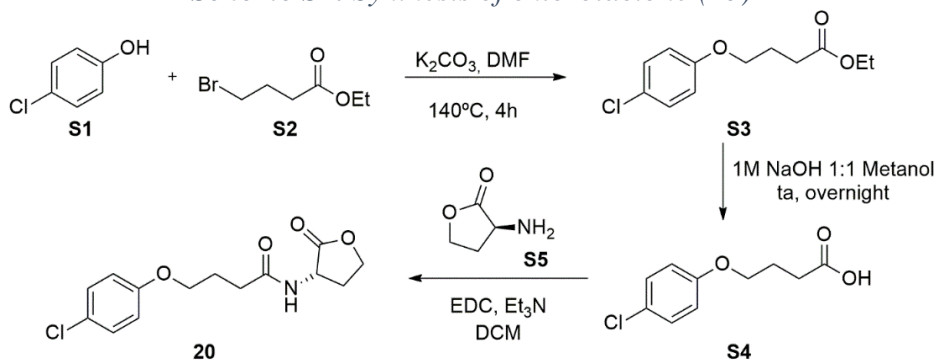
<b>S4.1.</b> HRMS data of <b>10E</b> .	<b>S4.2.</b> HRMS data of <b>10Z</b> .
<b>S4.3.</b> HRMS data of <b>11E</b> .	<b>S4.4.</b> HRMS data of <b>11Z</b> .
<b>S4.5.</b> HRMS data of <b>12E</b> .	<b>S4.6.</b> HRMS data of <b>12Z</b> .
<b>S4.7.</b> HRMS data of <b>13E</b> .	<b>S4.8.</b> HRMS data of <b>13Z</b> .
<b>S4.9.</b> HRMS data of <b>14E</b> .	<b>S4.10.</b> HRMS data of <b>15E</b> .
<b>S4.11.</b> HRMS data of <b>16E</b> .	<b>S4.12.</b> HRMS data of <b>17E</b> .
<b>S4.13.</b> HRMS data of <b>18E</b>	<b>S4.14.</b> HRMS data of <b>19E</b> .

**5. Purity analyses of compounds **10-20** by GC-MS.**

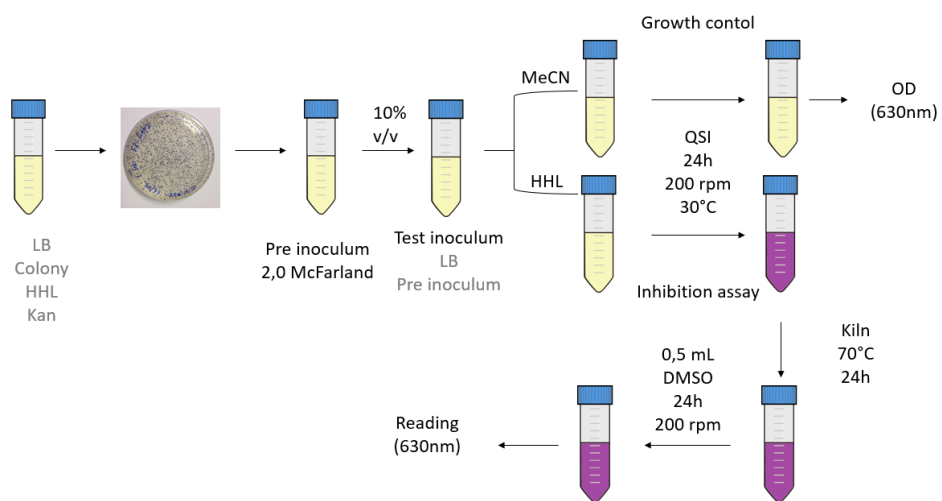
Page 92-105

<b>S5.1.</b> GC-MS data of <b>10E</b> .	<b>S5.2.</b> GC-MS data of <b>10Z</b> .
<b>S5.3.</b> GC-MS data of <b>11E</b> .	<b>S5.4.</b> GC-MS data of <b>11Z</b> .
<b>S5.5.</b> GC-MS data of <b>12E</b> .	<b>S5.6.</b> GC-MS data of <b>12Z</b> .
<b>S5.7.</b> GC-MS data of <b>13E</b> .	<b>S5.8.</b> GC-MS data of <b>13Z</b> .
<b>S5.9.</b> GC-MS data of <b>14E</b> .	<b>S5.10.</b> GC-MS data of <b>15E</b> .
<b>S5.11.</b> GC-MS data of <b>16E</b> .	<b>S5.12.</b> GC-MS data of <b>17E</b> .
<b>S5.13.</b> GC-MS data of <b>18E</b>	<b>S5.14.</b> GC-MS data of <b>19E</b> .
<b>S5.15.</b> GC-MS data of <b>20</b> .	

**Scheme S1.** Synthesis of chlorolactone (**20**)



**Scheme S2.** Violacein quantification assay.



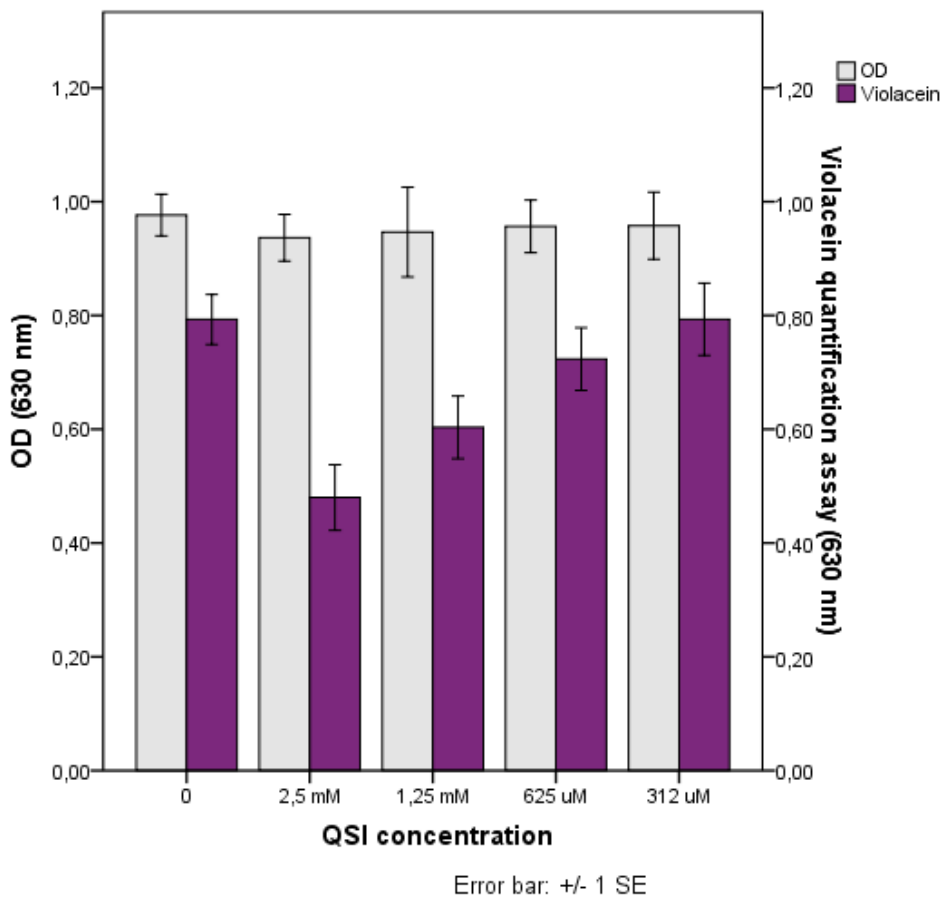


**Figure S1.** Violacein quantification assay for **10E**.

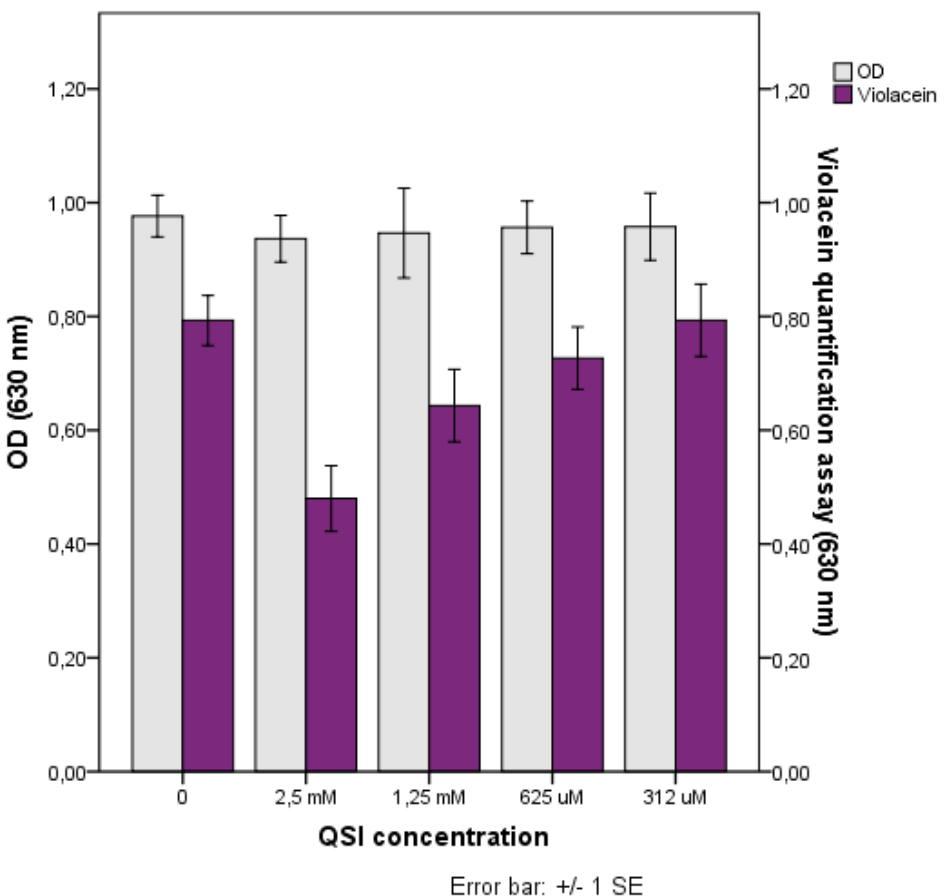


**Figure S2.** Violacein quantification assay for **10Z**.

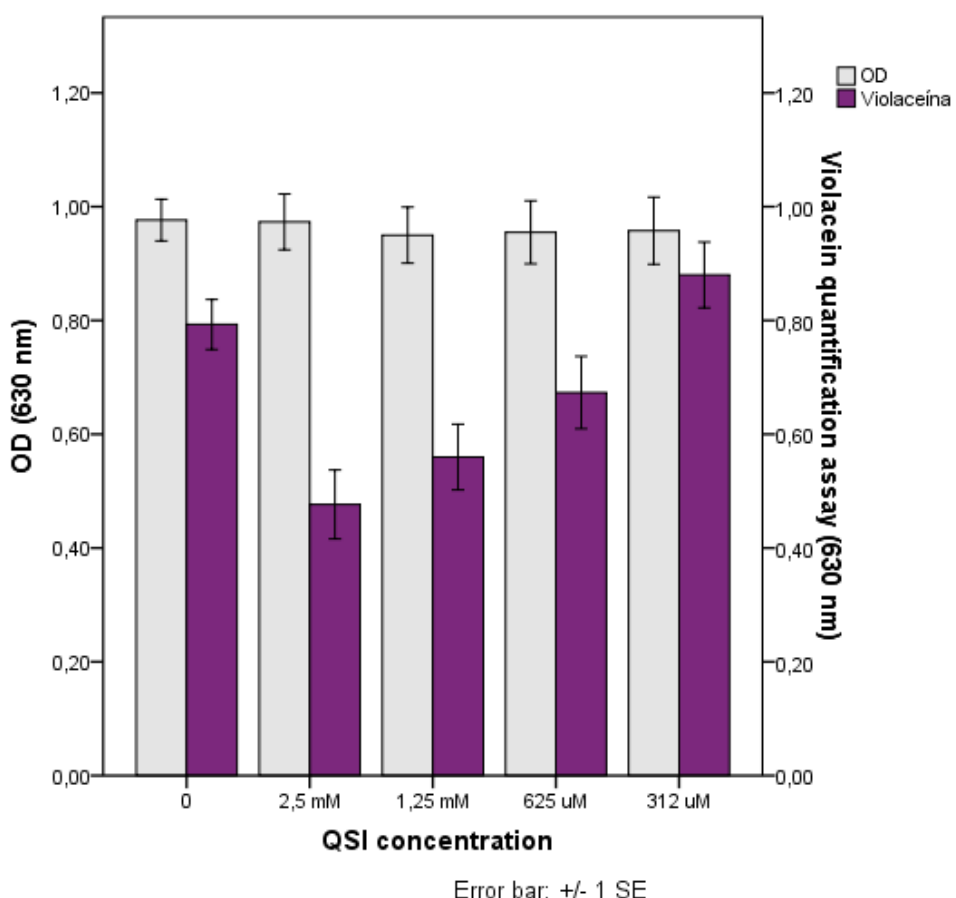


**Figure S3.** Violacein quantification assay for **11E**.

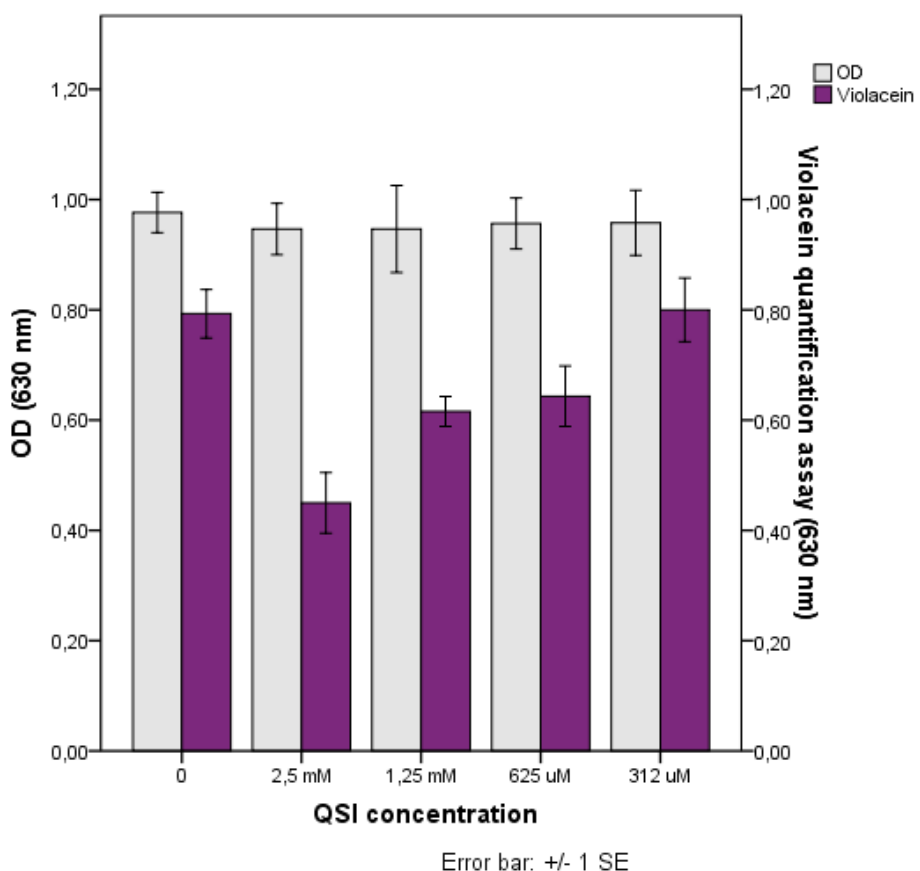


**Figure S4.** Violacein quantification assay for **11Z**.

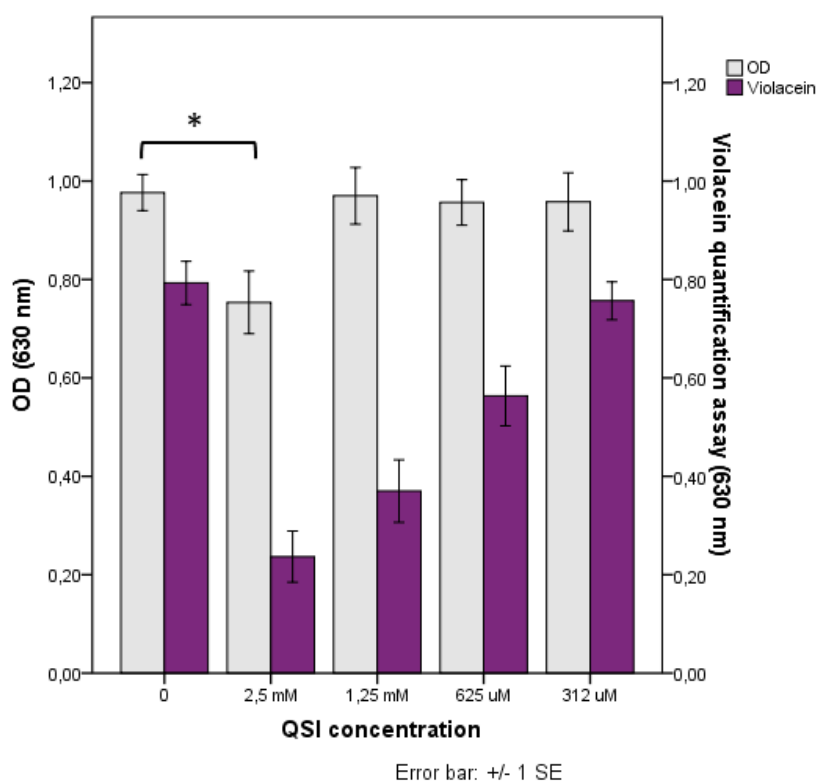


**Figure S5.** Violacein quantification assay for **12E**.

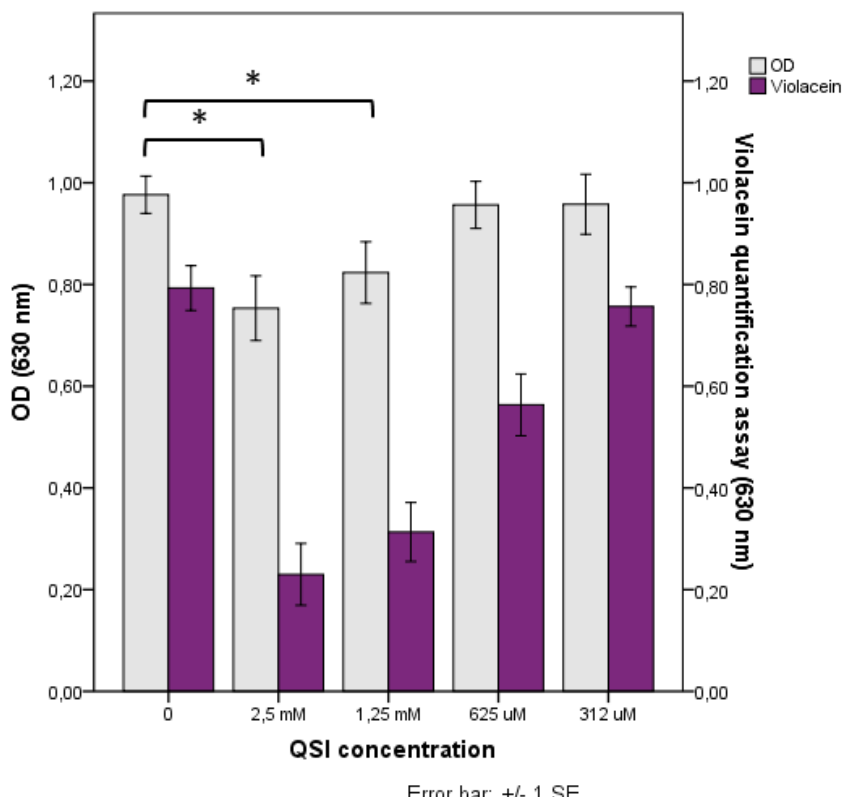


**Figure S6.** Violacein quantification assay for **12Z**.

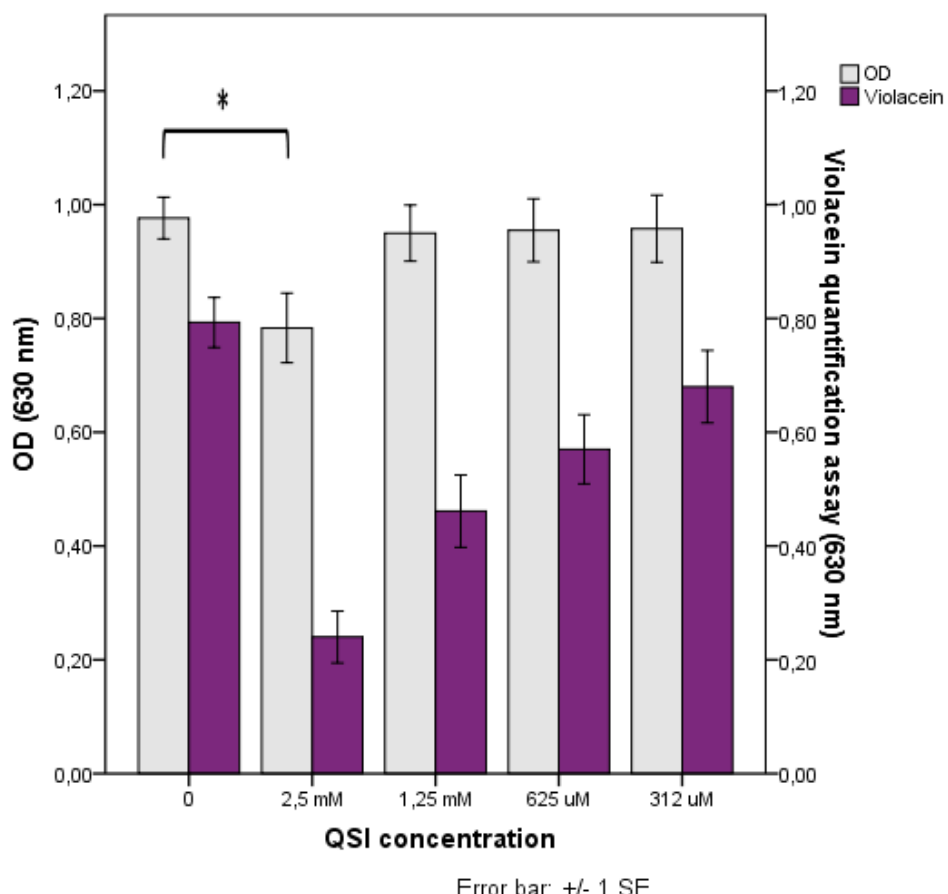


**Figure S7.** Violacein quantification assay for **13E**.

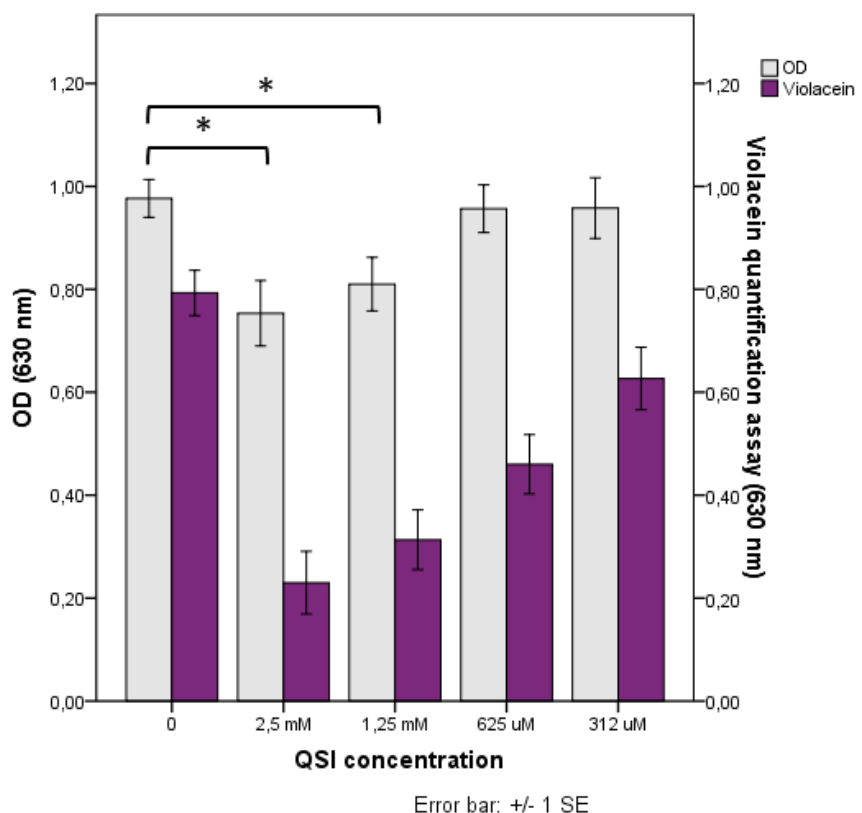


**Figure S8.** Violacein quantification assay for **13Z**.

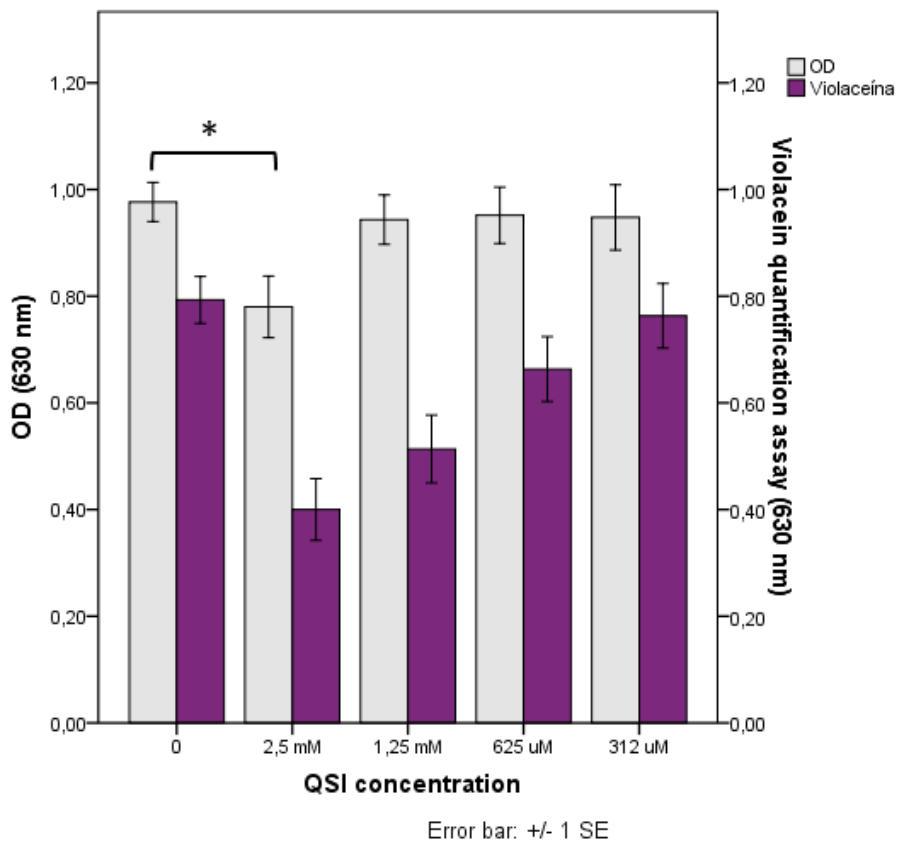


**Figure S9.** Violacein quantification assay for **14E**.

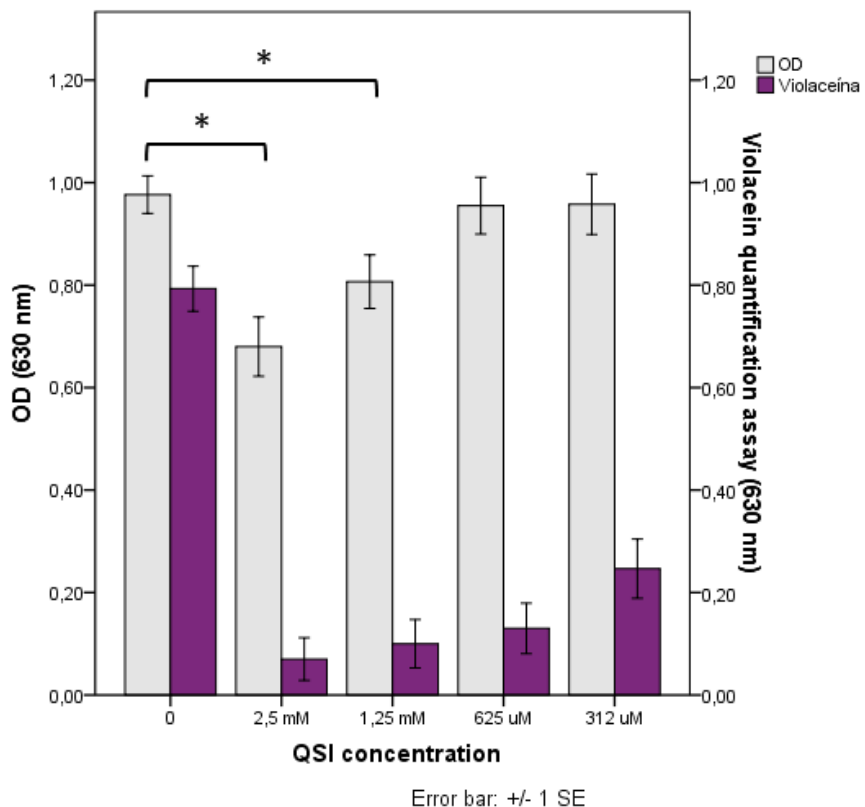


**Figure S10.** Violacein quantification assay for **15E**.

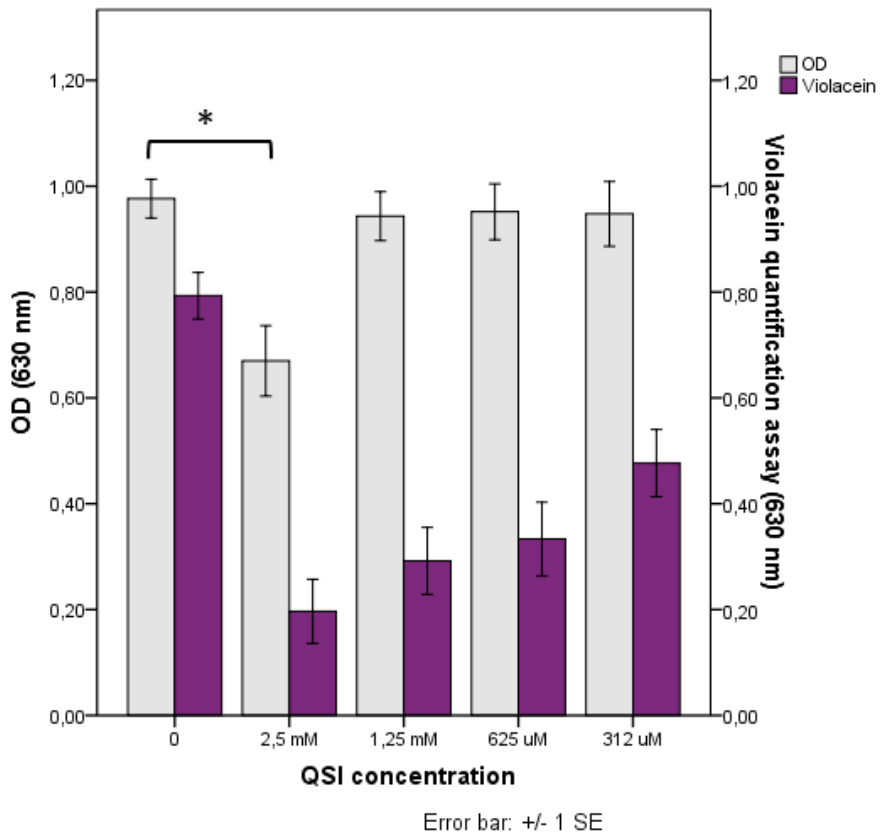


**Figure S11.** Violacein quantification assay for **16E**.

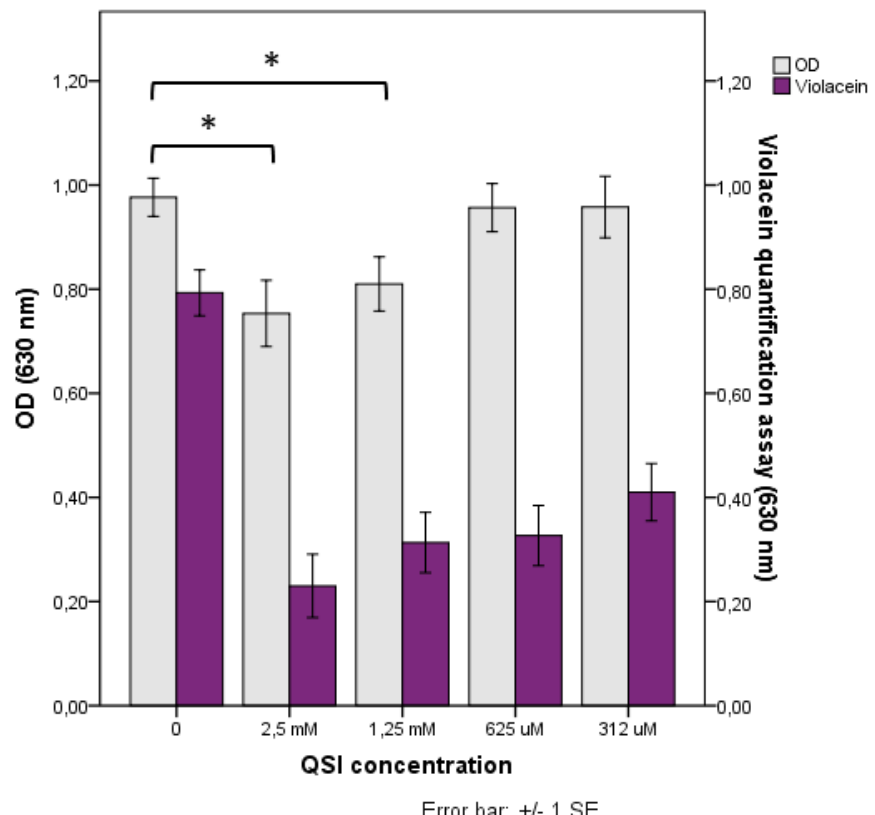


**Figure S12.** Violacein quantification assay for **17E**.

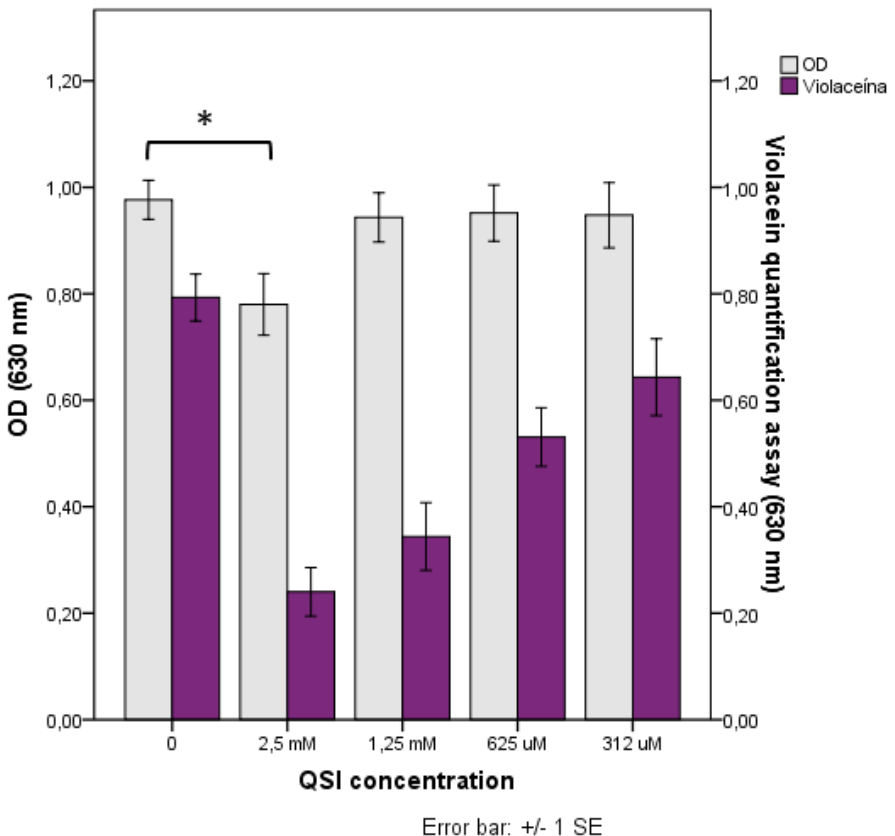


**Figure S13.** Violacein quantification assay for **18E**.

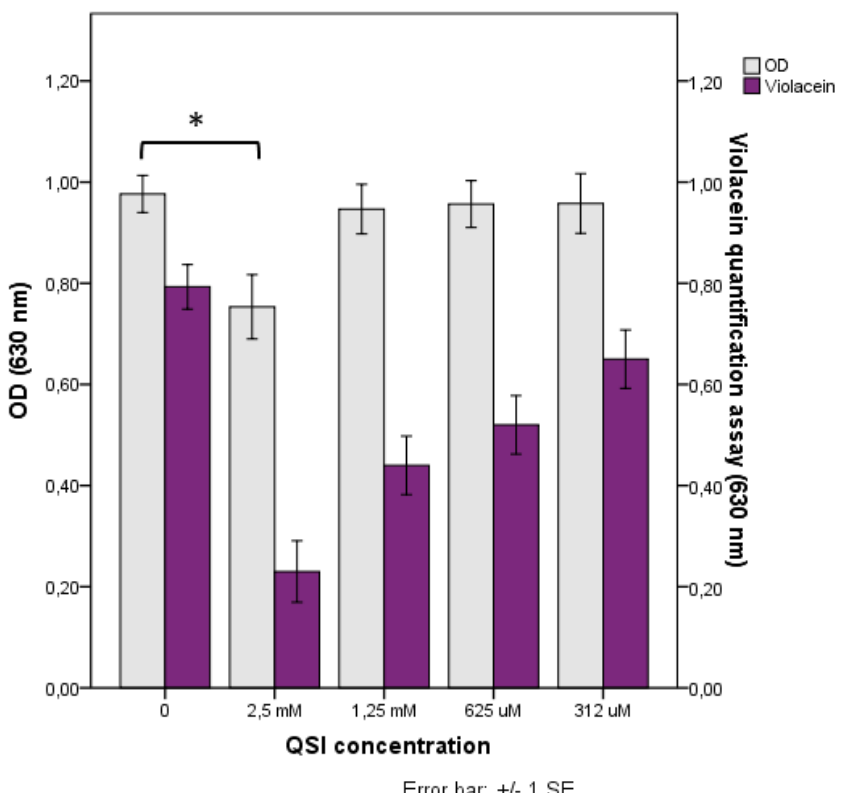


**Figure S14.** Violacein quantification assay for **19E**.

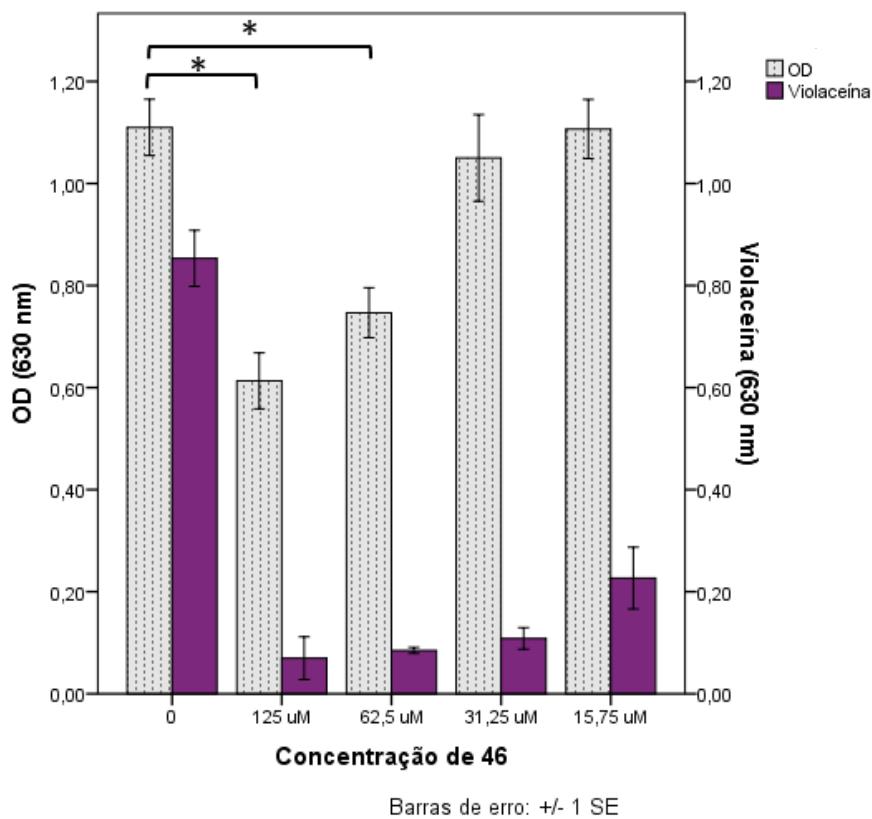


**Figure S15.** Violacein quantification assay for **20**.

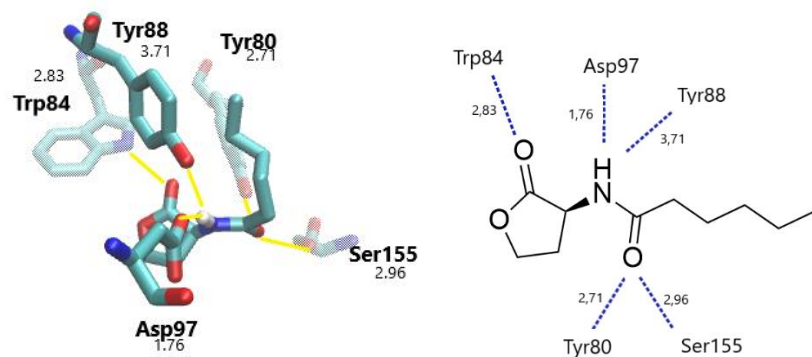


**Figure S16.** Ligand binding domain for **2/CviR**.

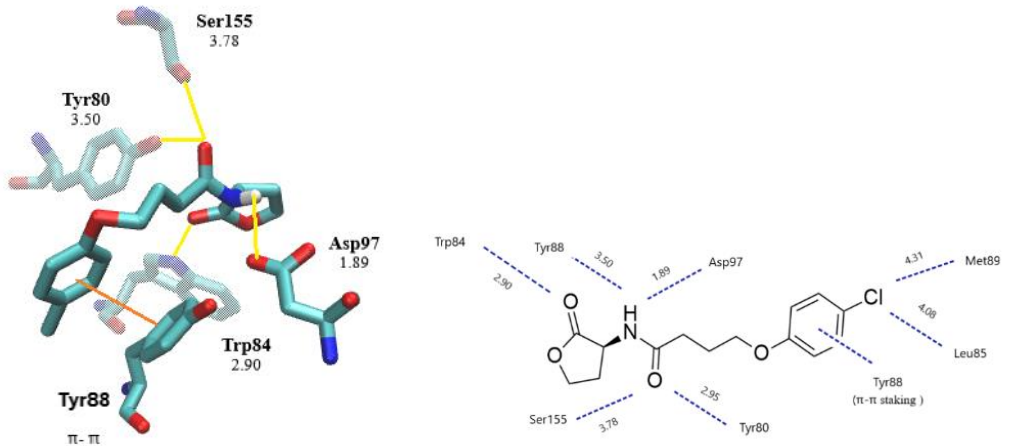


**Figure S17.** Ligand binding domain for **20**/CviR.

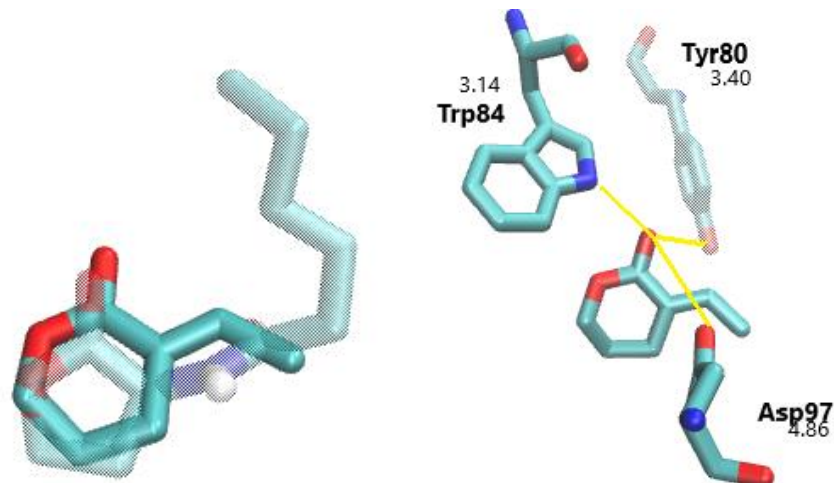


**Figure S18.** Overlap of **2** with **10E**, and ligand binding domain for **10E**/CviR, respectively.

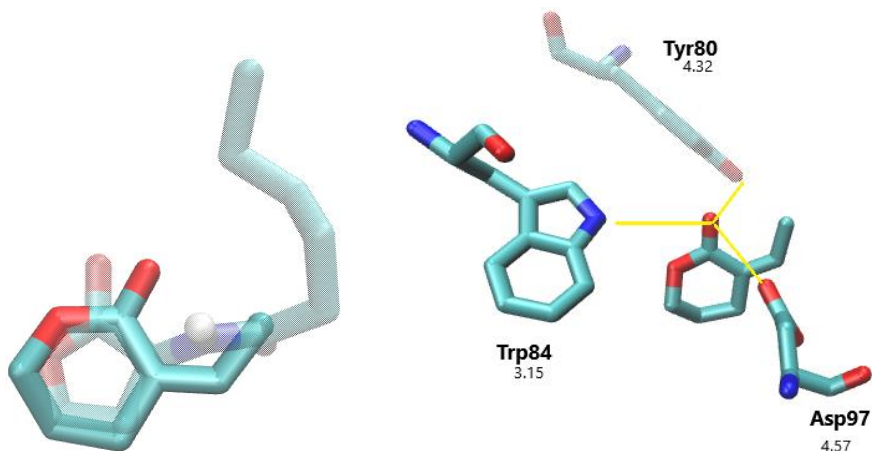


**Figure S19.** Overlap of **2** with **10Z**, and ligand binding domain for **10Z**/CviR, respectively.

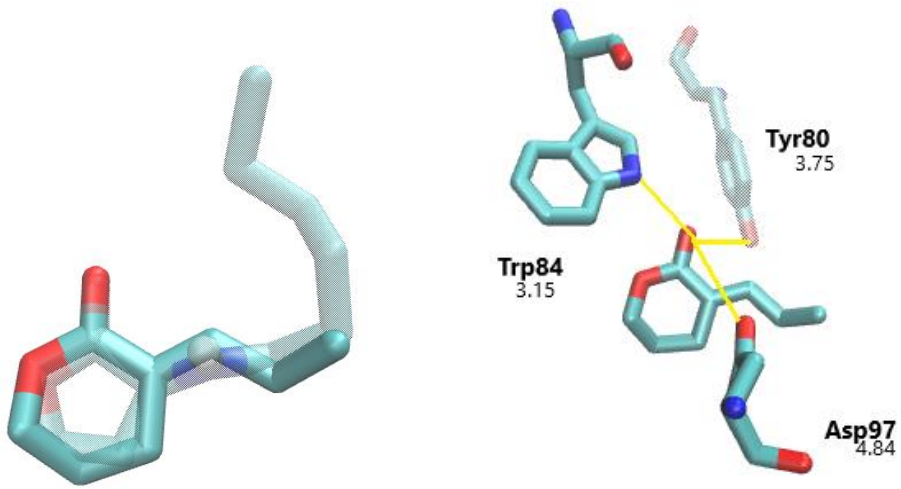


**Figure S20.** Overlap of **2** with **11E**, and ligand binding domain for **11E/CviR**, respectively.

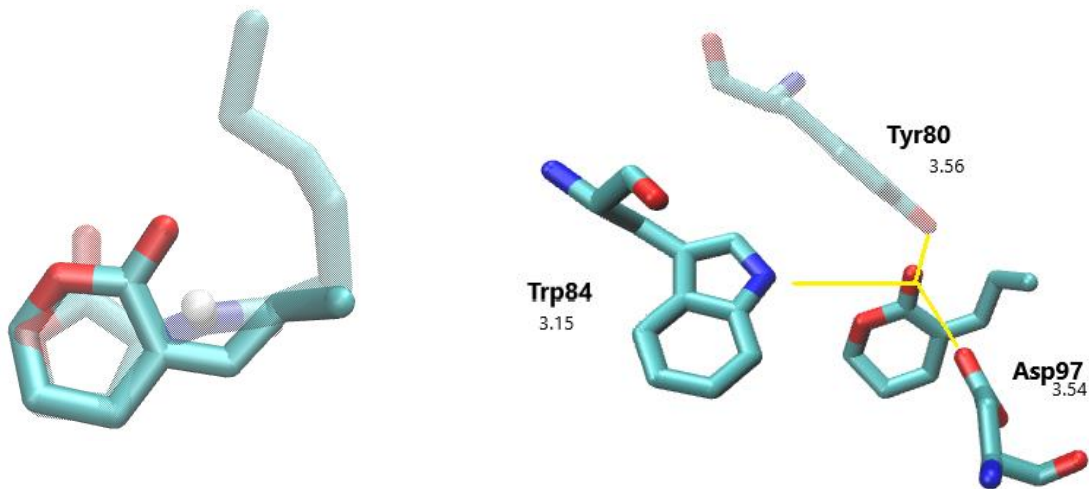


**Figure S21.** Overlap of **2** with **11Z**, and ligand binding domain for **11Z/CviR**, respectively.

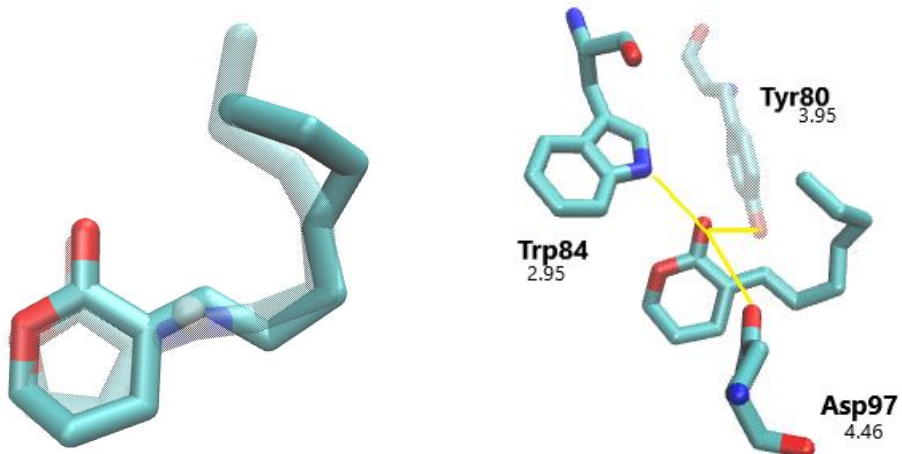


**Figure S22.** Overlap of **2** with **12E**, and ligand binding domain for **12E/CviR**, respectively.

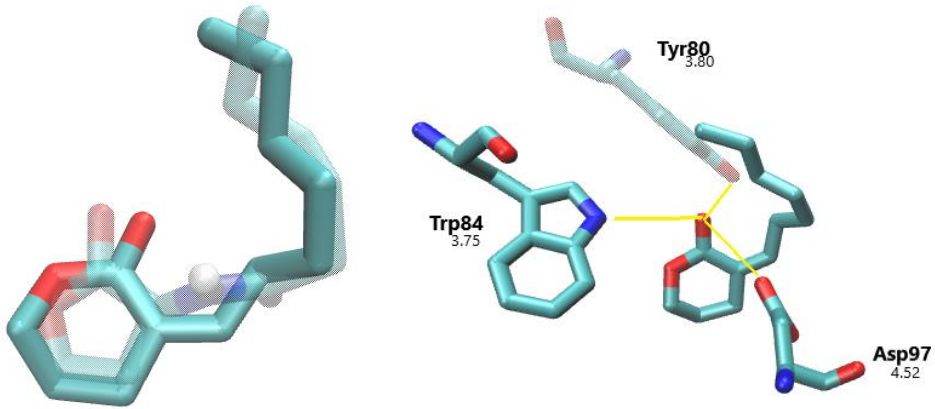


**Figure S23.** Overlap of **2** with **12Z**, and ligand binding domain for **12Z/CviR**, respectively.

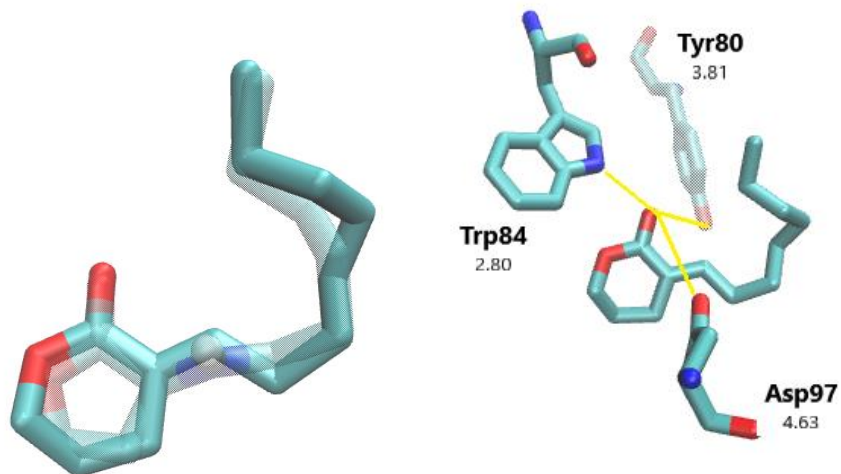


**Figure S24.** Overlap of **2** with **13E**, and ligand binding domain for **13E/CviR**, respectively.

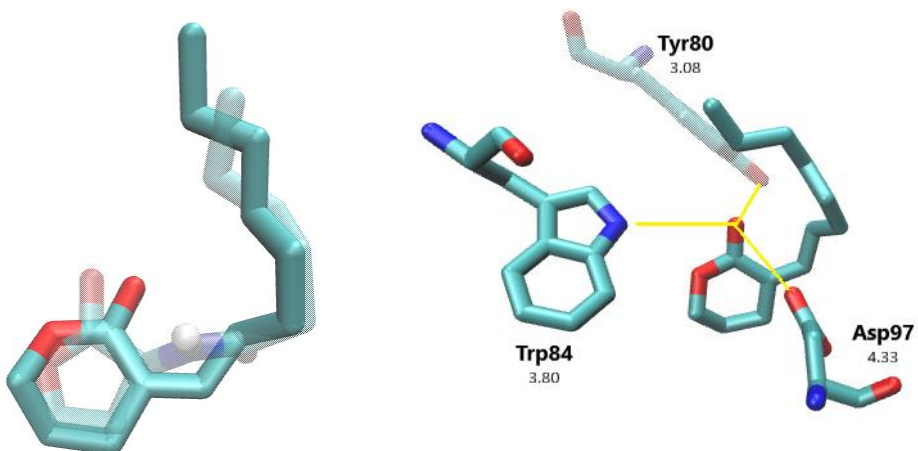


**Figure S25.** Overlap of **2** with **13Z**, and ligand binding domain for **13Z/CviR**, respectively.

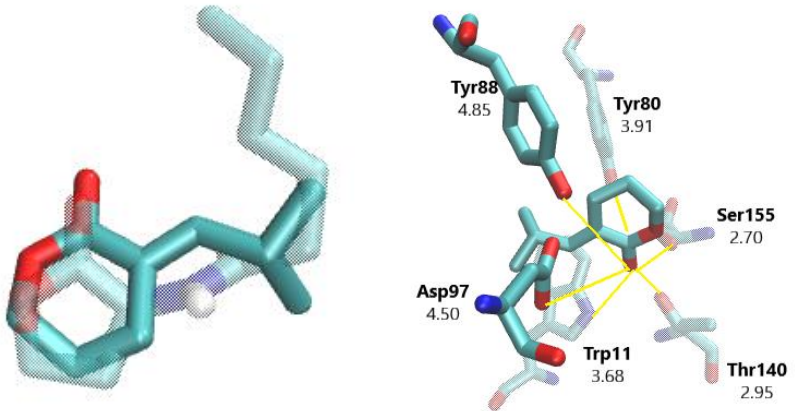


**Figure S26.** Overlap of **2** with **14E**, and ligand binding domain for **14E/CviR**, respectively.

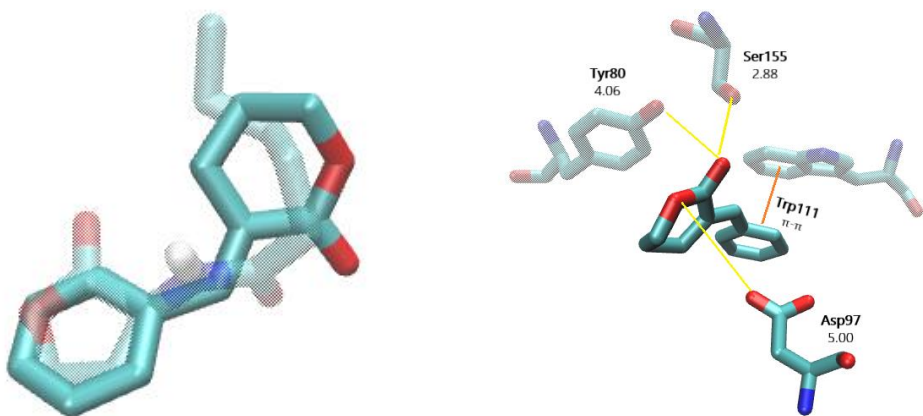


**Figure S27.** Overlap of **2** with **15E**, and ligand binding domain for **15E/CviR**, respectively.

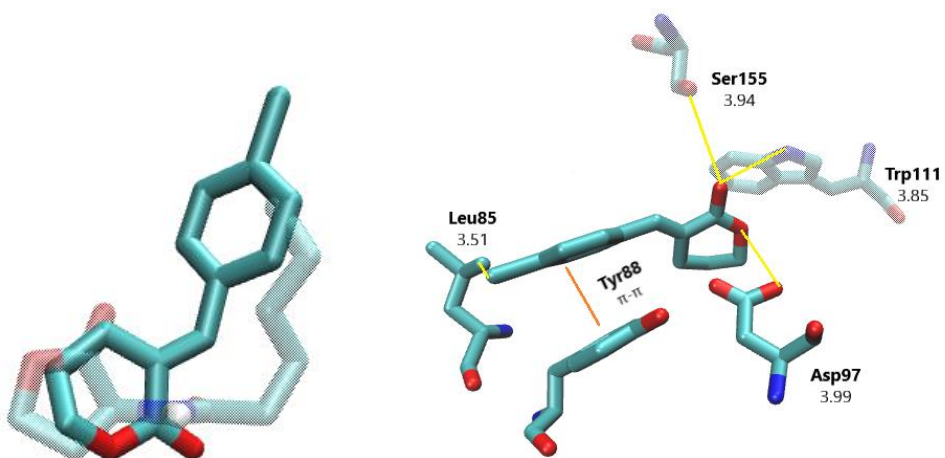


**Figure S28.** Overlap of **2** with **16E**, and ligand binding domain for **16E/CviR**, respectively.

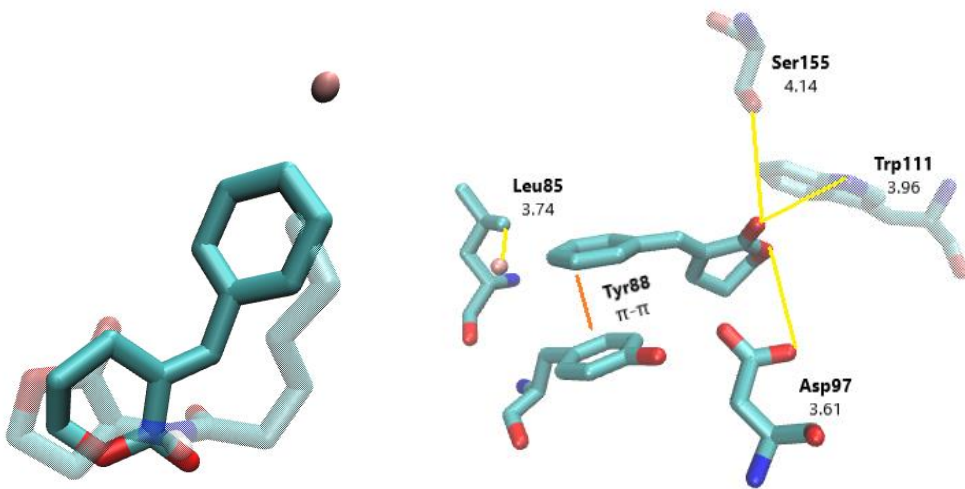


**Figure S29.** Overlap of **2** with **17E**, and ligand binding domain for **17E/CviR**, respectively.

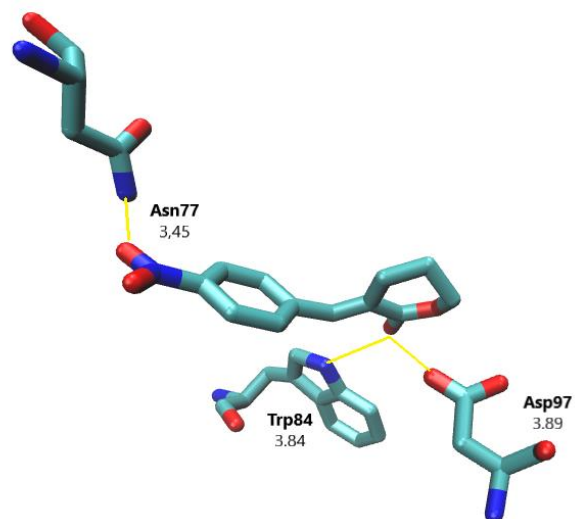


**Figure S30.** Overlap of **2** with **18E**, and ligand binding domain for **18E/CviR**, respectively.

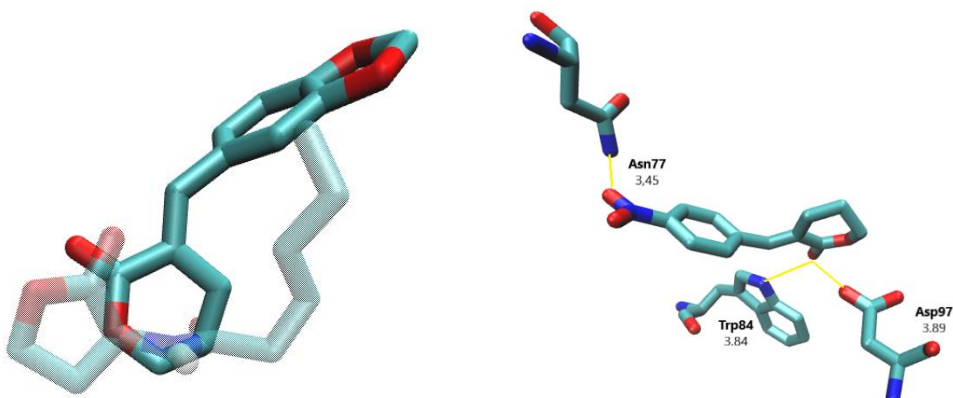


**Figure S31.** Overlap of **2** with **19E**, and ligand binding domain for **19E/CviR**, respectively.

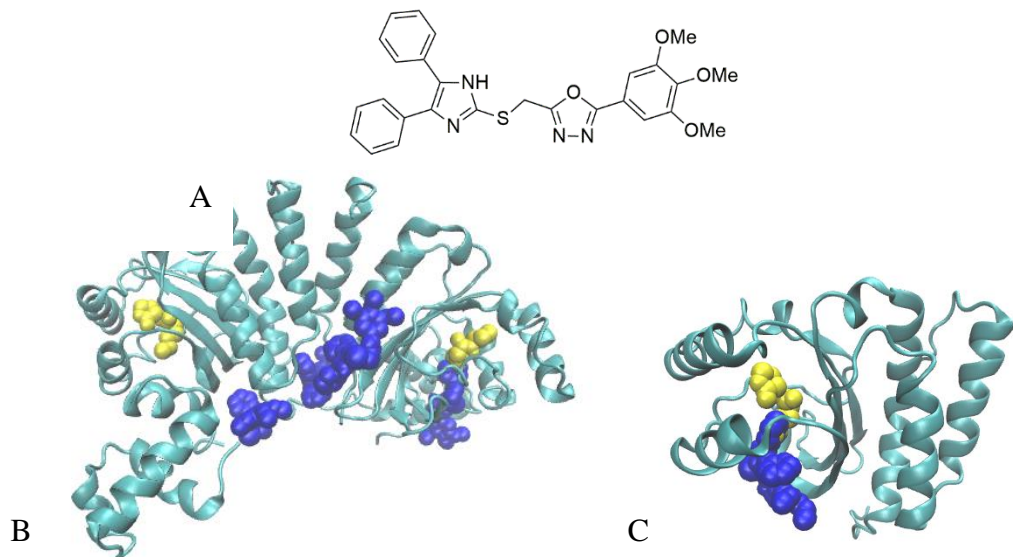
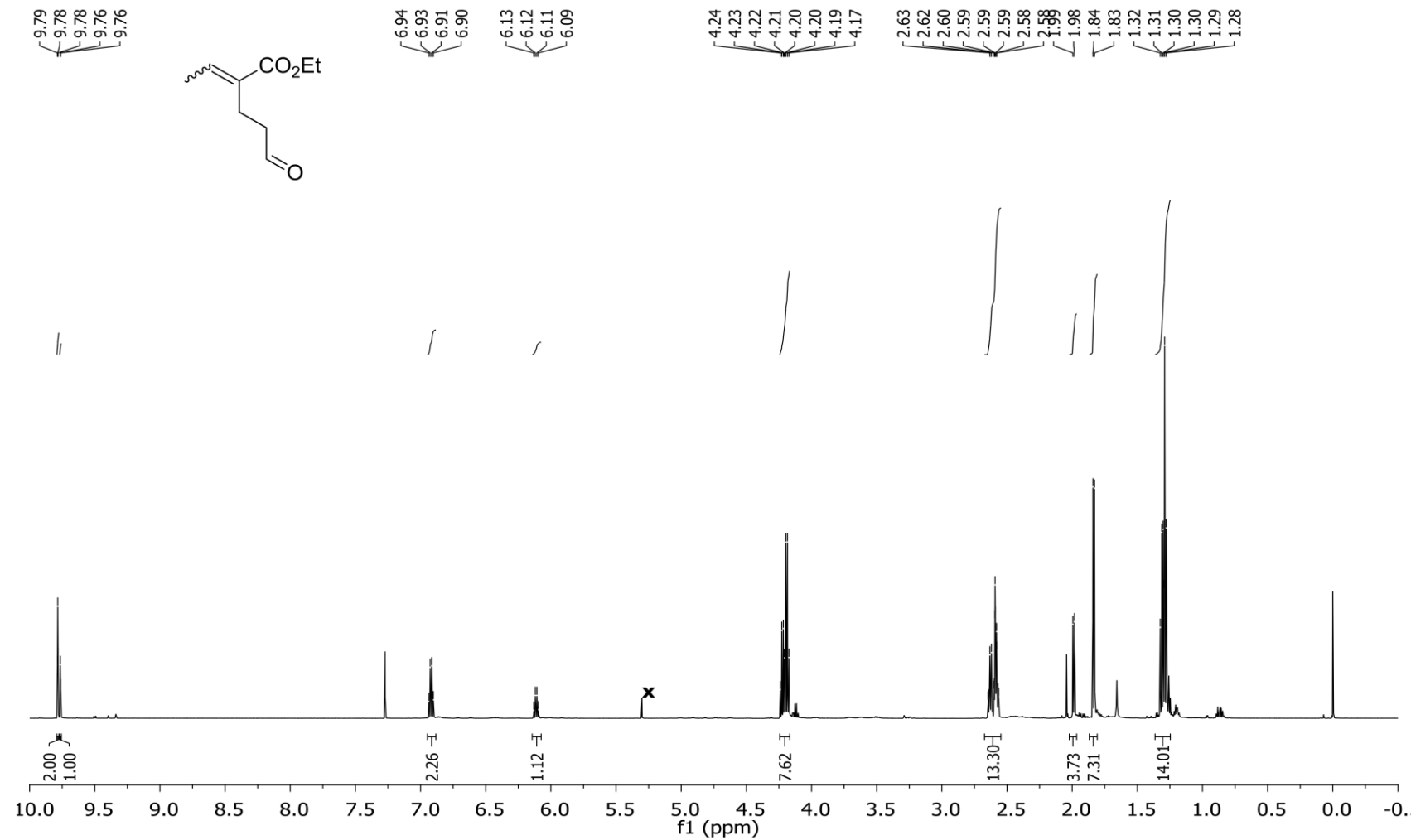


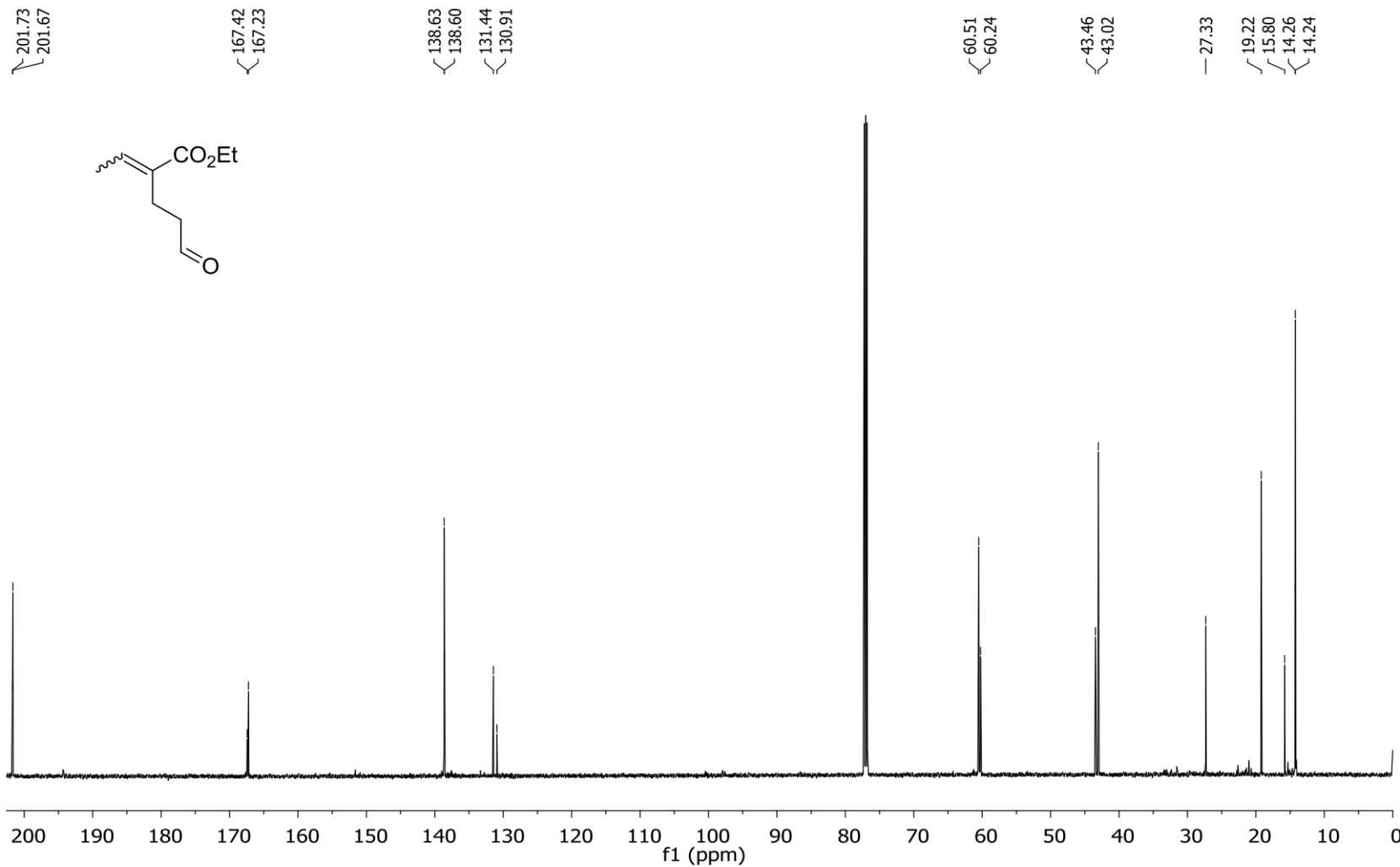
**Figure S32.** (A): Chemical structure of **21**; B: CviR (PDB ID: 3PQ5) complex with **21**(blue), in yellow is shown HHL to exemplify the LBD.; (C): LBD complex with **21**(blue), in yellow is shown HHL (**2**) to exemplify the LBD.

2. NMR spectrums:

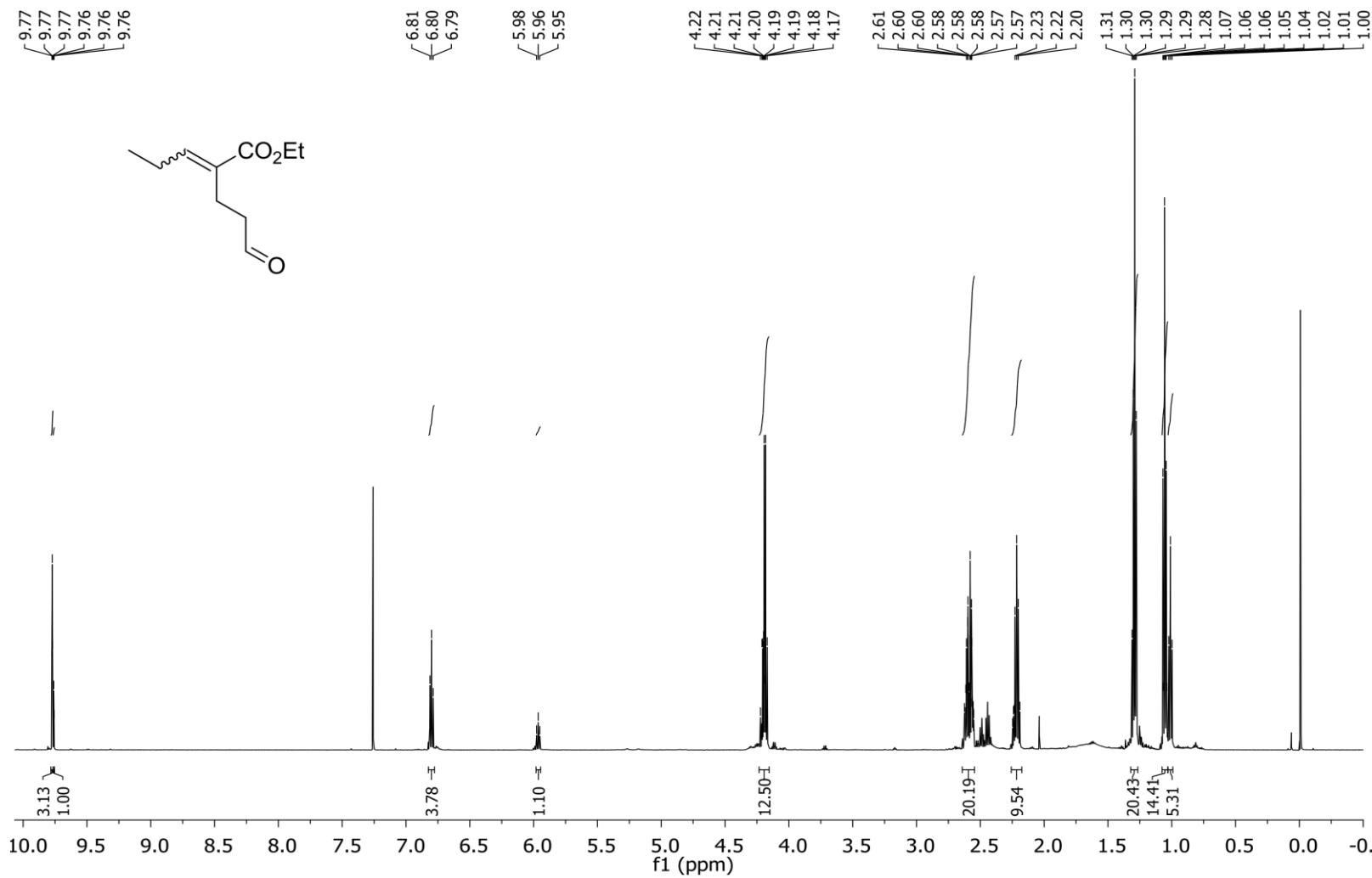
S2.1.  $^1\text{H}$  NMR (600 MHz) spectrum of **8 (E/Z)** R = Methyl in  $\text{CDCl}_3$ .



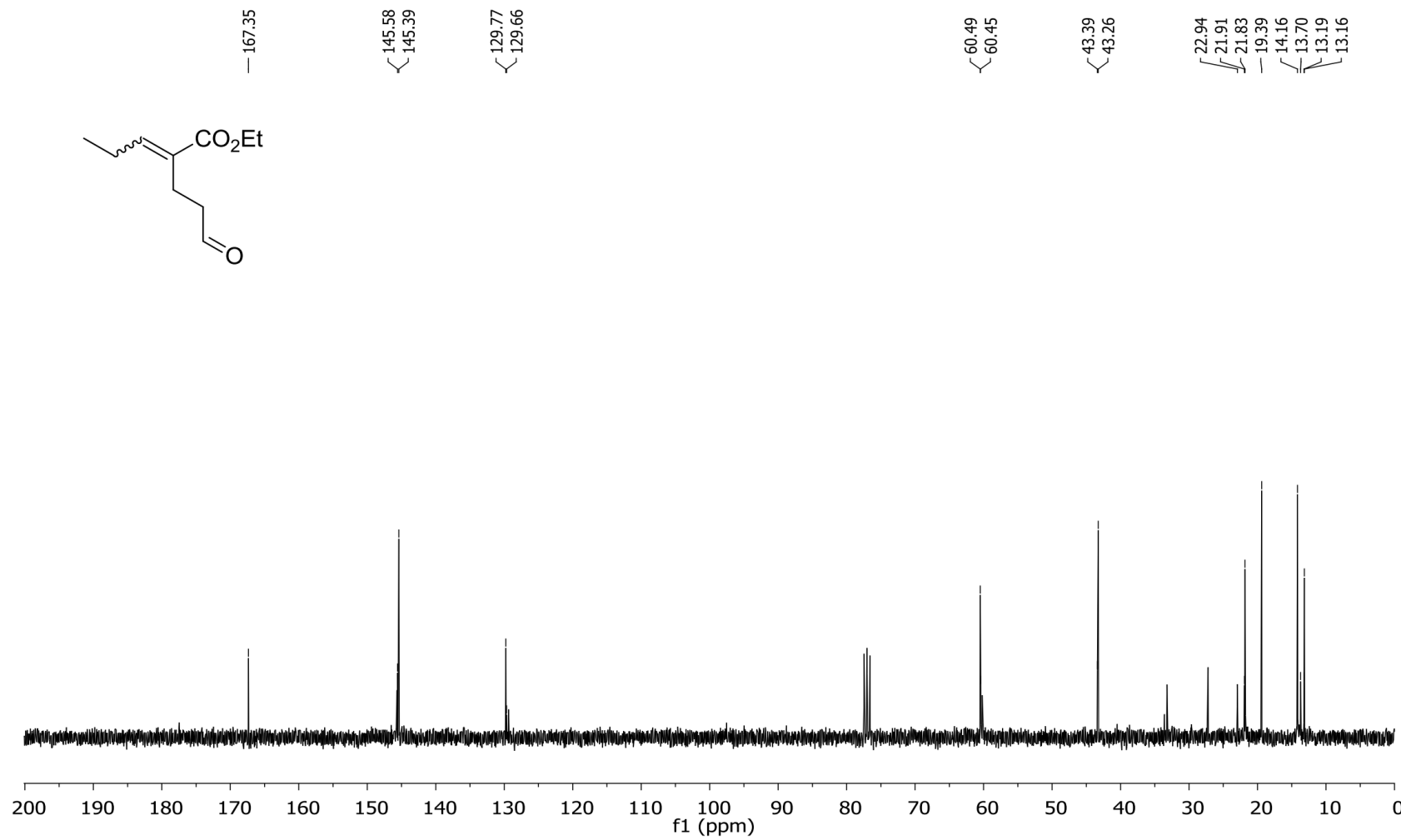
S2.2.  $^{13}\text{C}$  NMR (75 MHz) spectrum of **8** (*E/Z*) **R = Methyl** in  $\text{CDCl}_3$



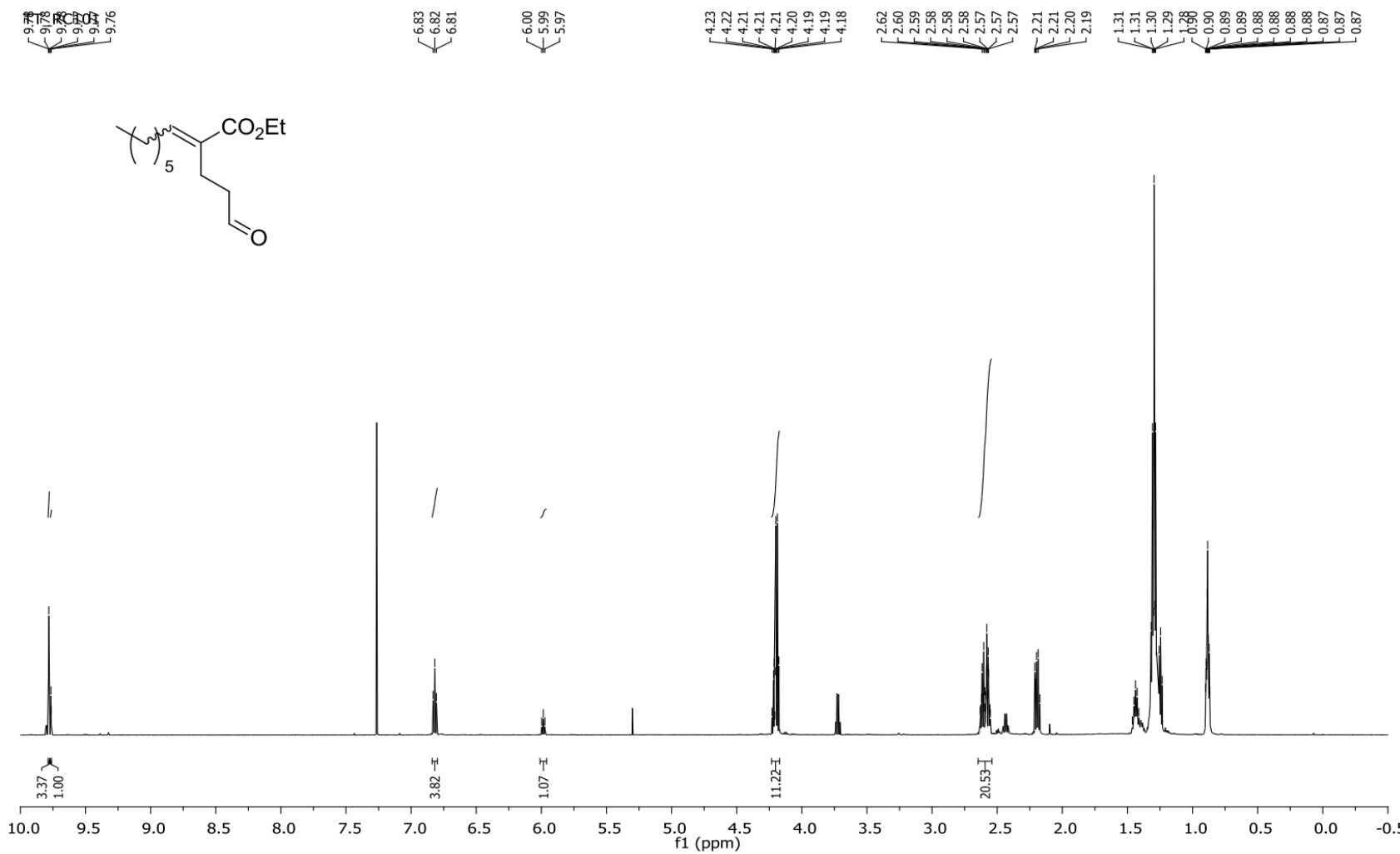
S2.3.  $^1\text{H}$  NMR (600 MHz) spectrum of **8** (*E/Z*) R = Ethyl in  $\text{CDCl}_3$ .



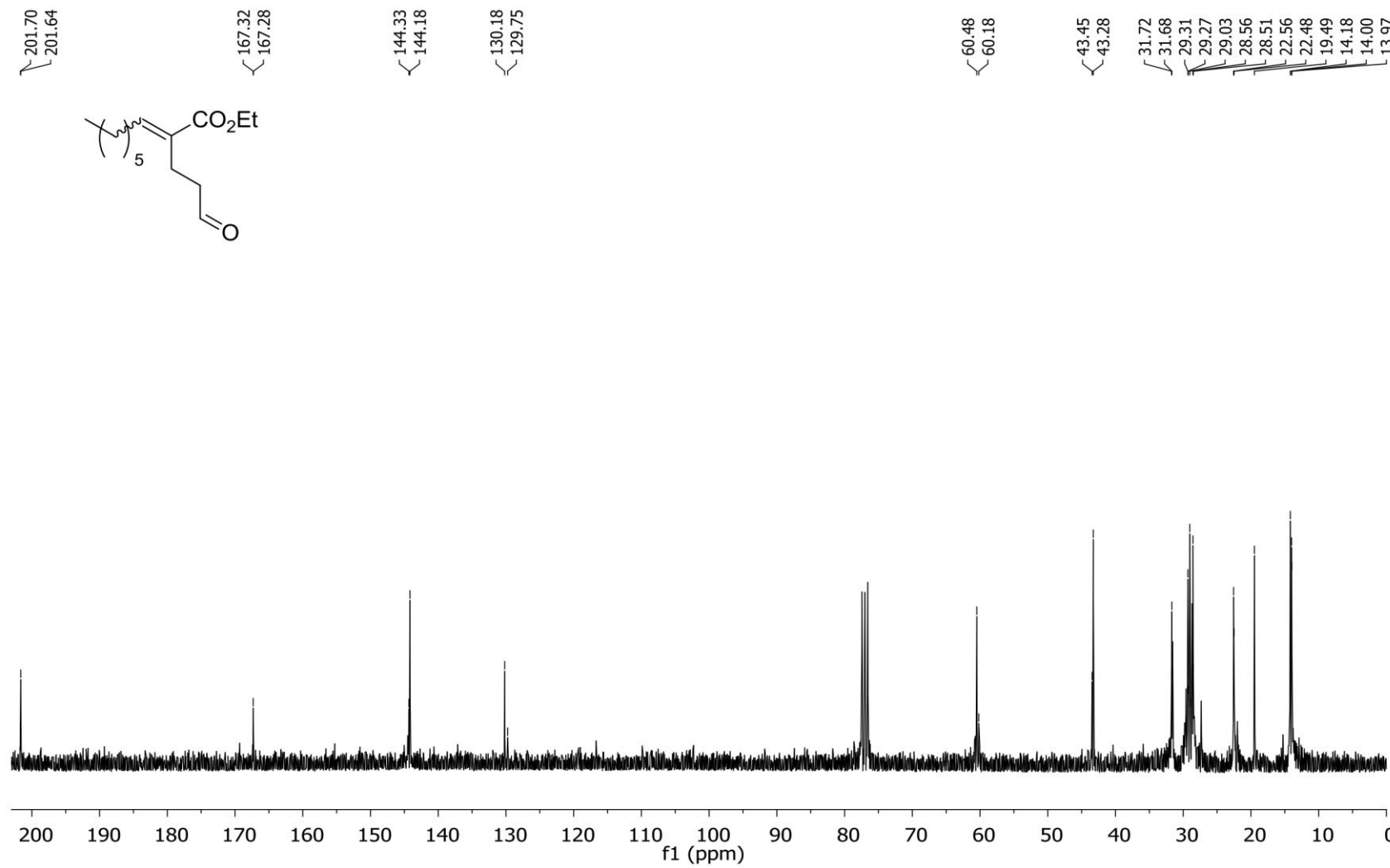
S2.4.  $^{13}\text{C}$  NMR (75 MHz) spectrum of **8** (*E/Z*) **R = Ethyl** in  $\text{CDCl}_3$ .



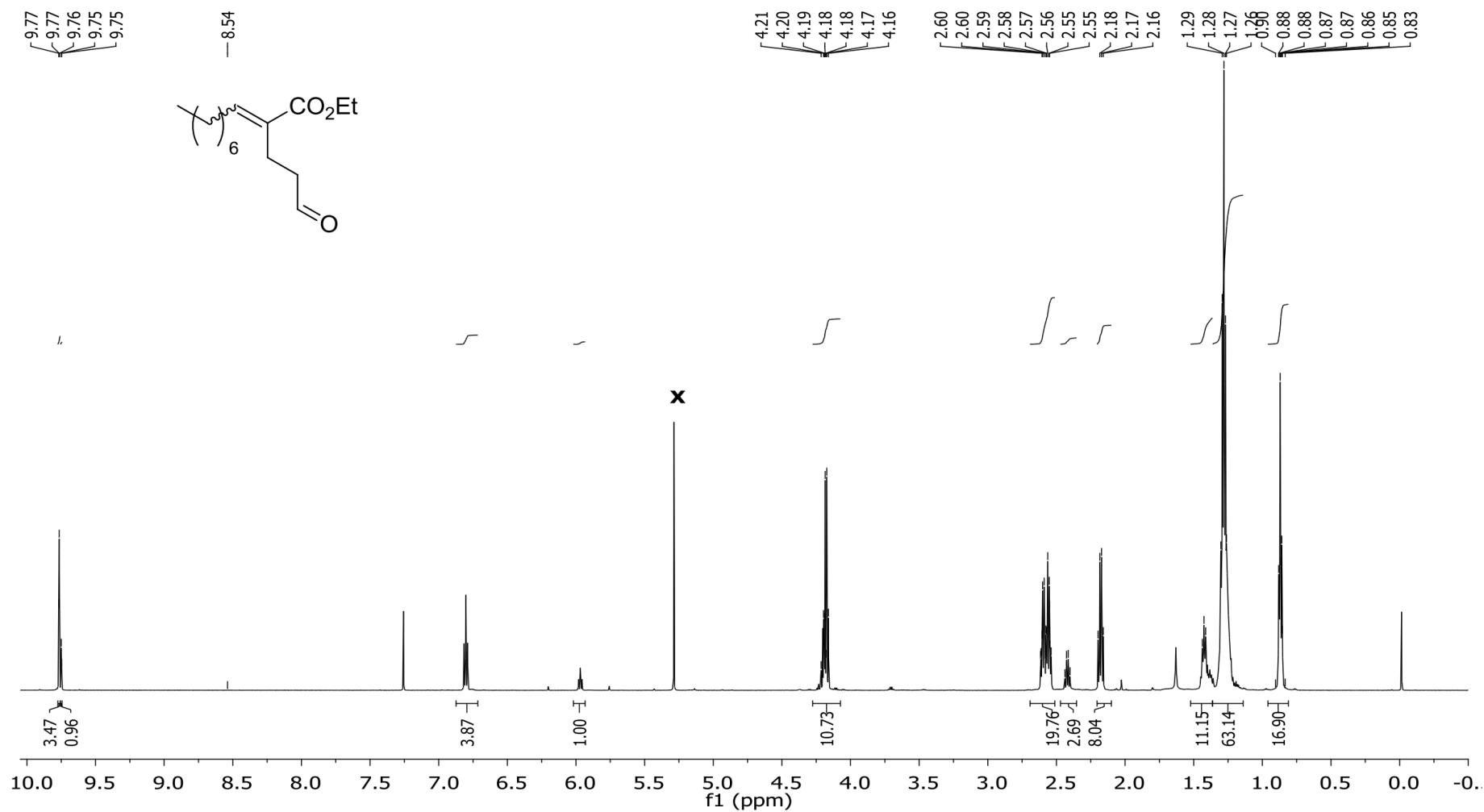
S2.5.  $^1\text{H}$  NMR (600 MHz) spectrum of **8** (*E/Z*) R = *n*-Hexyl in  $\text{CDCl}_3$ .



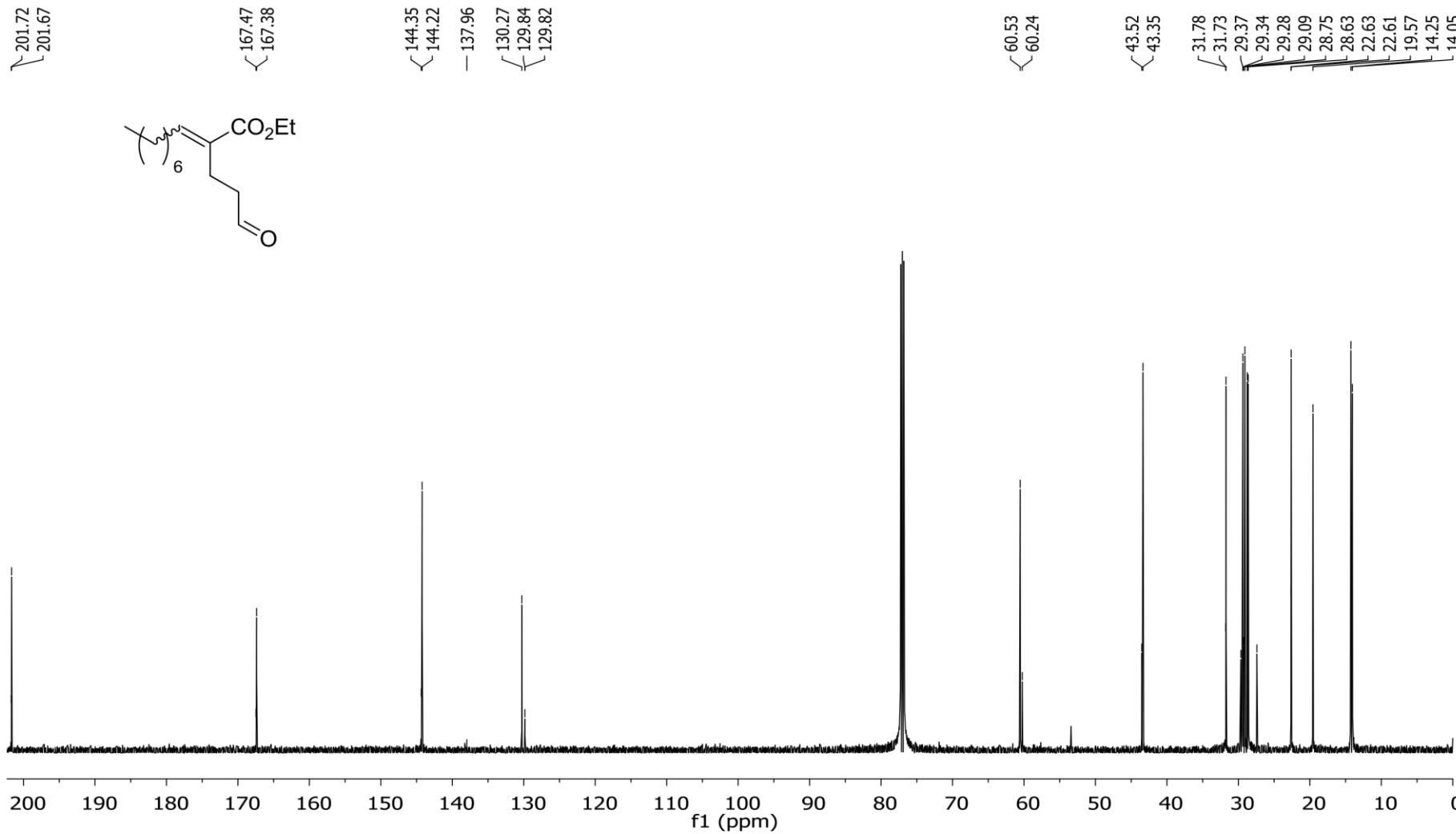
S2.6.  $^{13}\text{C}$  NMR (151 MHz) spectrum of **8** (*E/Z*) R = *n*-Hexyl in  $\text{CDCl}_3$ .



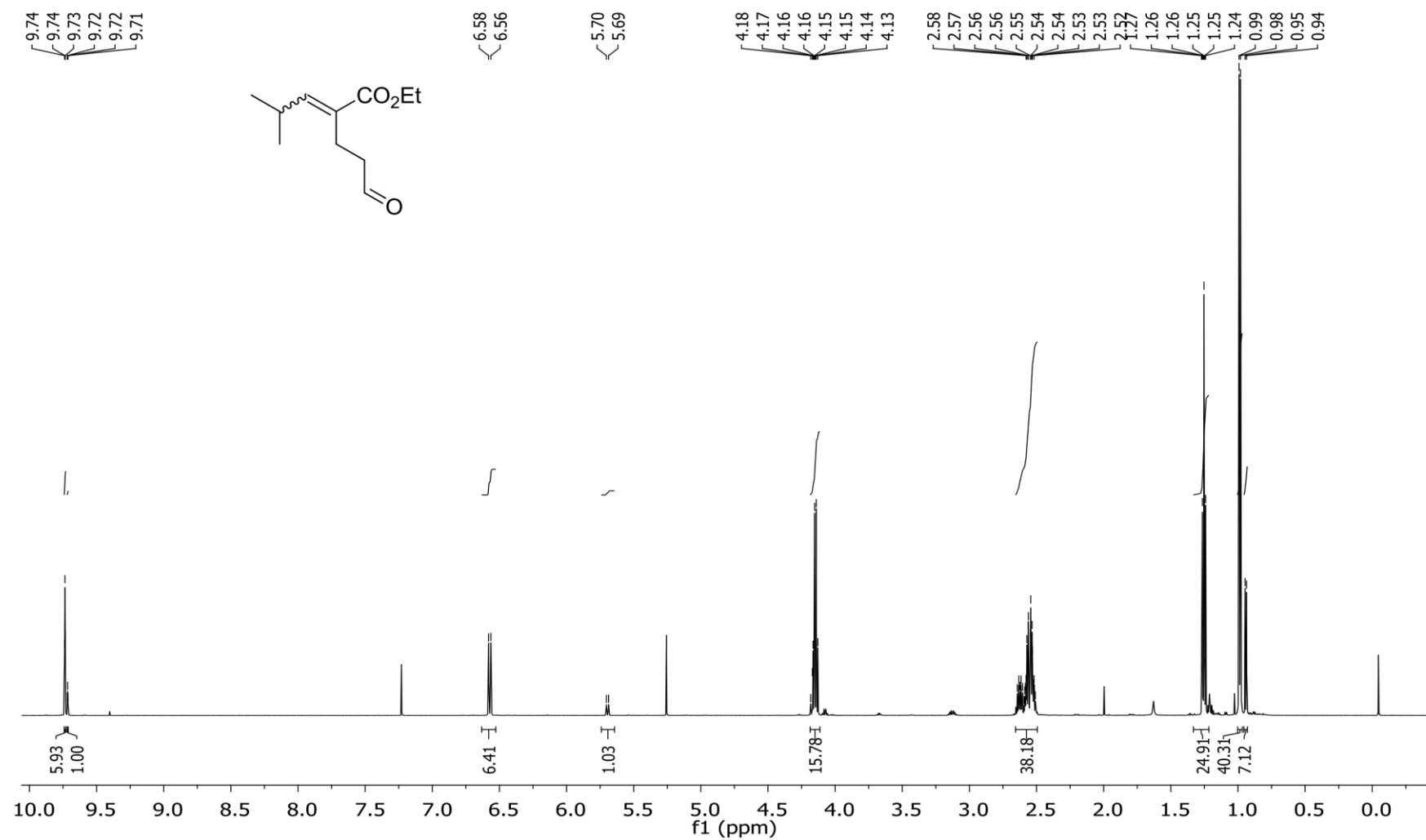
S2.7.  $^1\text{H}$  NMR (600 MHz) spectrum of **8** (*E/Z*) R = *n*-Heptyl in  $\text{CDCl}_3$ .



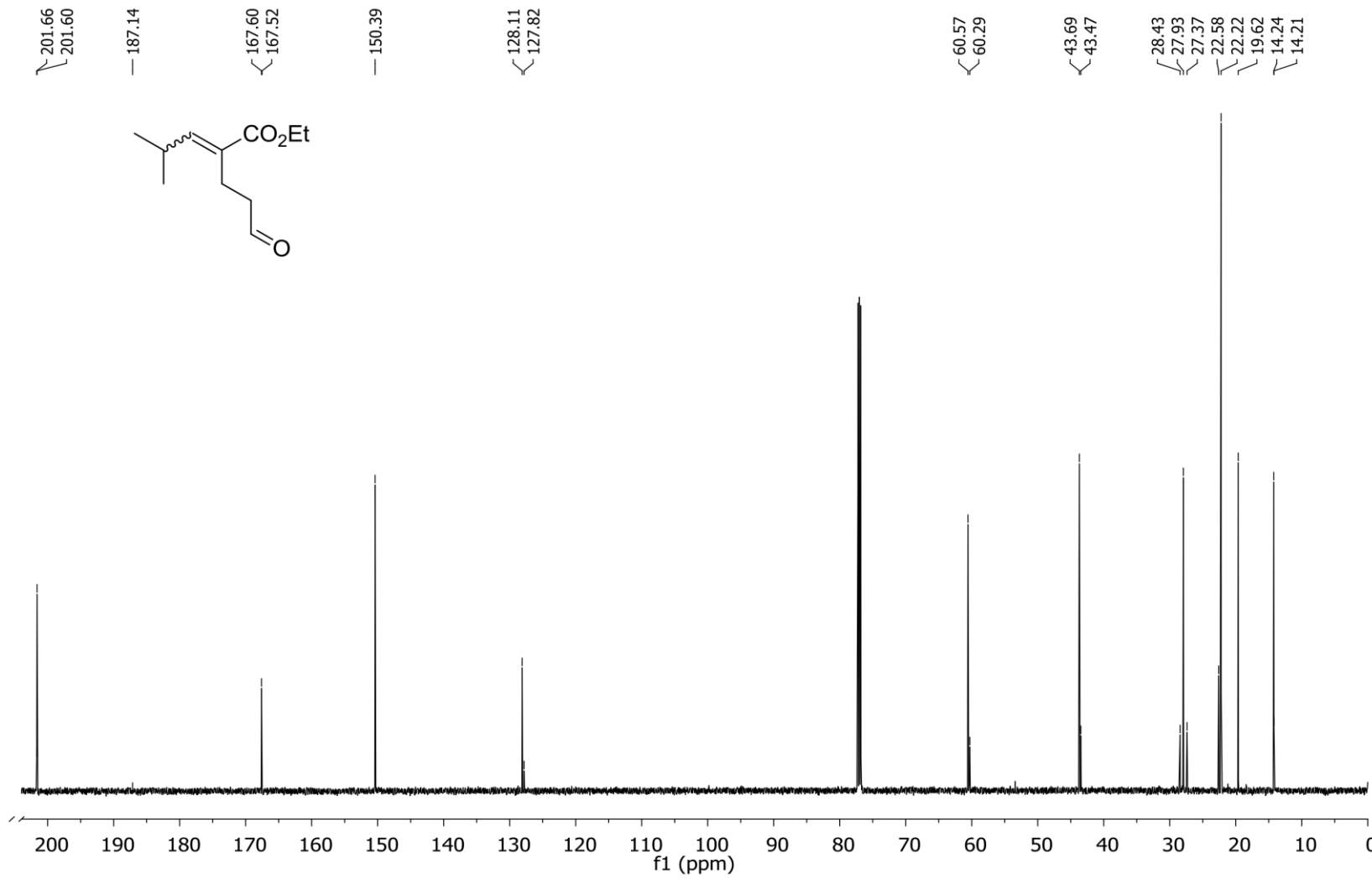
S2.8.  $^{13}\text{C}$  NMR (151 MHz) spectrum of **8** (*E/Z*) R = *n*-Heptyl in  $\text{CDCl}_3$ .



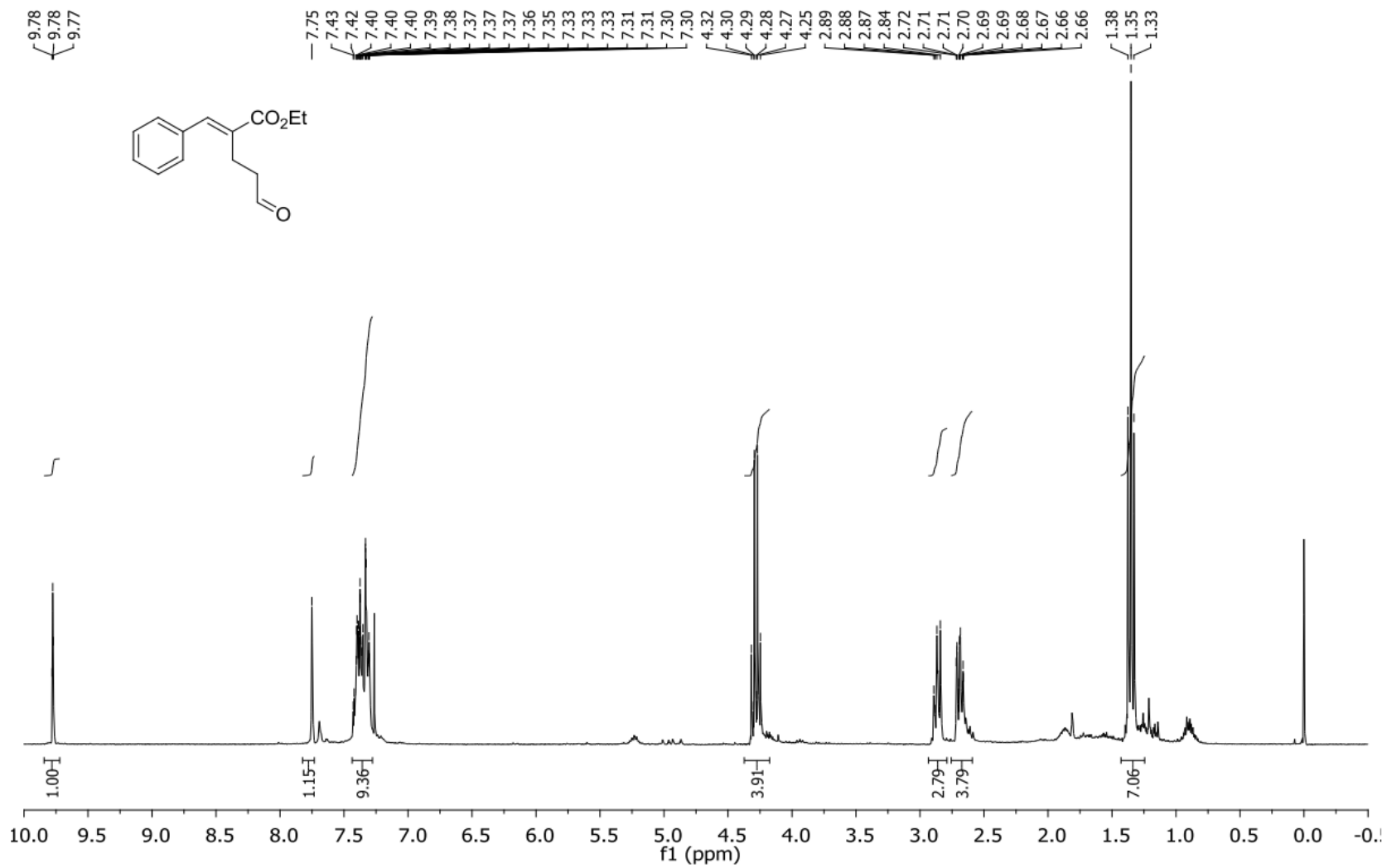
S2.9.  $^1\text{H}$  NMR (600 MHz) spectrum of **8** (*E/Z*) R = *iso*-Propyl in  $\text{CDCl}_3$ .



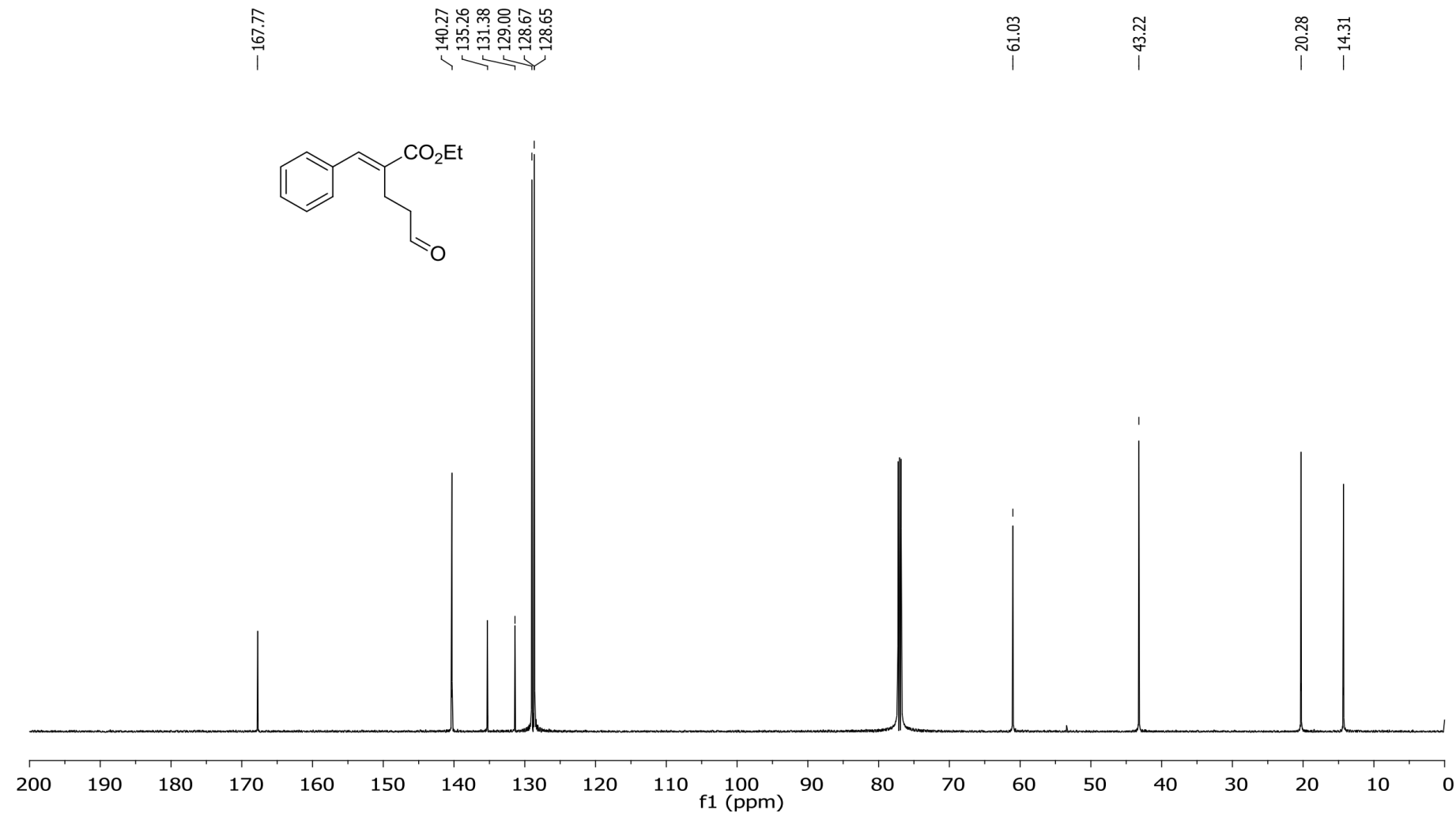
S2.10.  $^{13}\text{C}$  NMR (151 MHz) spectrum of **8** (*E/Z*) **R** = *iso*-Propyl in  $\text{CDCl}_3$ .



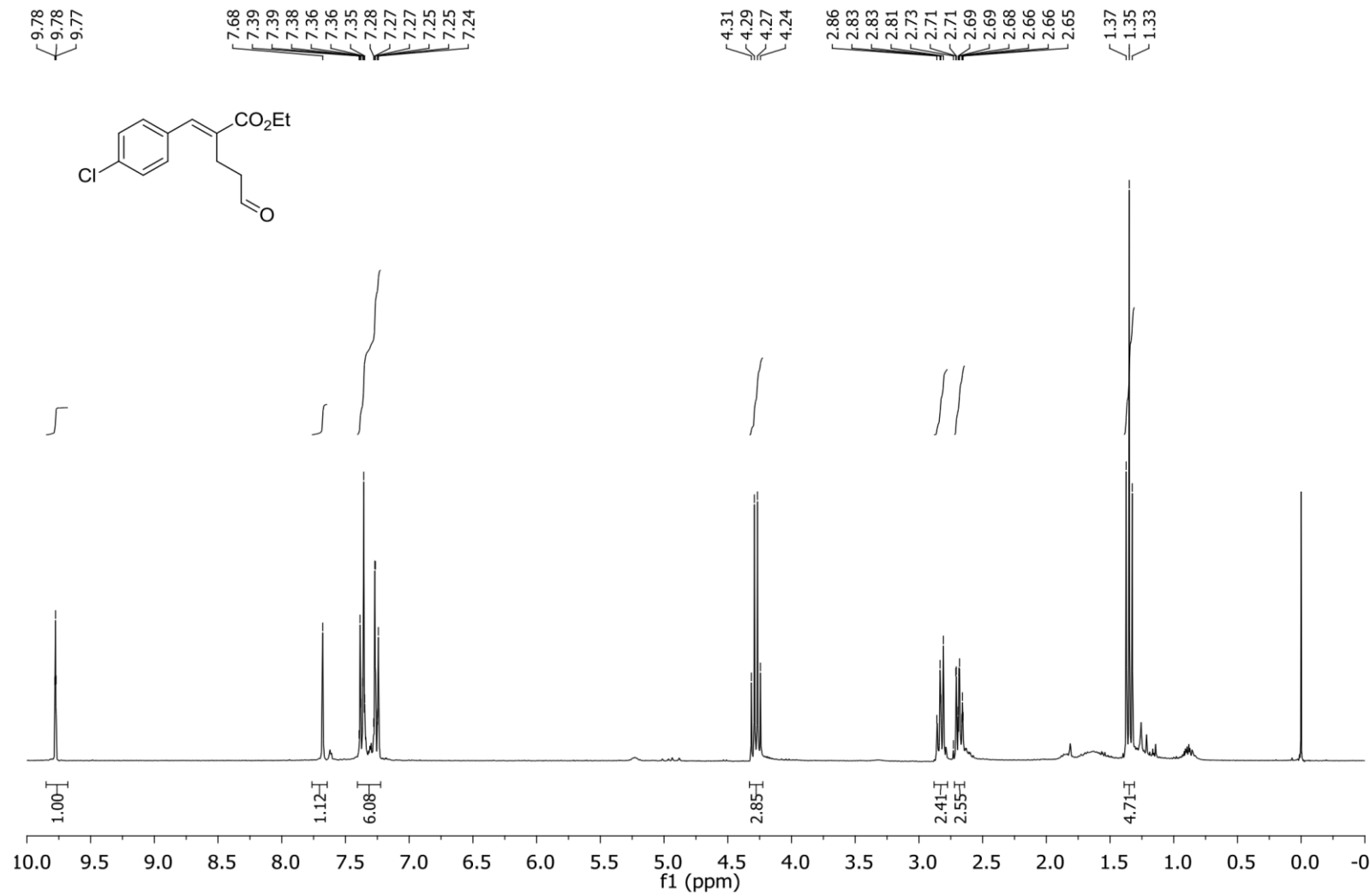
S2.11.  $^1\text{H}$  NMR (600 MHz) spectrum of **8** (*E*) R = Phenyl in  $\text{CDCl}_3$ .



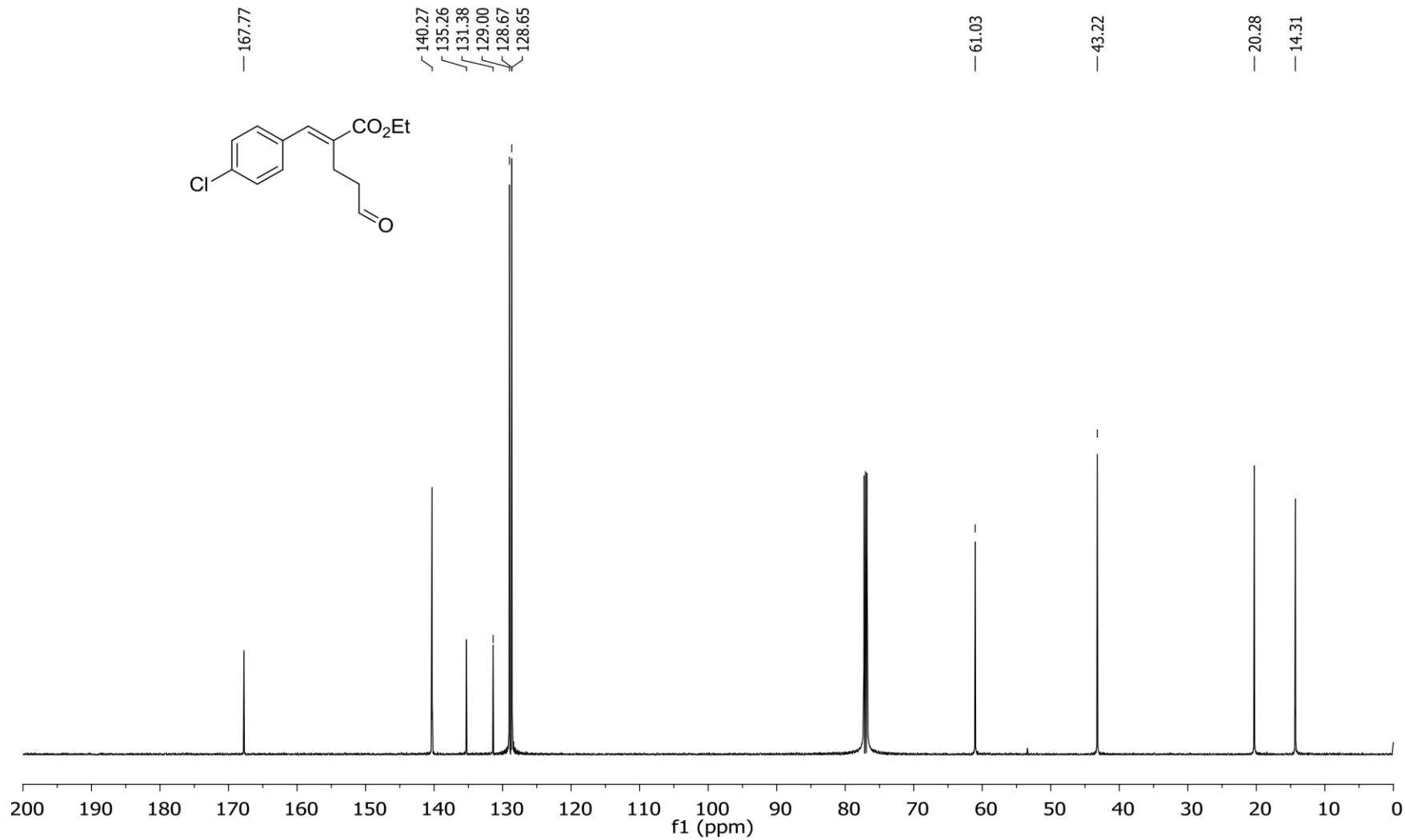
S2.12.  $^{13}\text{C}$  NMR (151 MHz) spectrum of **8 (E)** R = Phenyl in  $\text{CDCl}_3$ .



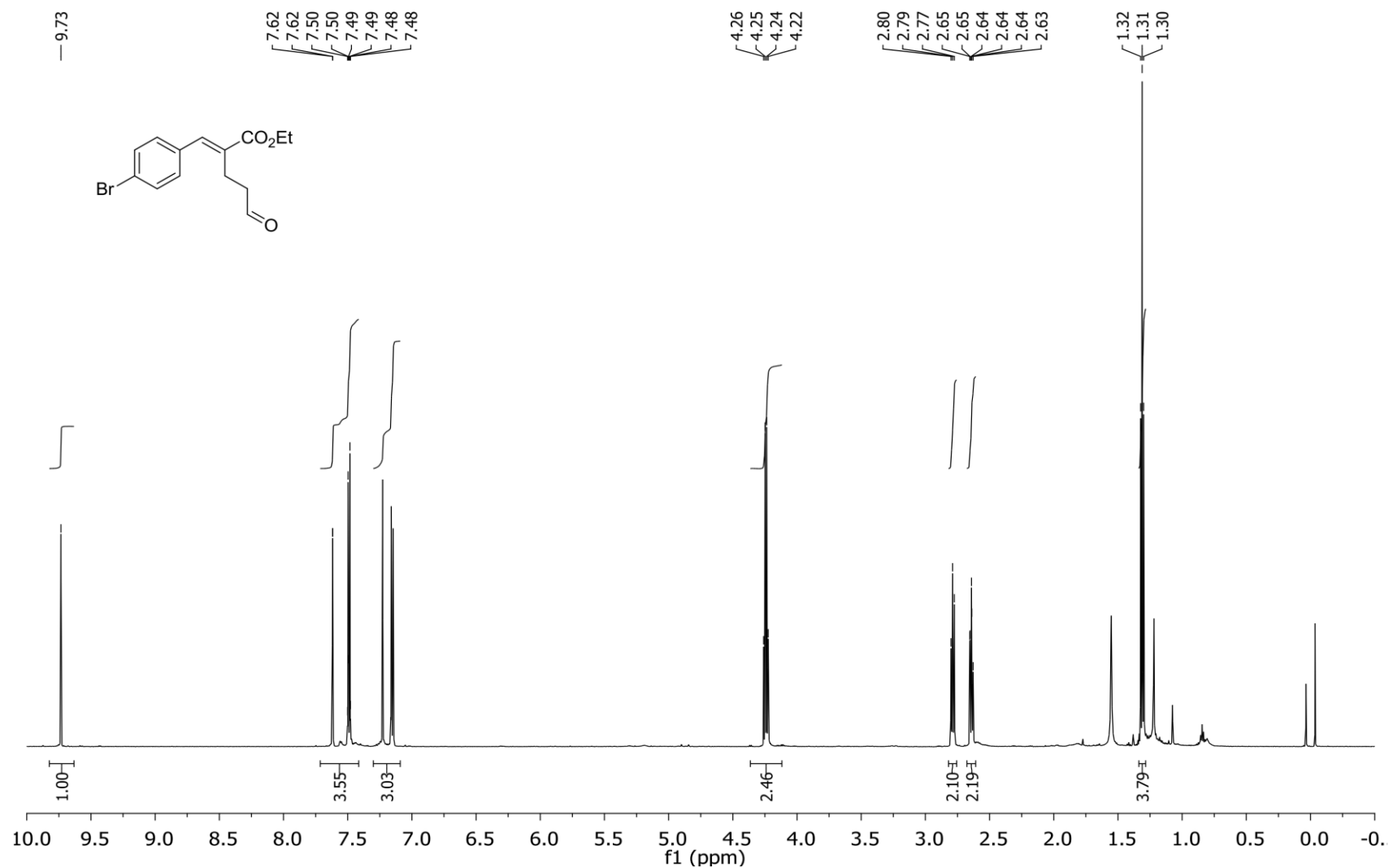
S2.13.  $^1\text{H}$  NMR (300 MHz) spectrum of **8** (*E*) R = 4-Cl-Phenyl in  $\text{CDCl}_3$ .



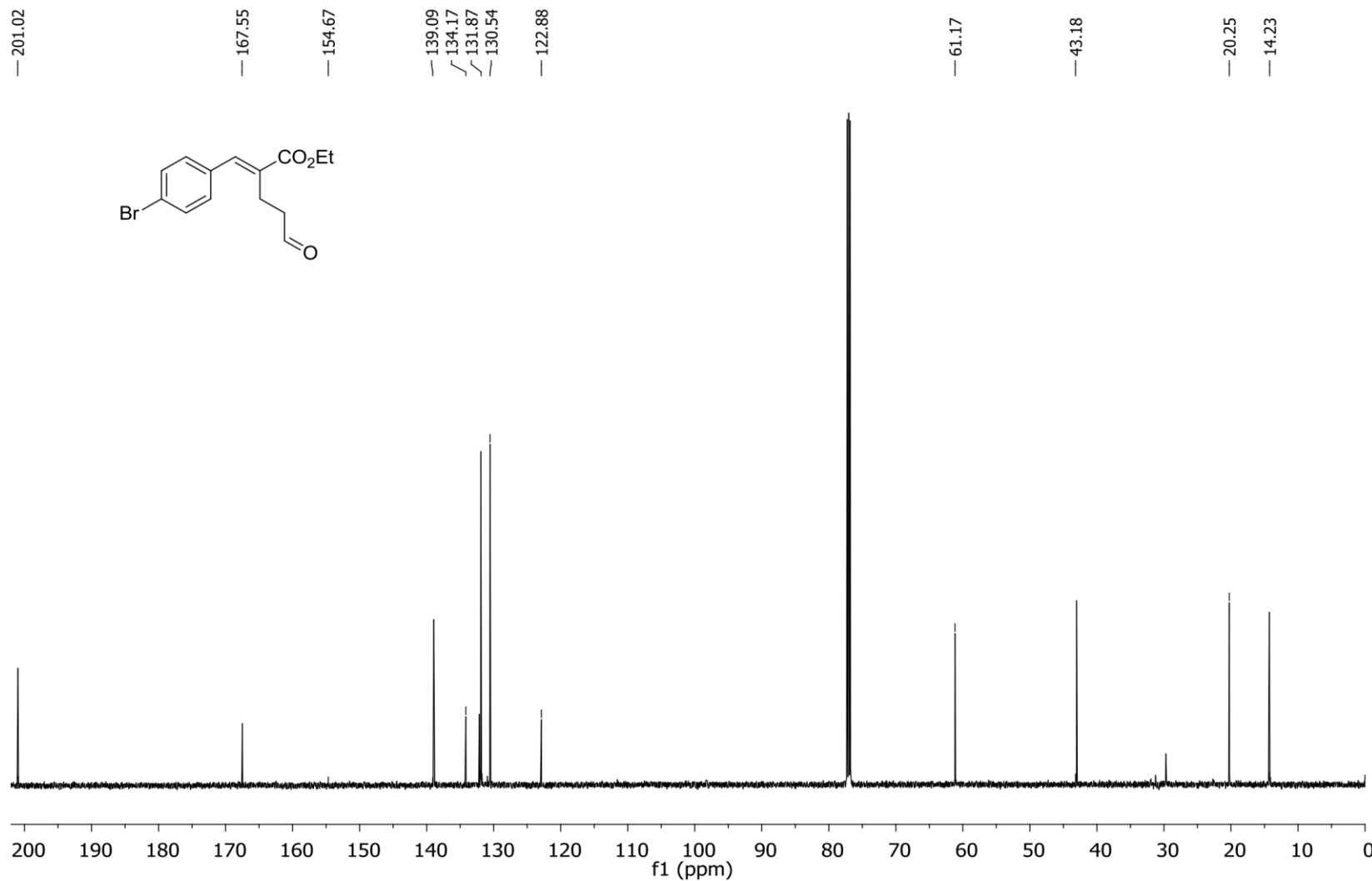
S2.14.  $^{13}\text{C}$  NMR (151 MHz) spectrum of **8** (*E*) **R** = 4-Cl-Phenyl in  $\text{CDCl}_3$ .



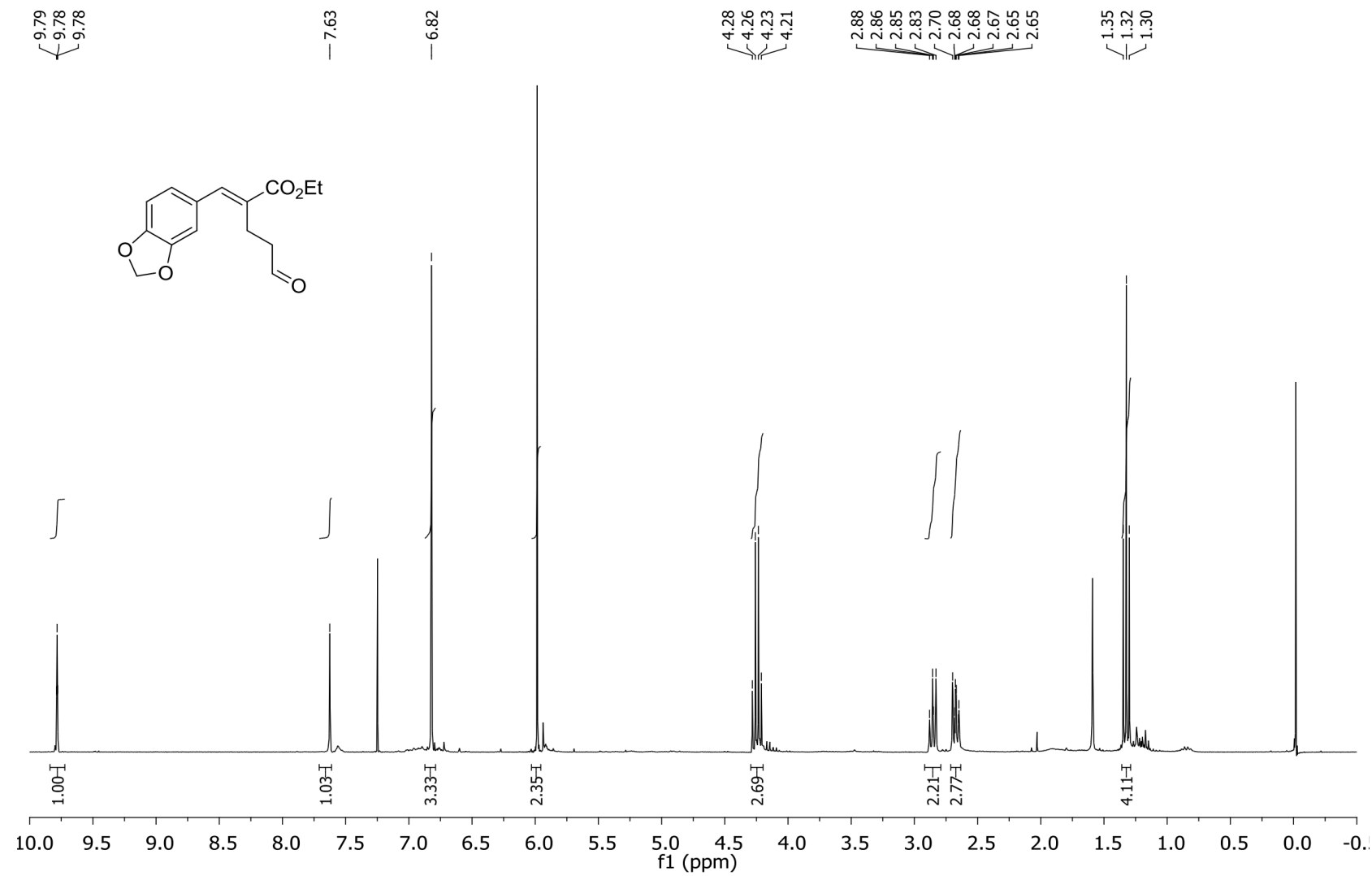
S2.15.  $^1\text{H}$  NMR (600 MHz) spectrum of **8** (*E*) R = 4-Br-Phenyl in  $\text{CDCl}_3$ .



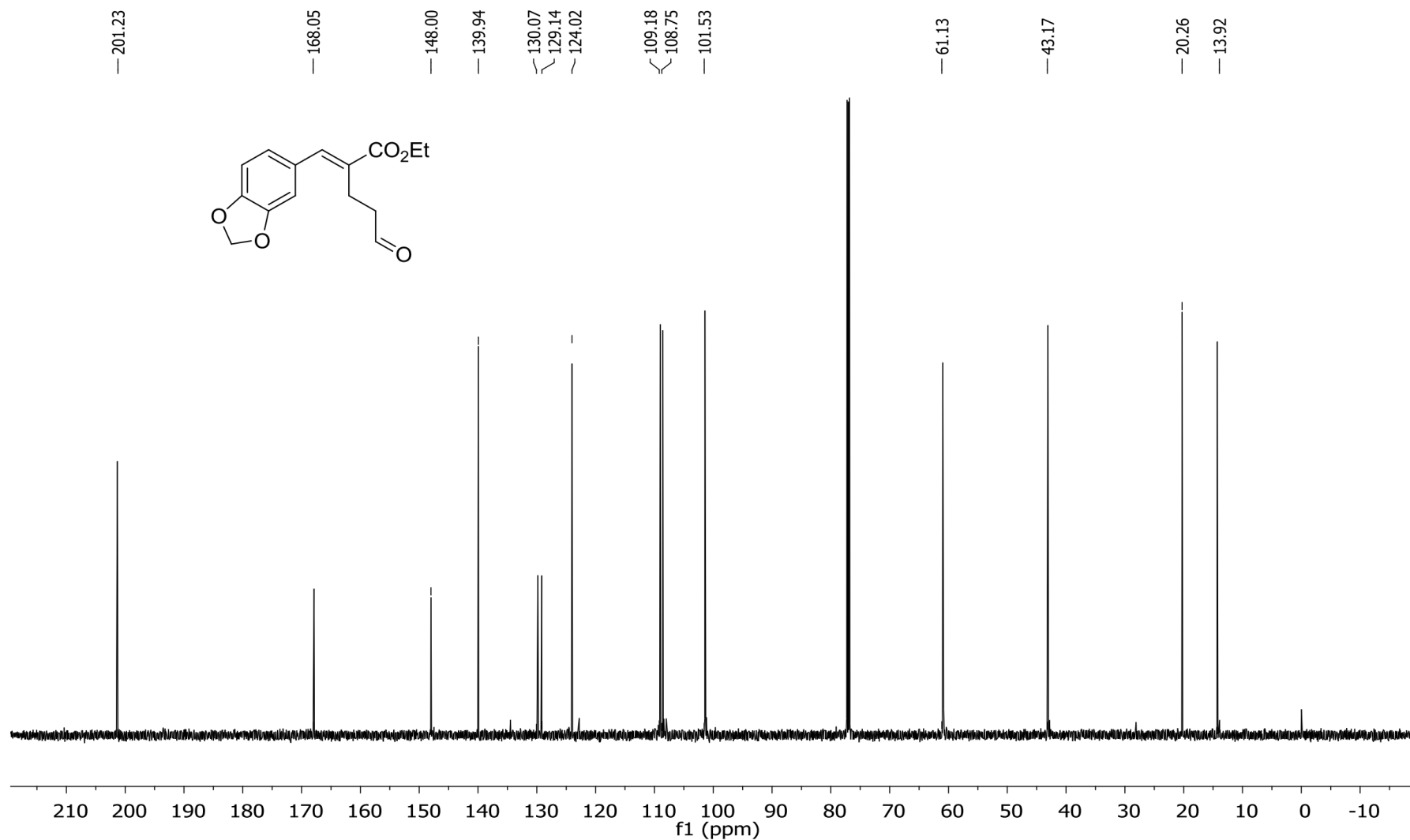
S2.16.  $^{13}\text{C}$  NMR (151 MHz) spectrum of **8** (*E*) R = 4-Br-Phenyl in  $\text{CDCl}_3$ .



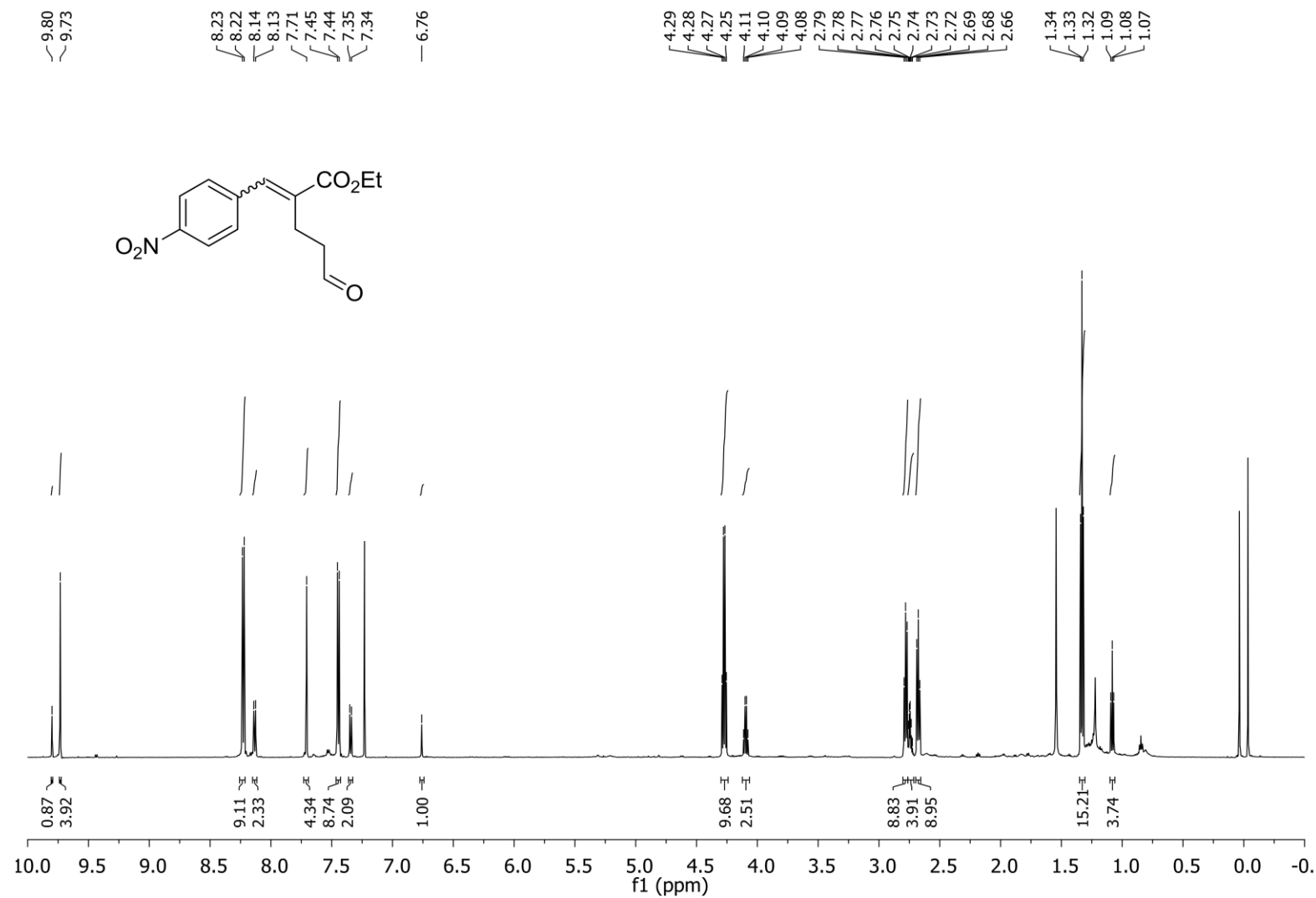
S2.17.  $^1\text{H}$  NMR (600 MHz) spectrum of **8** (*E*) R = 3,4-Methylenedioxyphenyl in  $\text{CDCl}_3$ .



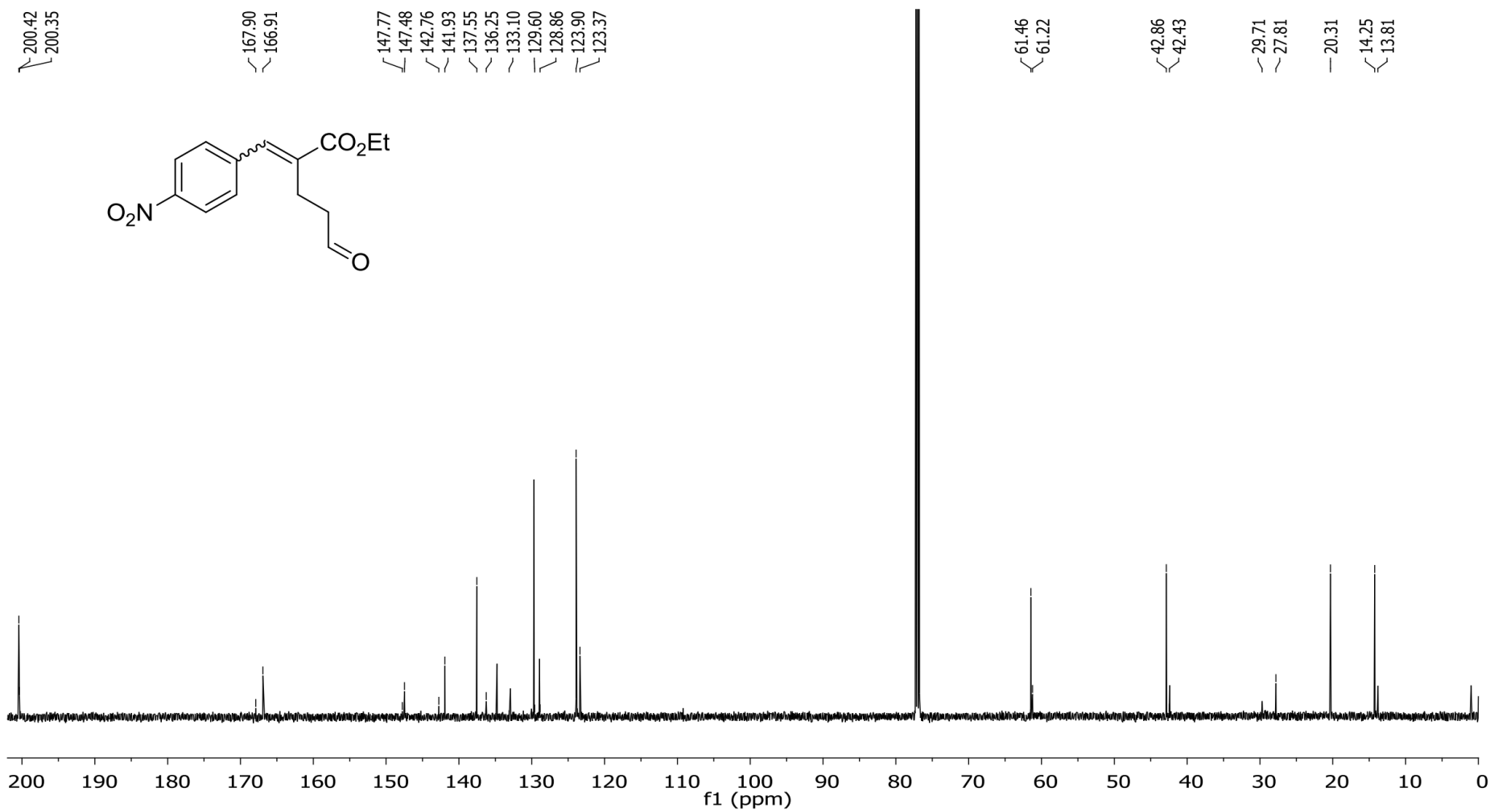
S2.18.  $^{13}\text{C}$  NMR (151 MHz) spectrum of **8 (E)** R = 3,4-Methylenedioxyphenyl in  $\text{CDCl}_3$ .



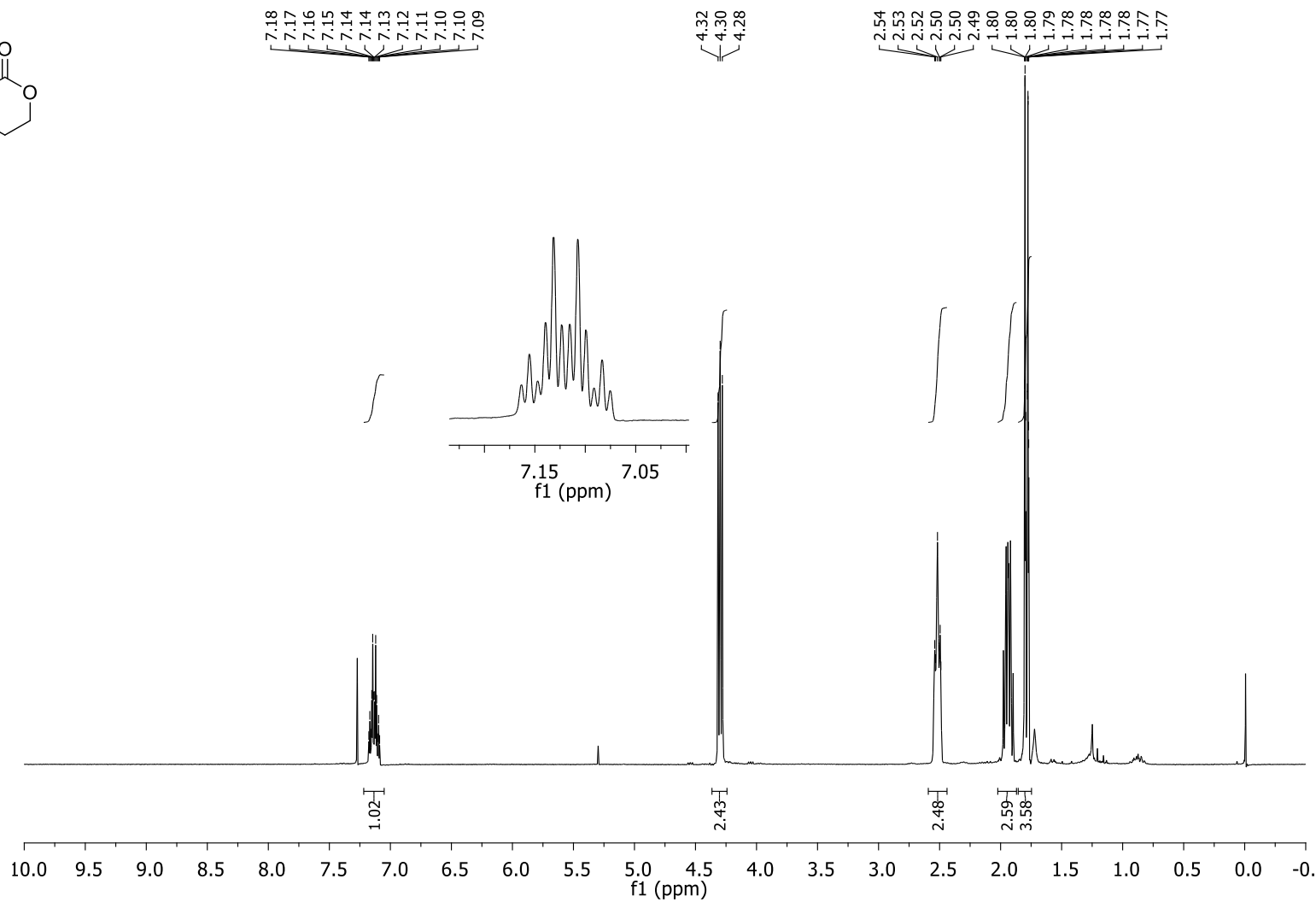
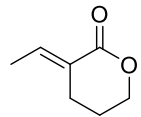
S2.19.  $^1\text{H}$  NMR (600 MHz) spectrum of **8** (*E*) R = 4-NO<sub>2</sub>-Phenyl in CDCl<sub>3</sub>.



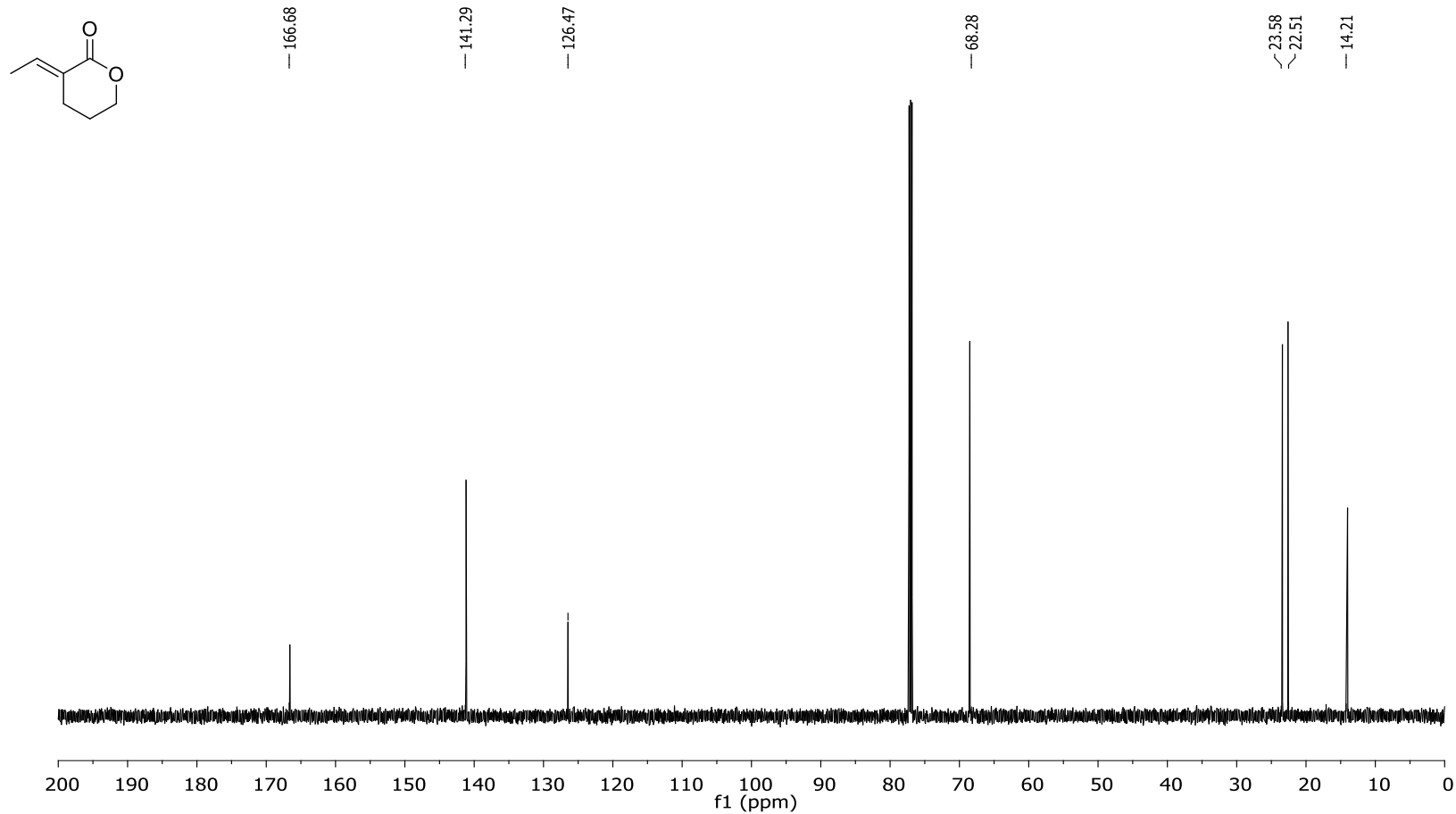
S2.20.  $^{13}\text{C}$  NMR (151 MHz) spectrum of **8** (*E*) **R** = 4-NO<sub>2</sub>-Phenyl in CDCl<sub>3</sub>.



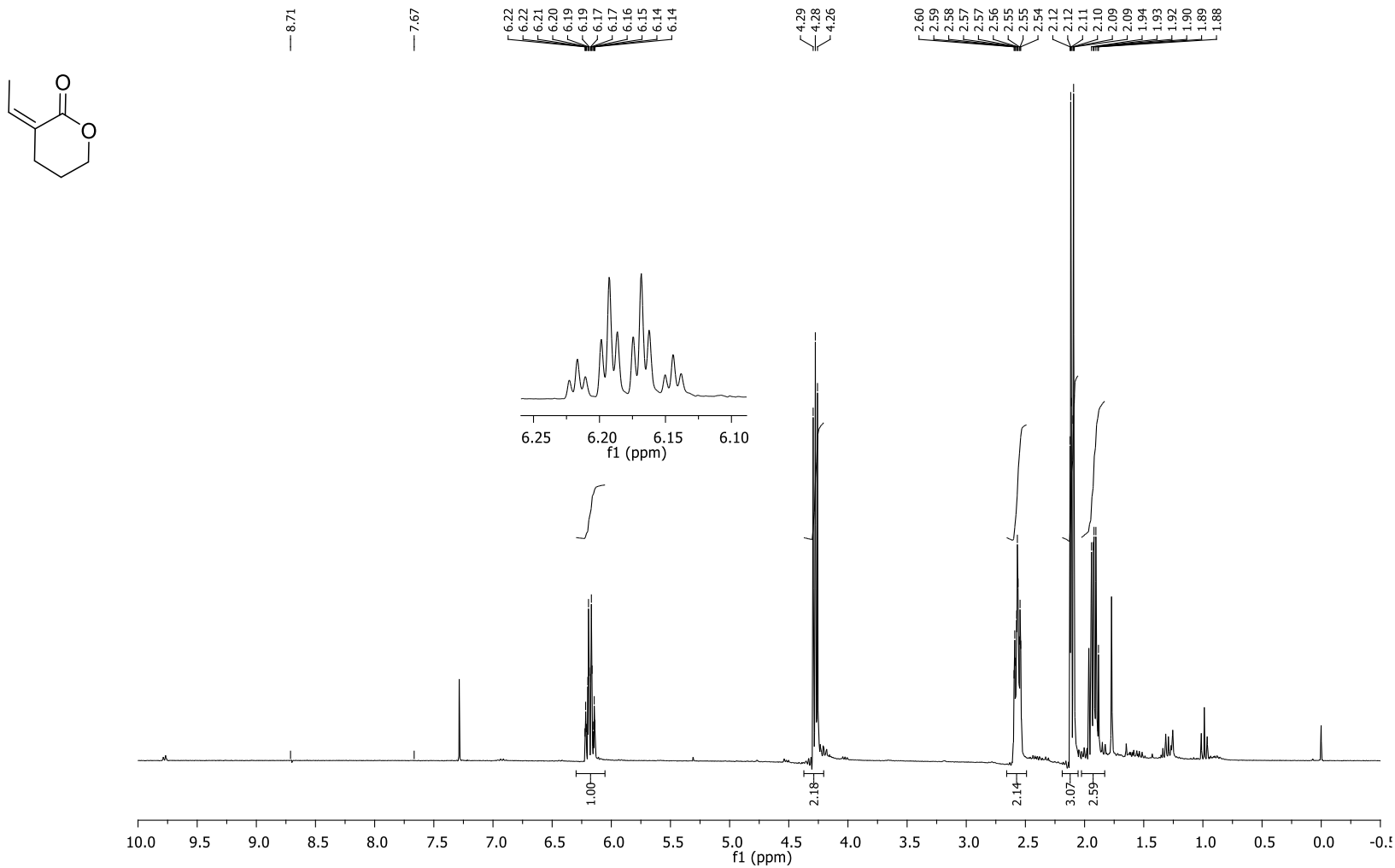
S2.21.  $^1\text{H}$  NMR (600 MHz) spectrum of **10E** in  $\text{CDCl}_3$ .



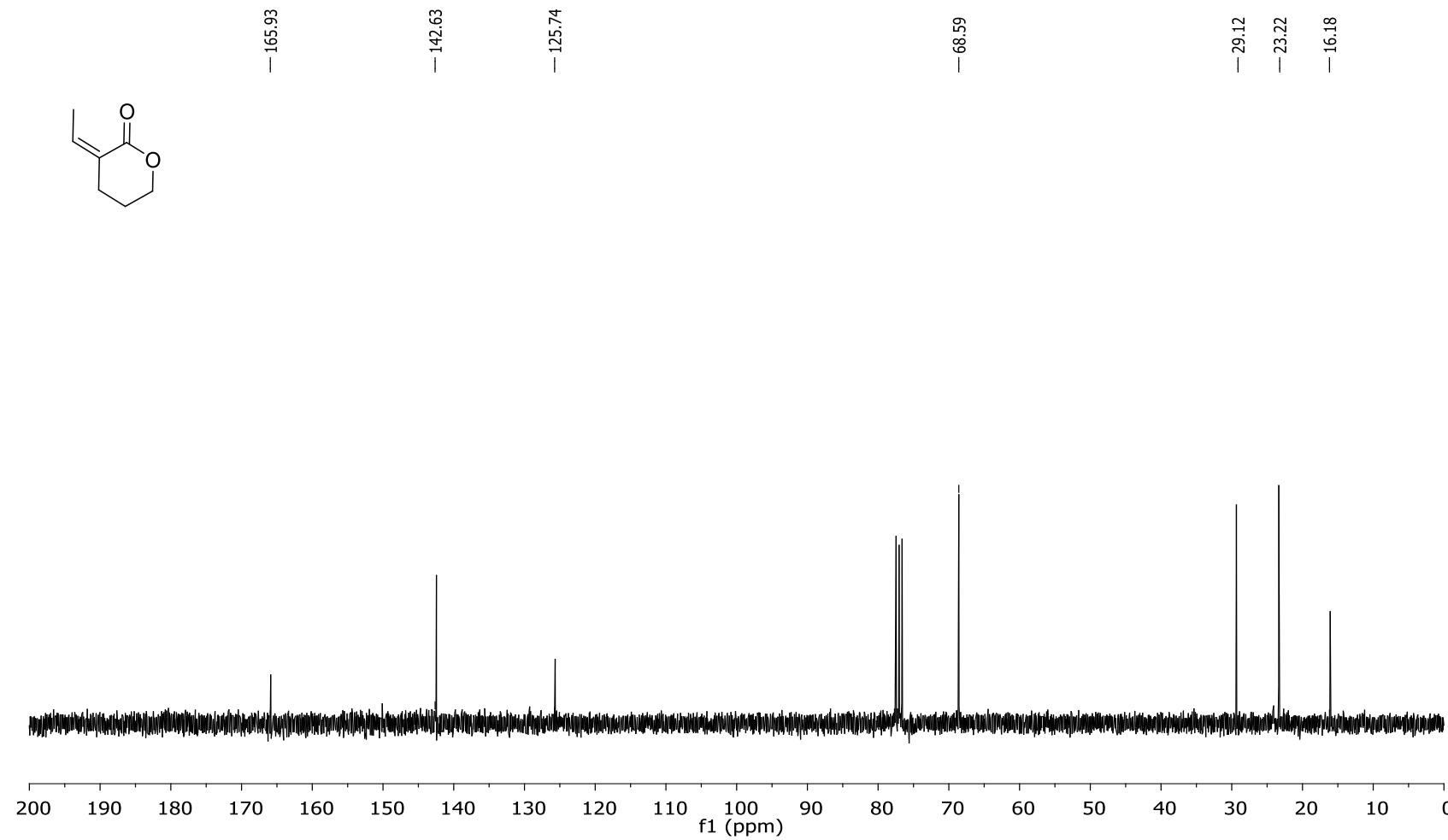
S2.22.  $^{13}\text{C}$  NMR (151 MHz) spectrum of **10E** in  $\text{CDCl}_3$ .



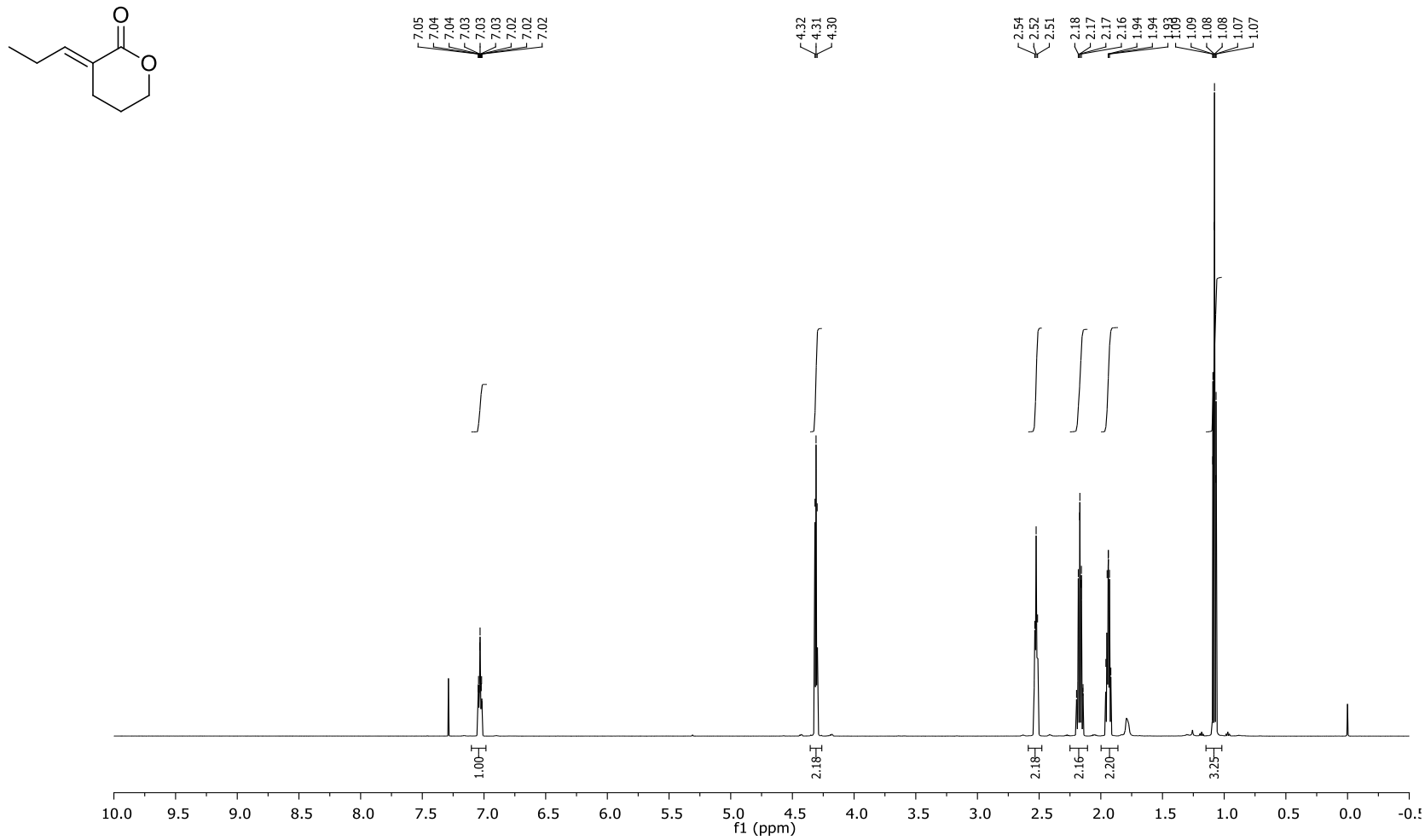
S2.23.  $^1\text{H}$  NMR (300 MHz) spectrum of **10Z** in  $\text{CDCl}_3$ .



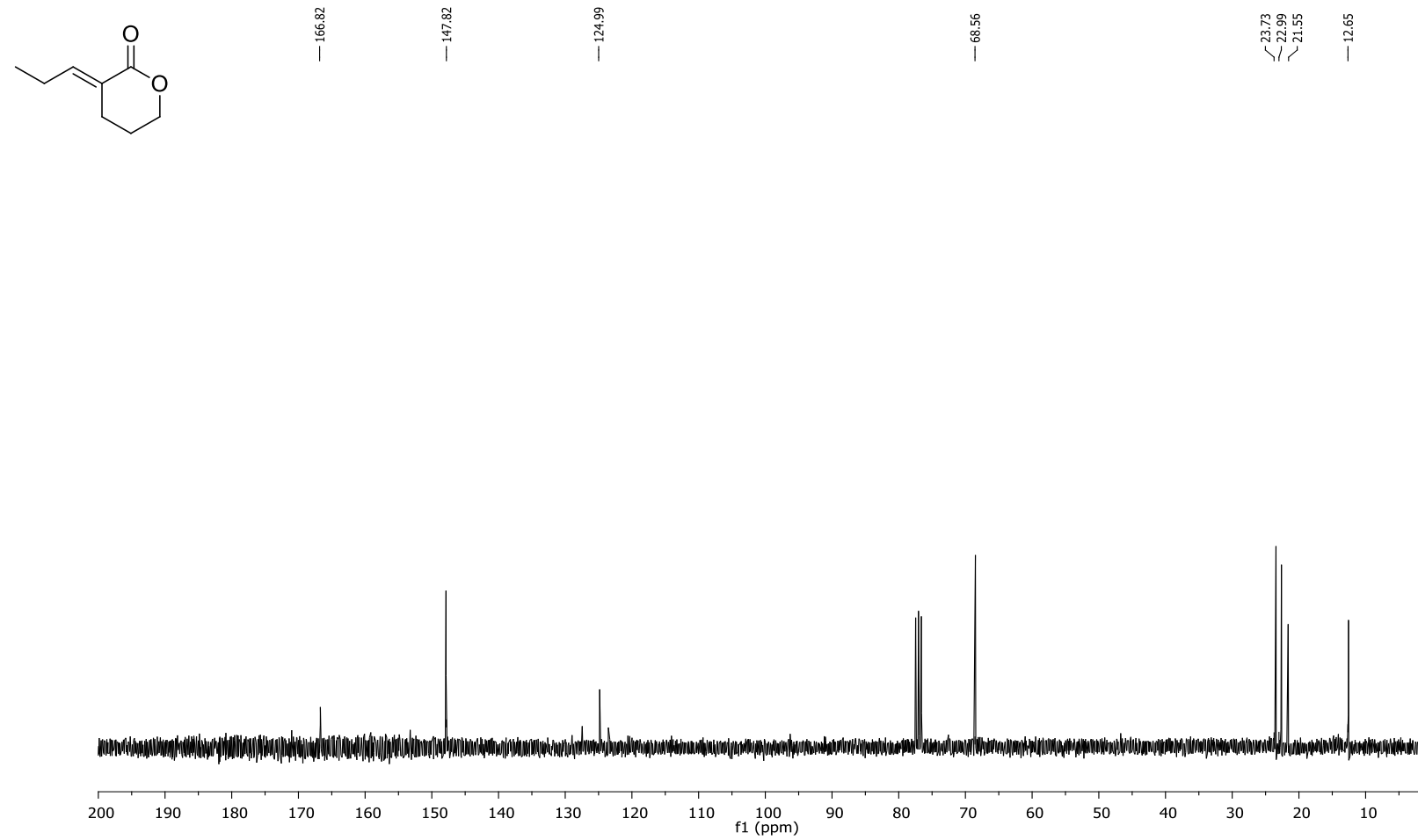
S2.24.  $^{13}\text{C}$  NMR (75 MHz) spectrum of **10Z** in  $\text{CDCl}_3$ .



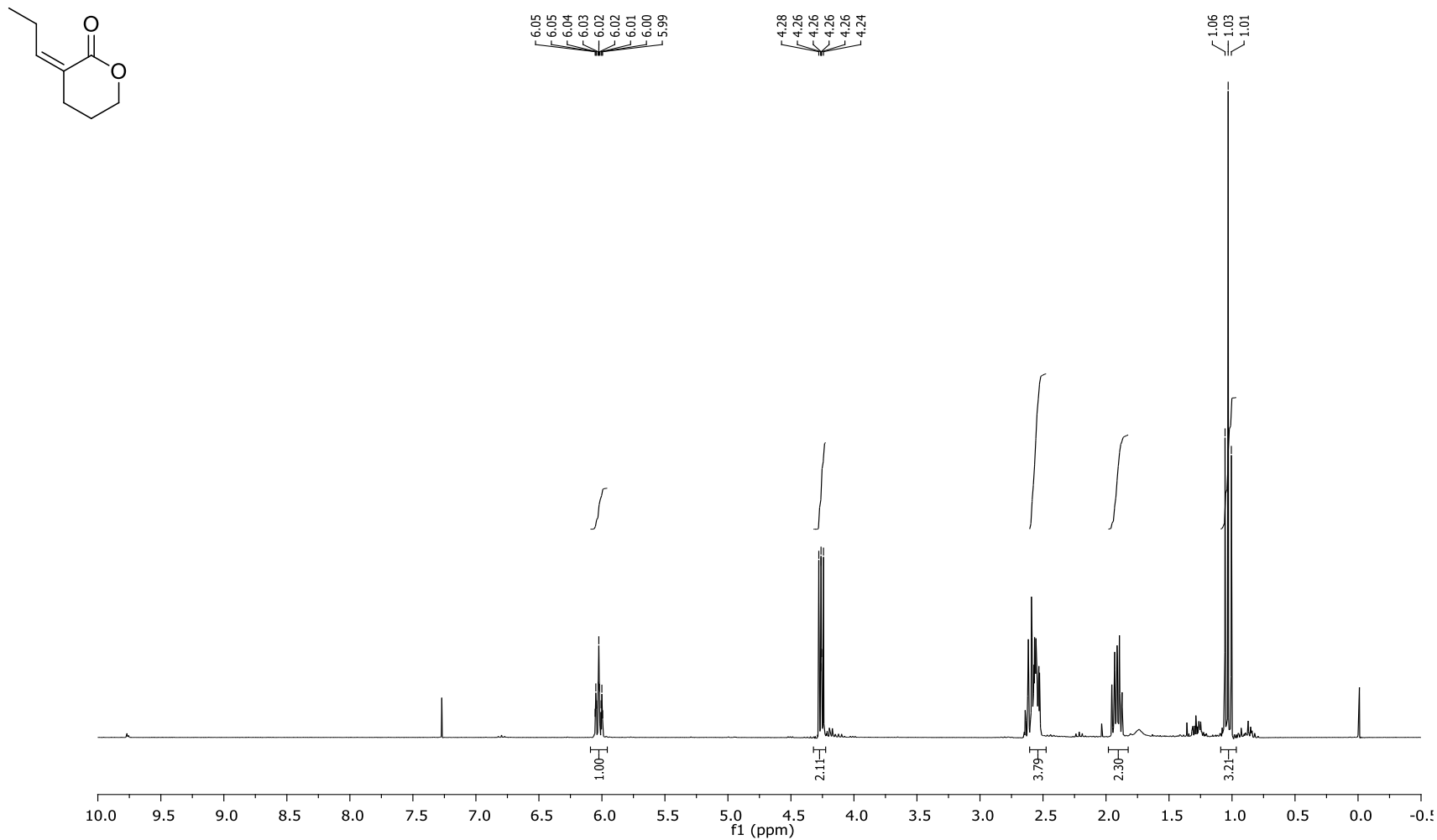
S2.25.  $^1\text{H}$  NMR (600 MHz) spectrum of **11E** in  $\text{CDCl}_3$ .



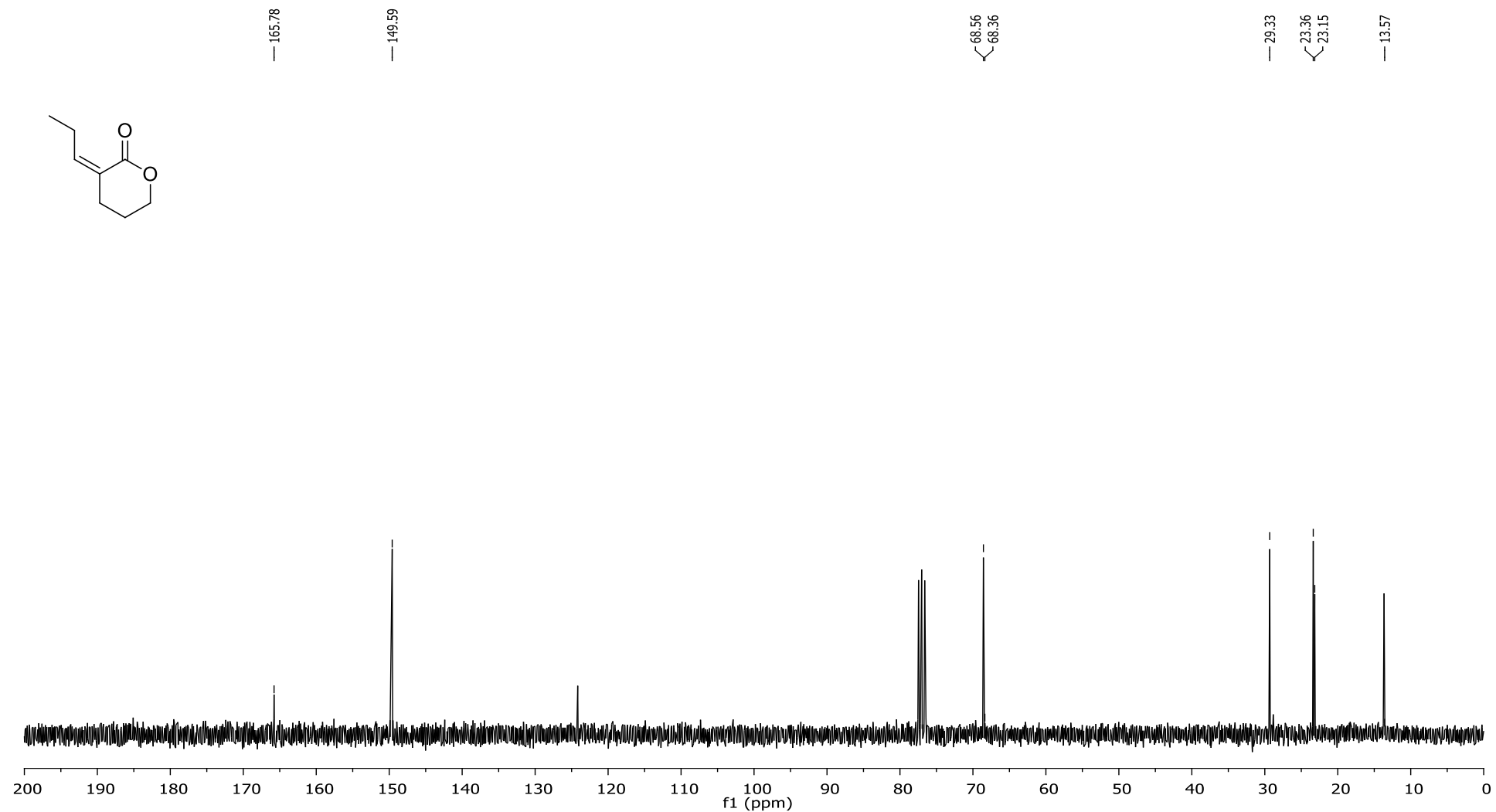
S2.26.  $^{13}\text{C}$  NMR (75 MHz) spectrum of **11E** in  $\text{CDCl}_3$ .



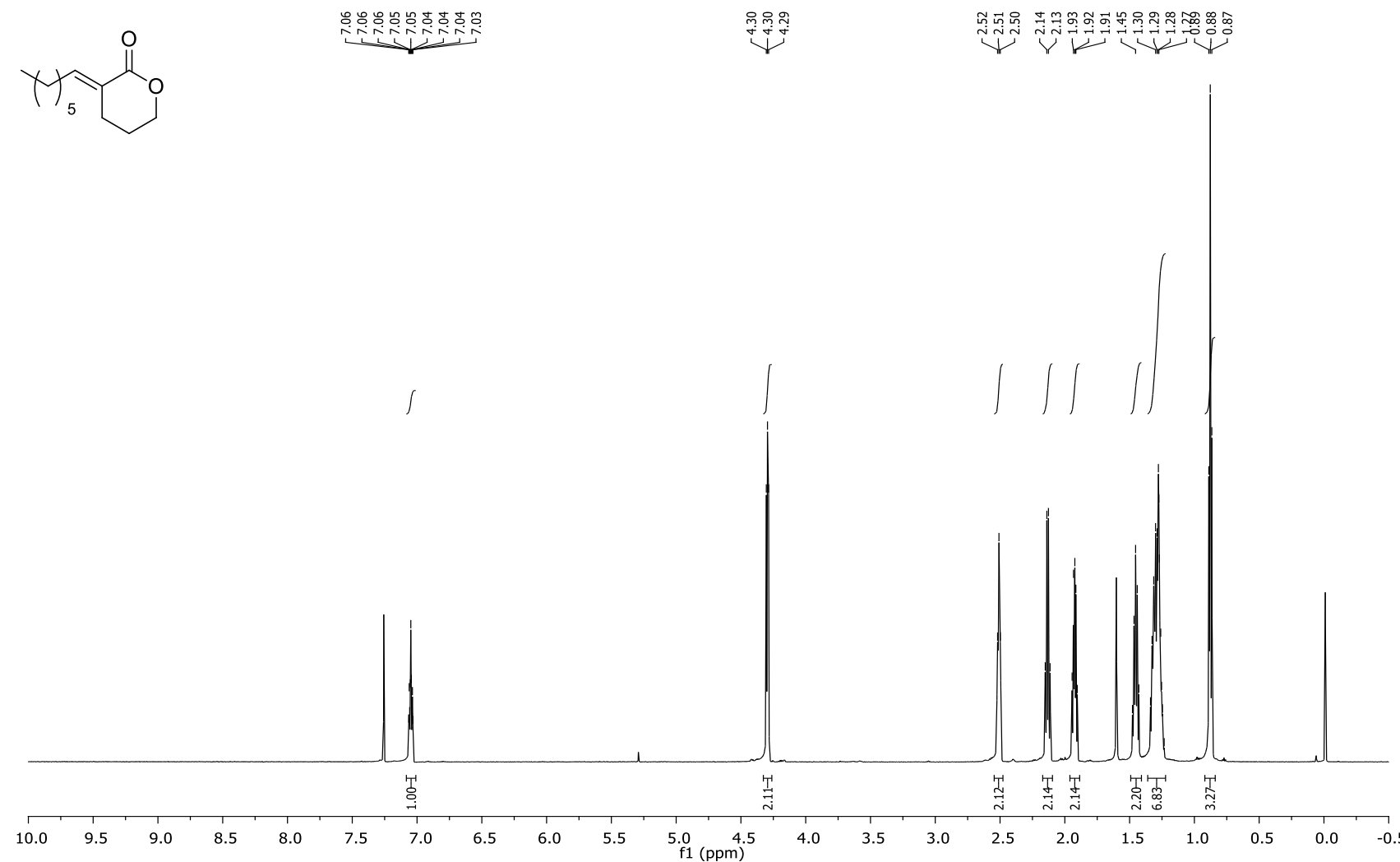
S2.27.  $^1\text{H}$  NMR (300 MHz) spectrum of **11Z** in  $\text{CDCl}_3$ .



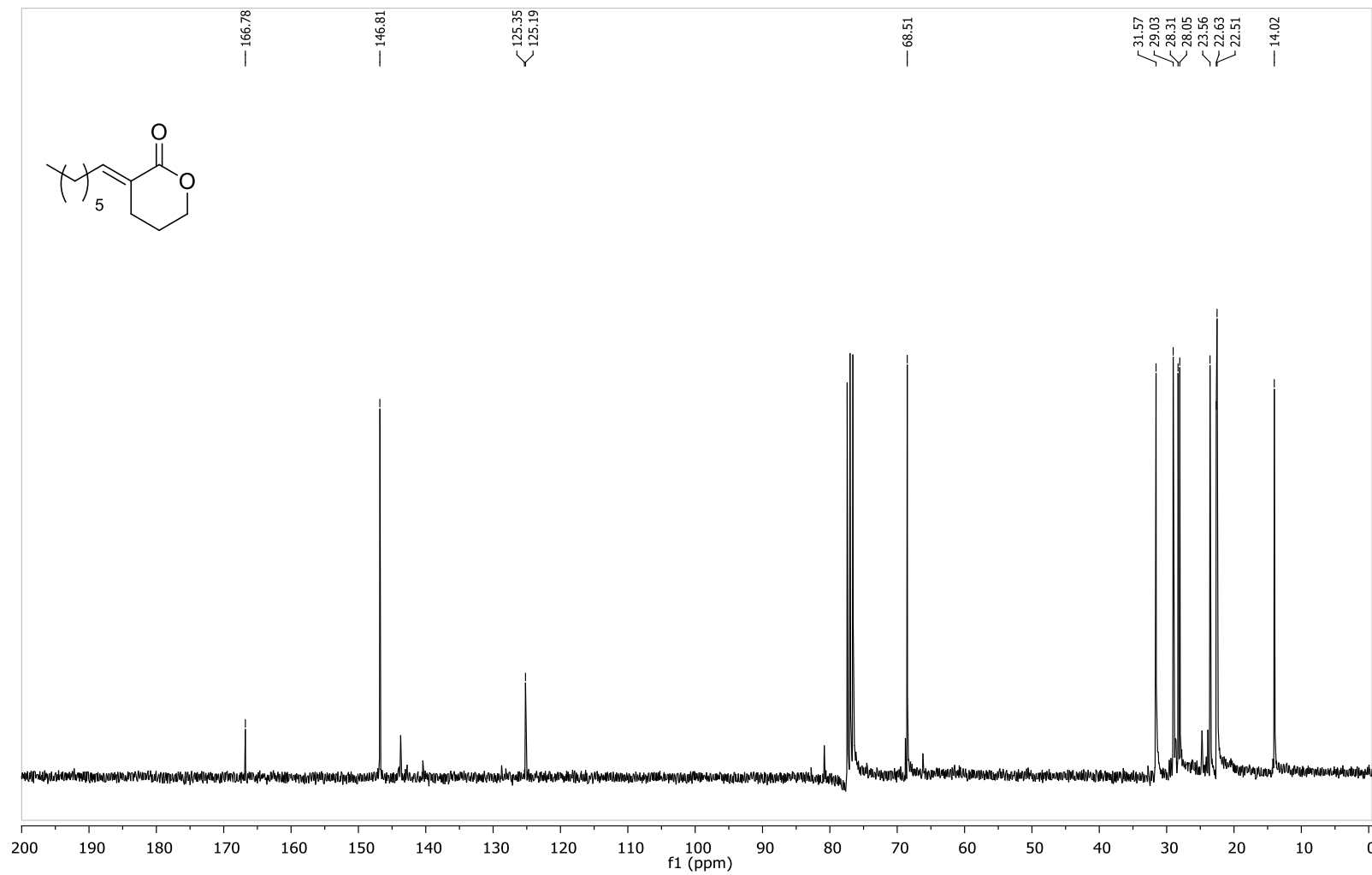
S2.28.  $^{13}\text{C}$  NMR (75 MHz) spectrum of **11Z** in  $\text{CDCl}_3$ .



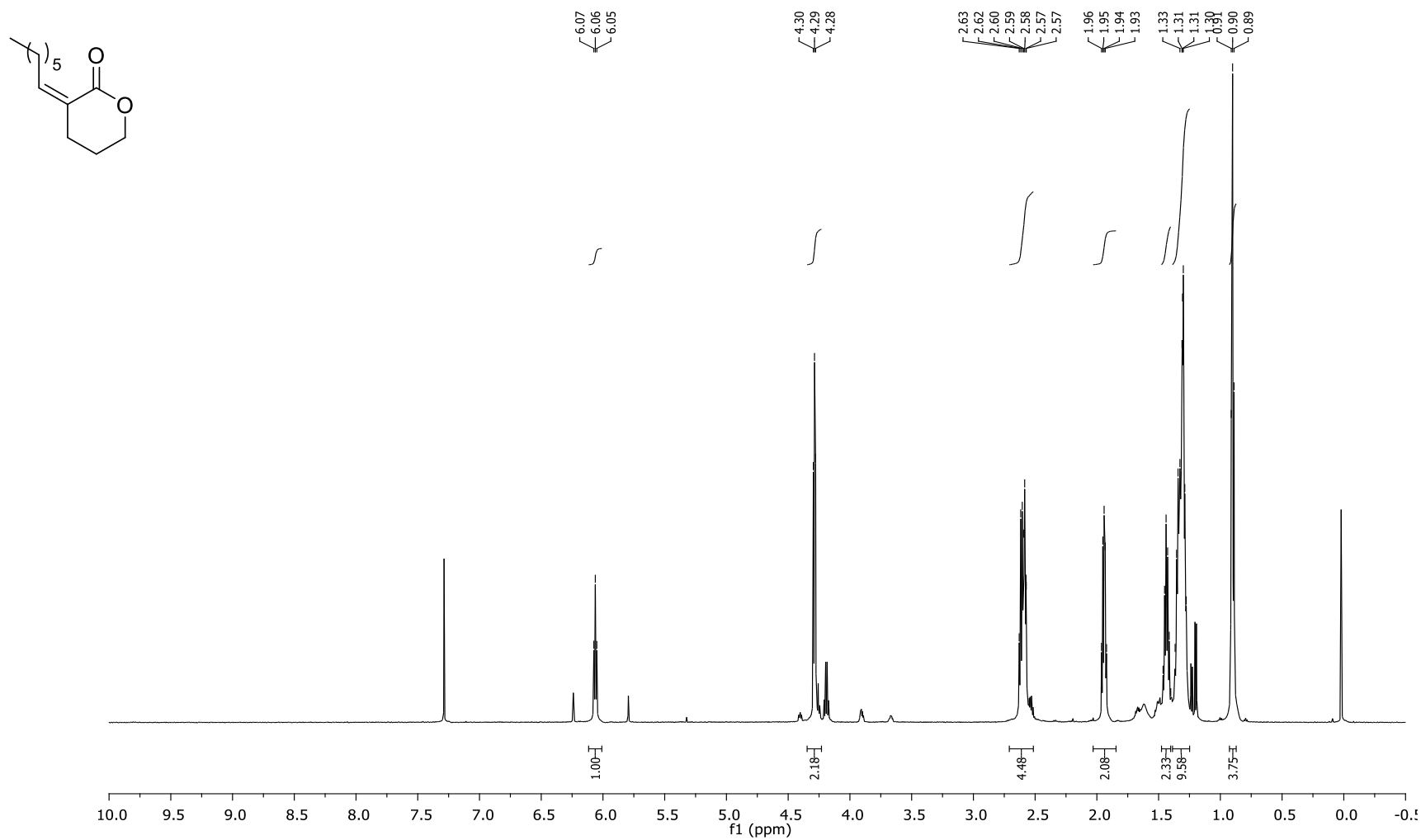
S2.29.  $^1\text{H}$  NMR (600 MHz) spectrum of **12E** in  $\text{CDCl}_3$ .



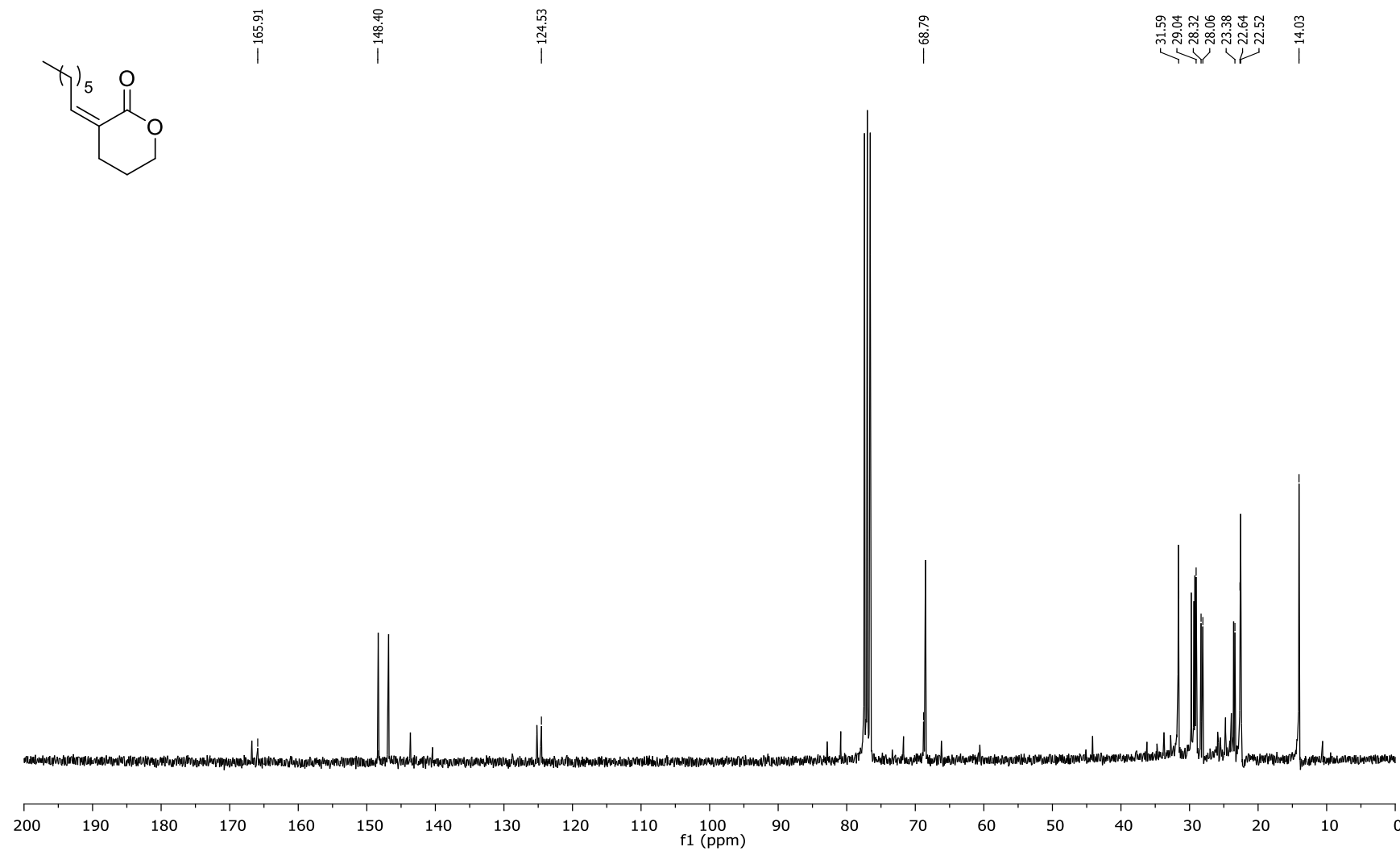
S2.30.  $^{13}\text{C}$  NMR (75 MHz) spectrum of **12E** in  $\text{CDCl}_3$ .



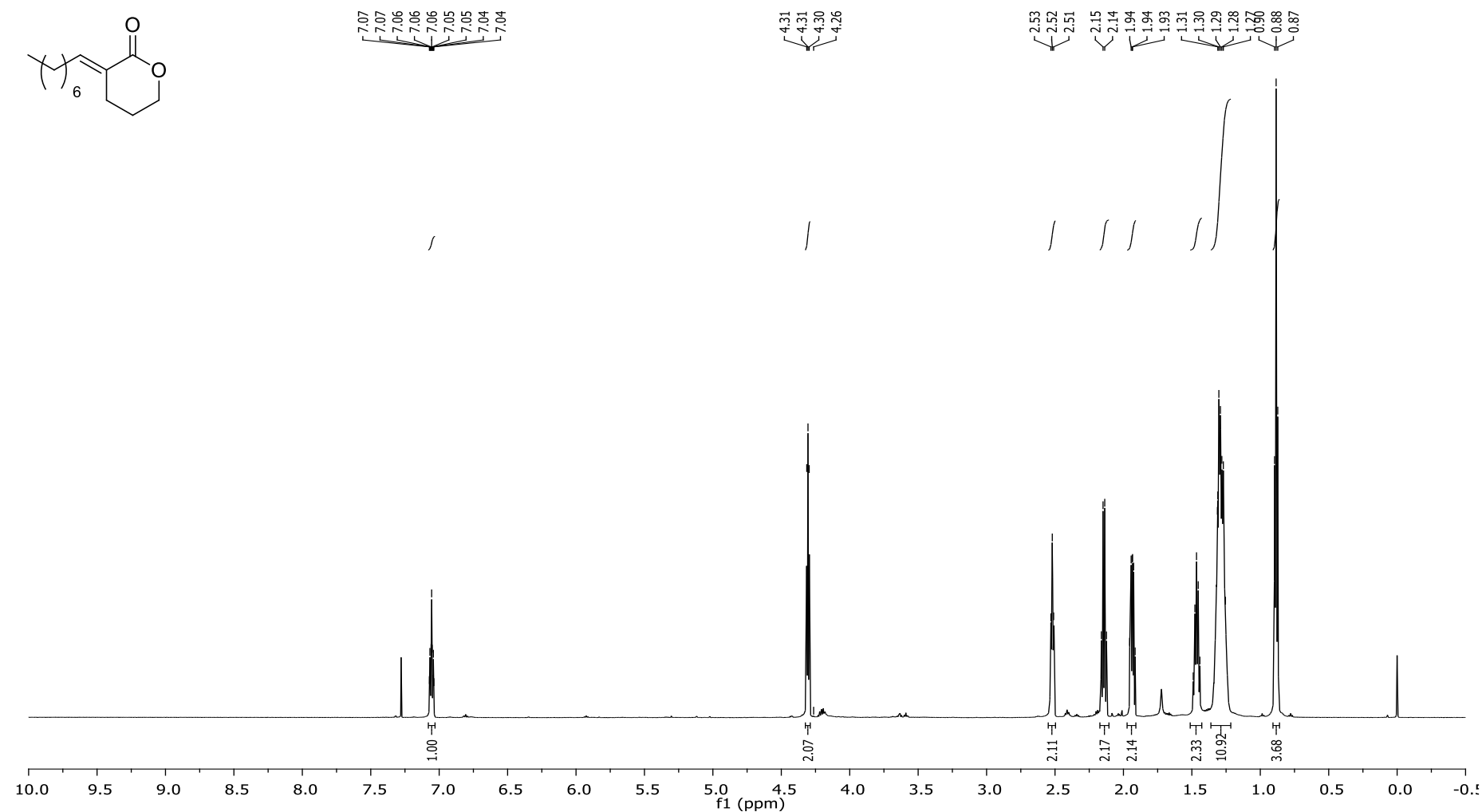
S2.31.  $^1\text{H}$  NMR (600 MHz) spectrum of **12Z** in  $\text{CDCl}_3$ .



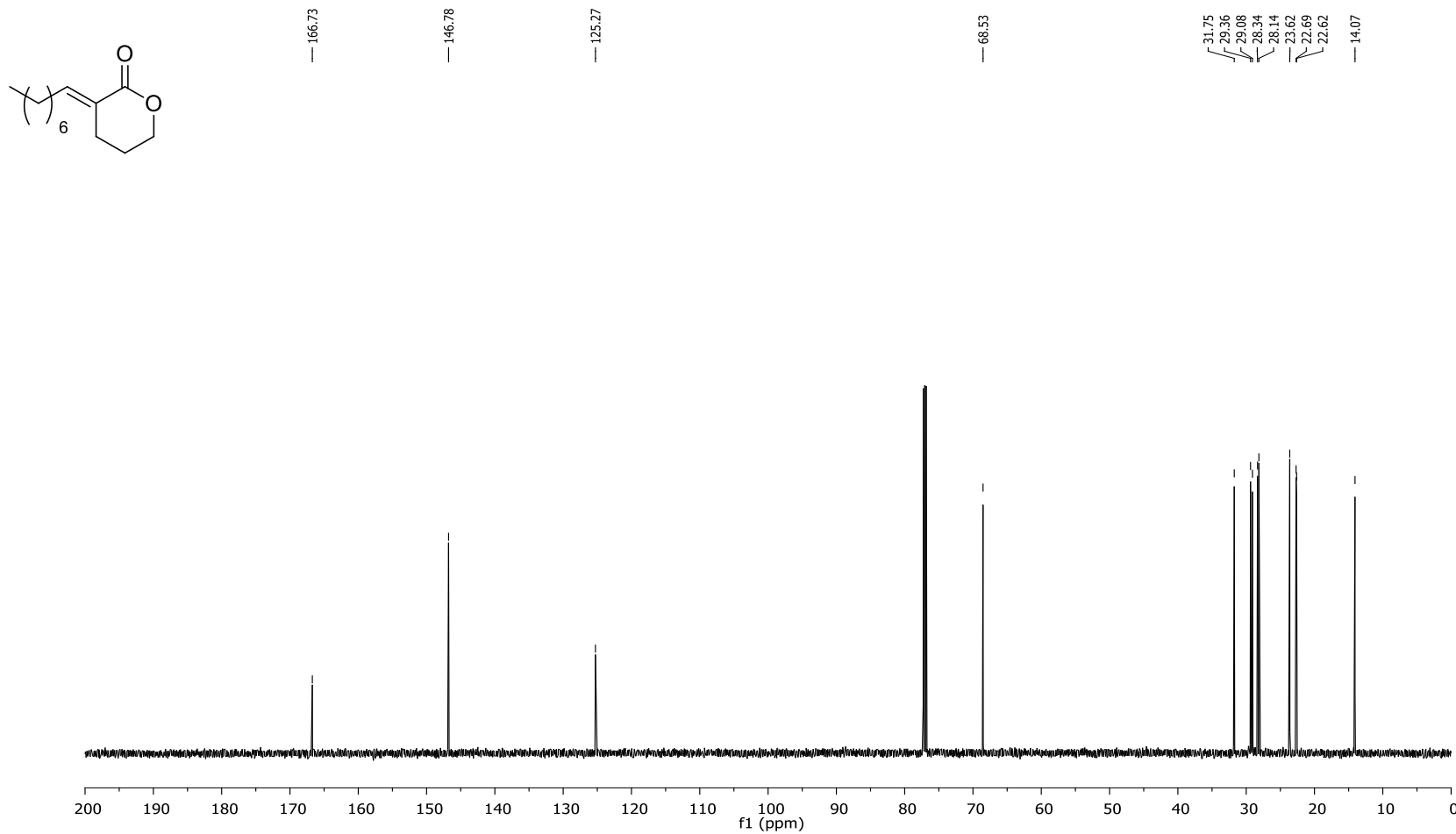
S2.32.  $^{13}\text{C}$  NMR (75 MHz) spectrum of **12Z** in  $\text{CDCl}_3$ .



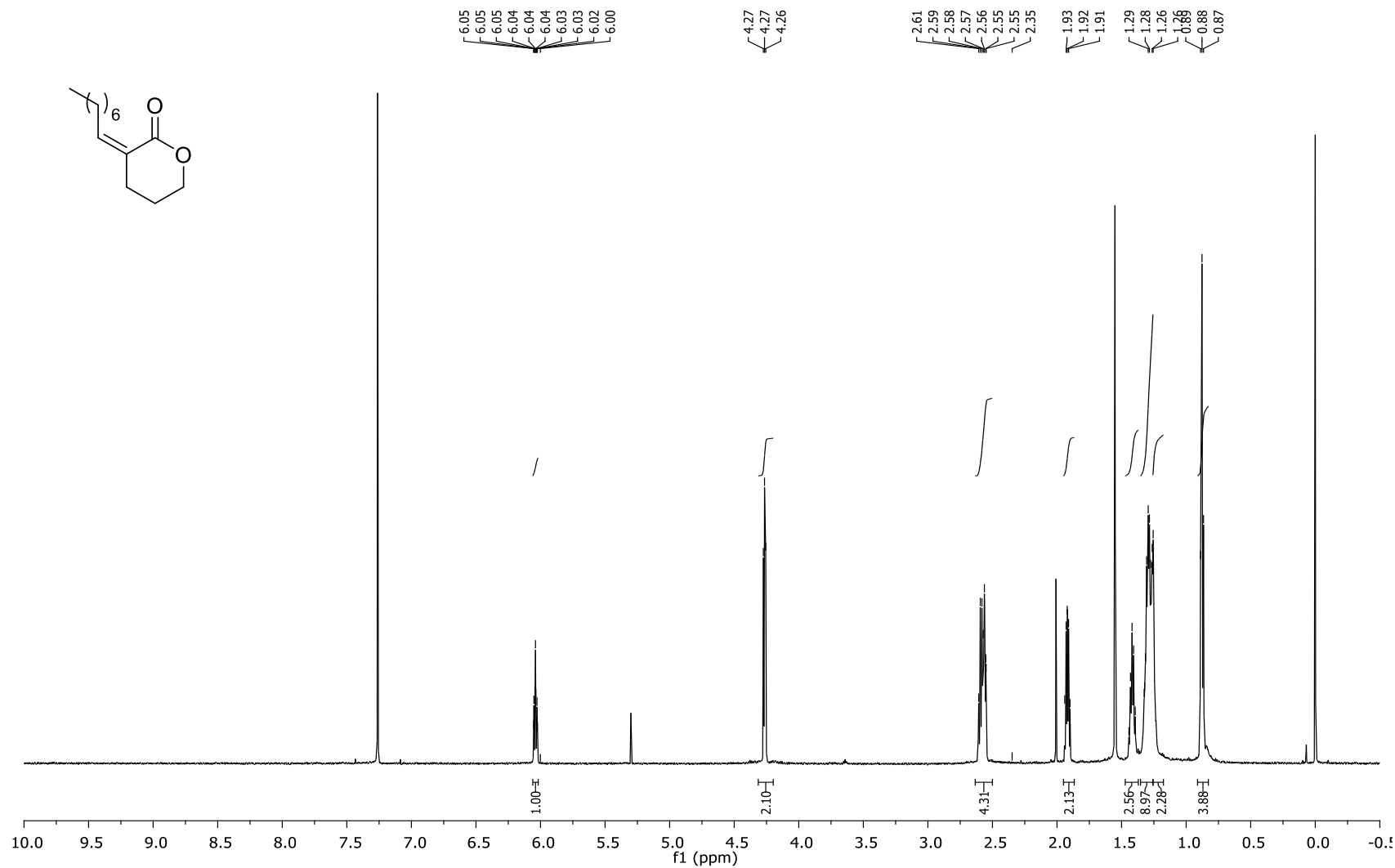
S2.33.  $^1\text{H}$  NMR (600 MHz) spectrum of **13E** in  $\text{CDCl}_3$ .



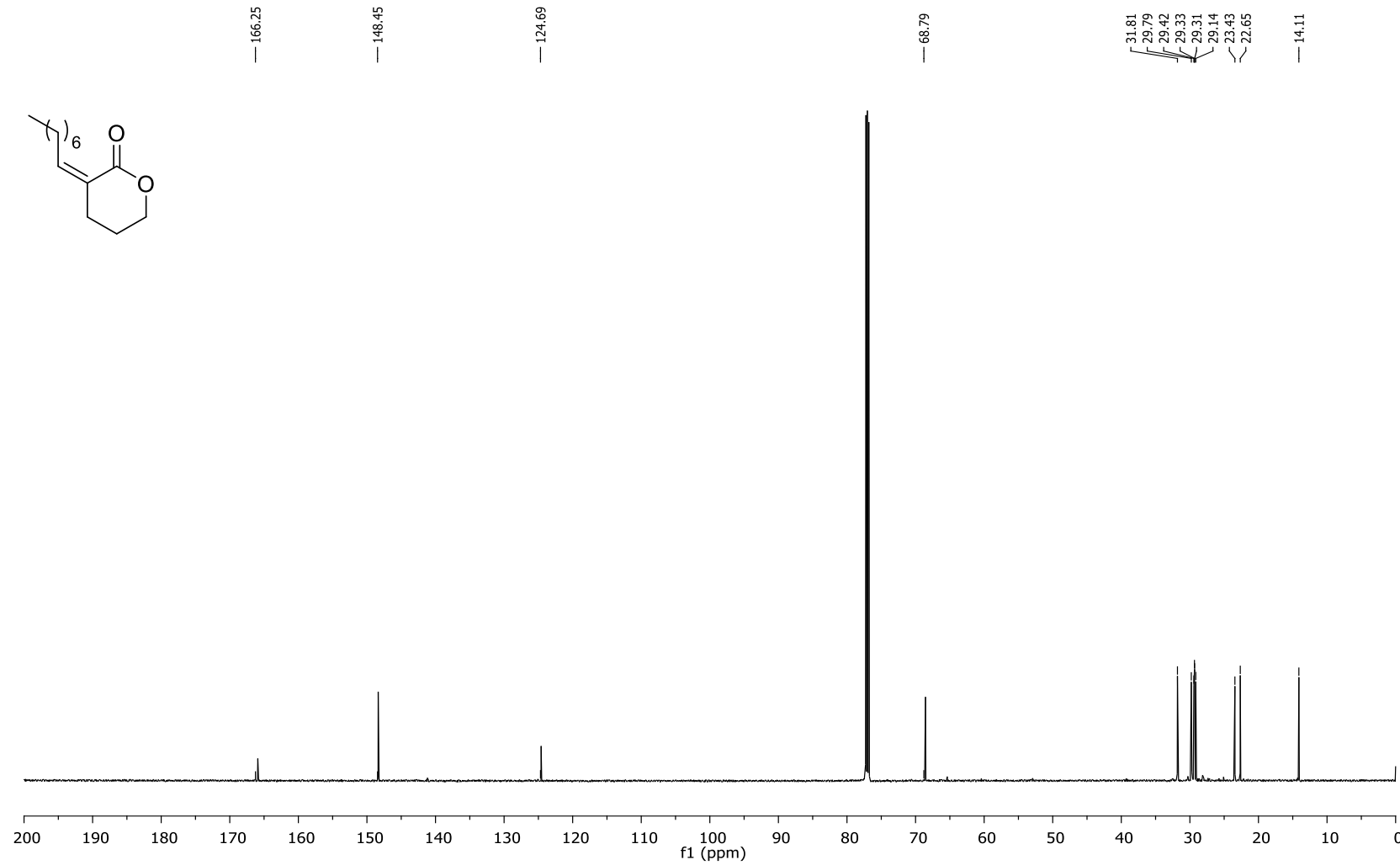
S2.34.  $^{13}\text{C}$  NMR (151 MHz) spectrum of **13E** in  $\text{CDCl}_3$ .



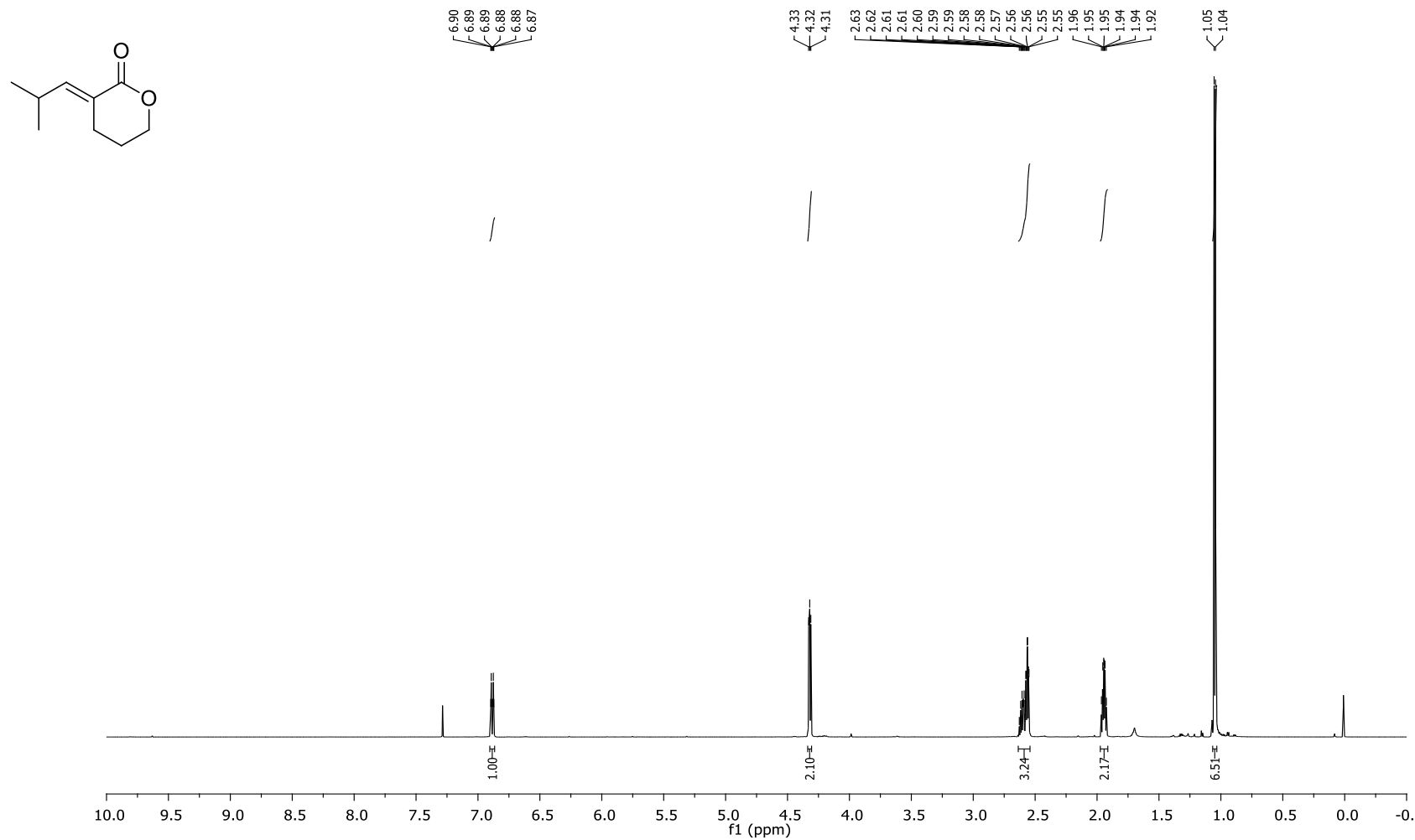
S2.35.  $^1\text{H}$  NMR (600 MHz) spectrum of **13Z** in  $\text{CDCl}_3$ .



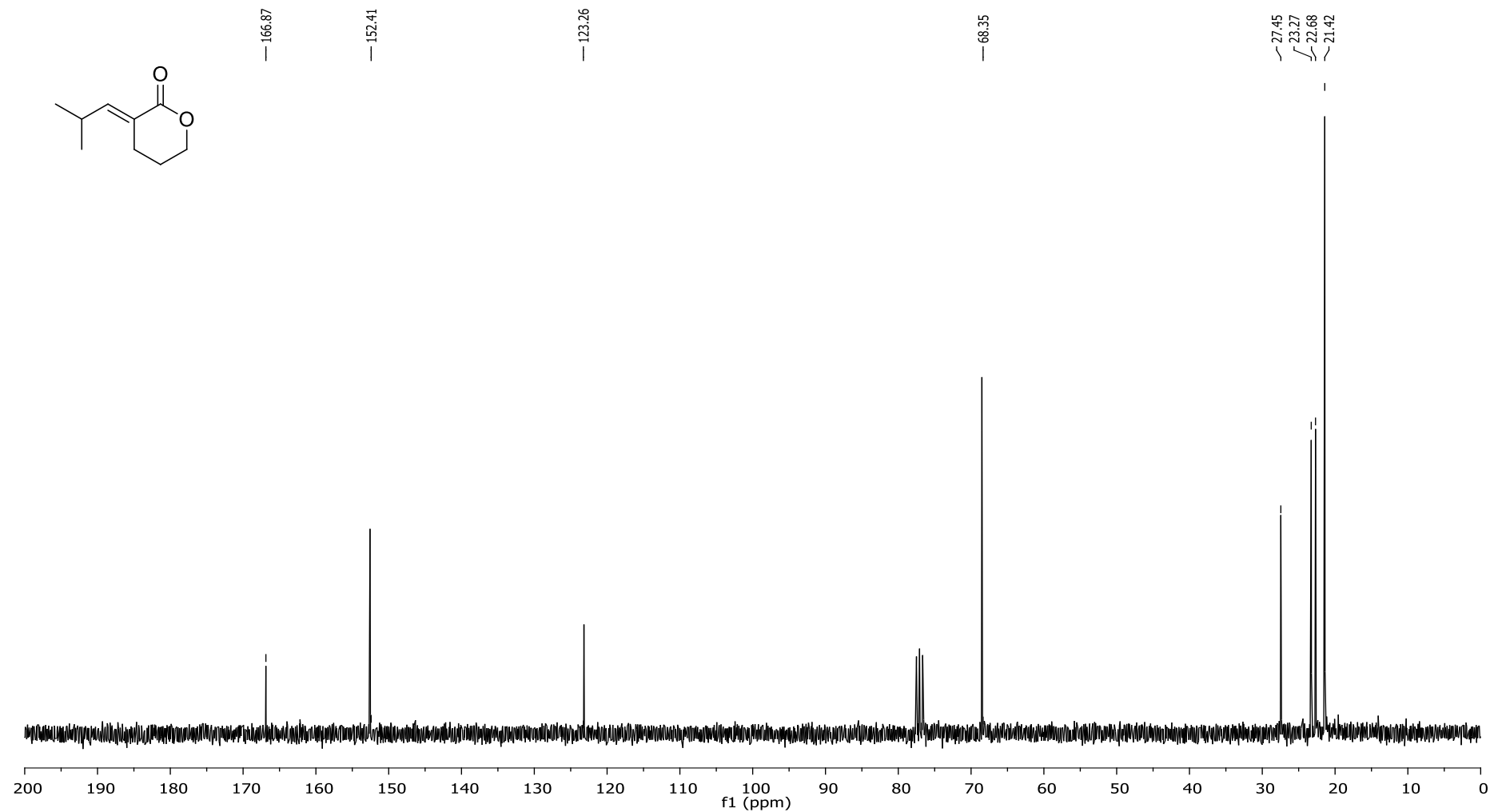
S2.36.  $^{13}\text{C}$  NMR (151 MHz) spectrum of **13Z** in  $\text{CDCl}_3$ .



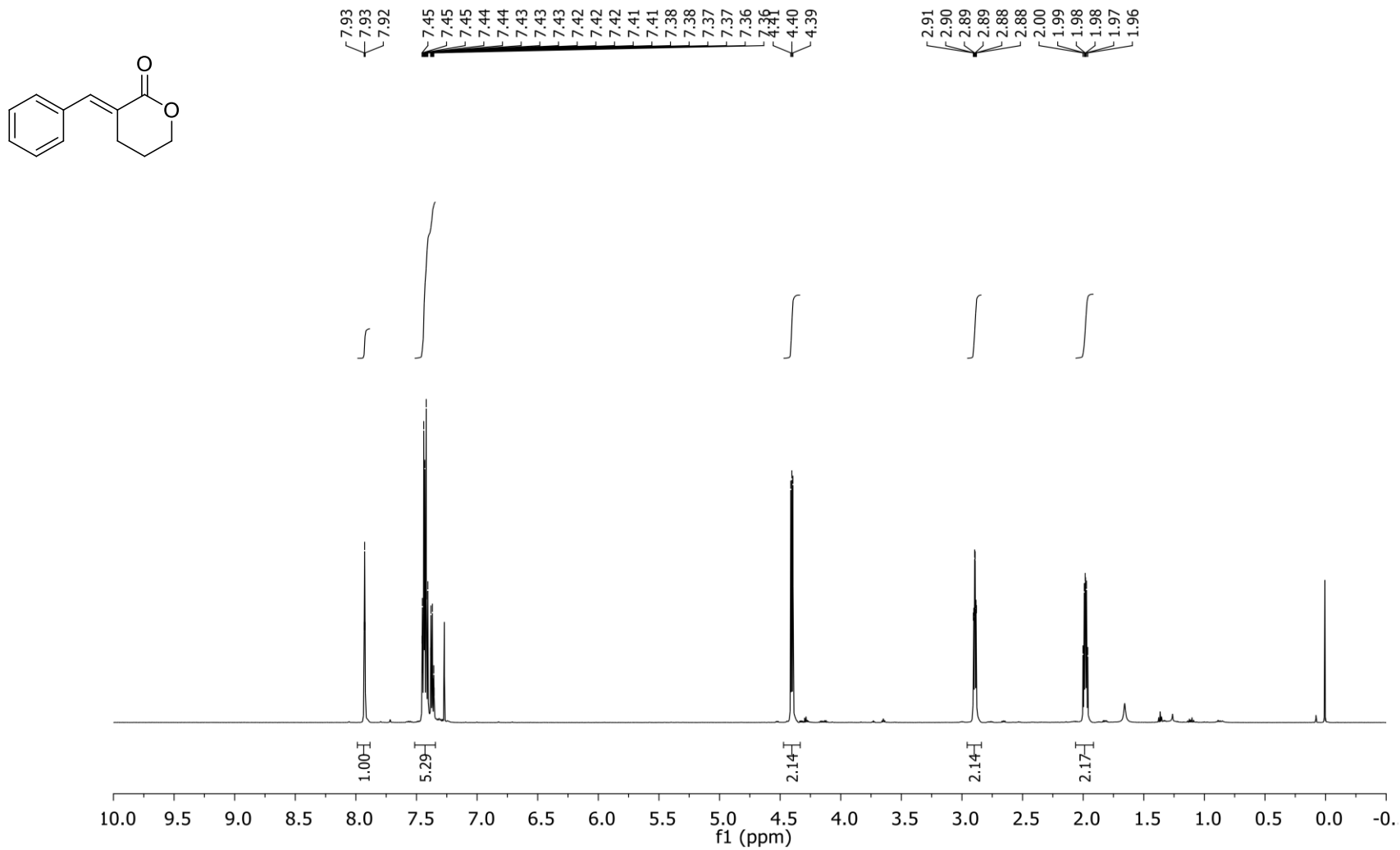
S2.37.  $^1\text{H}$  NMR (600 MHz) spectrum of **14E** in  $\text{CDCl}_3$ .



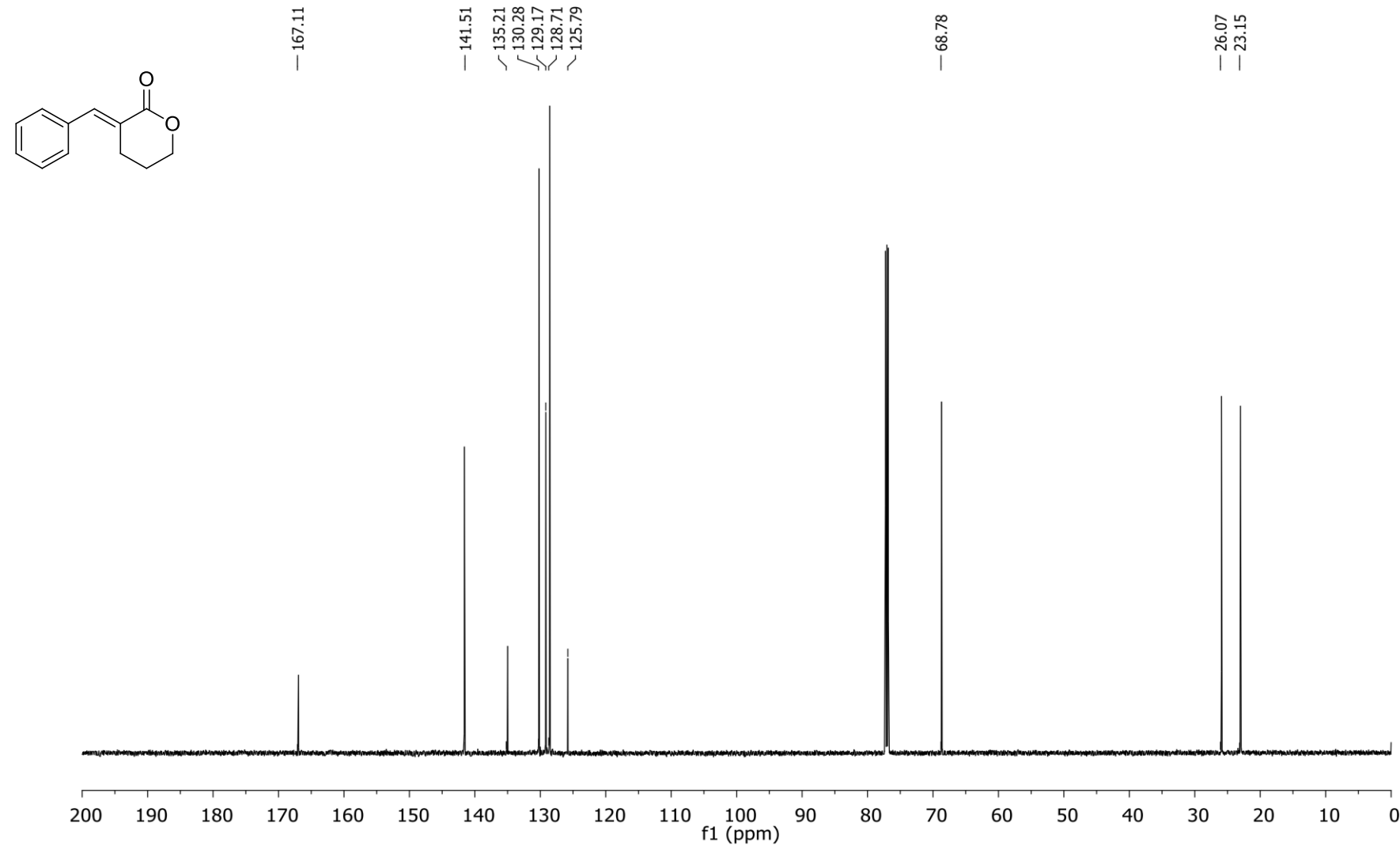
S2.38.  $^{13}\text{C}$  NMR (75 MHz) spectrum of **14E** in  $\text{CDCl}_3$ .



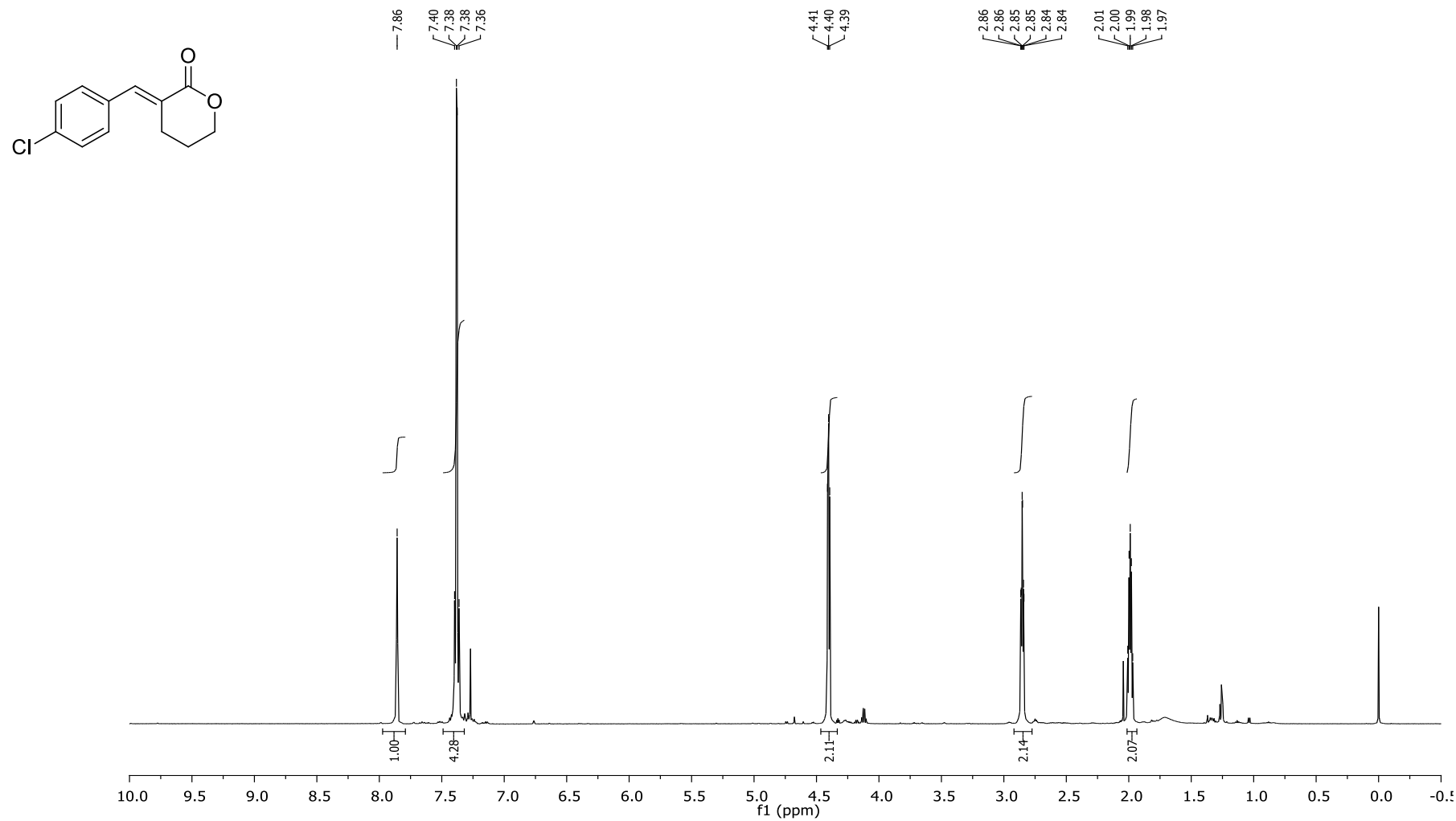
S2.39.  $^1\text{H}$  NMR (600 MHz) spectrum of **15E** in  $\text{CDCl}_3$ .



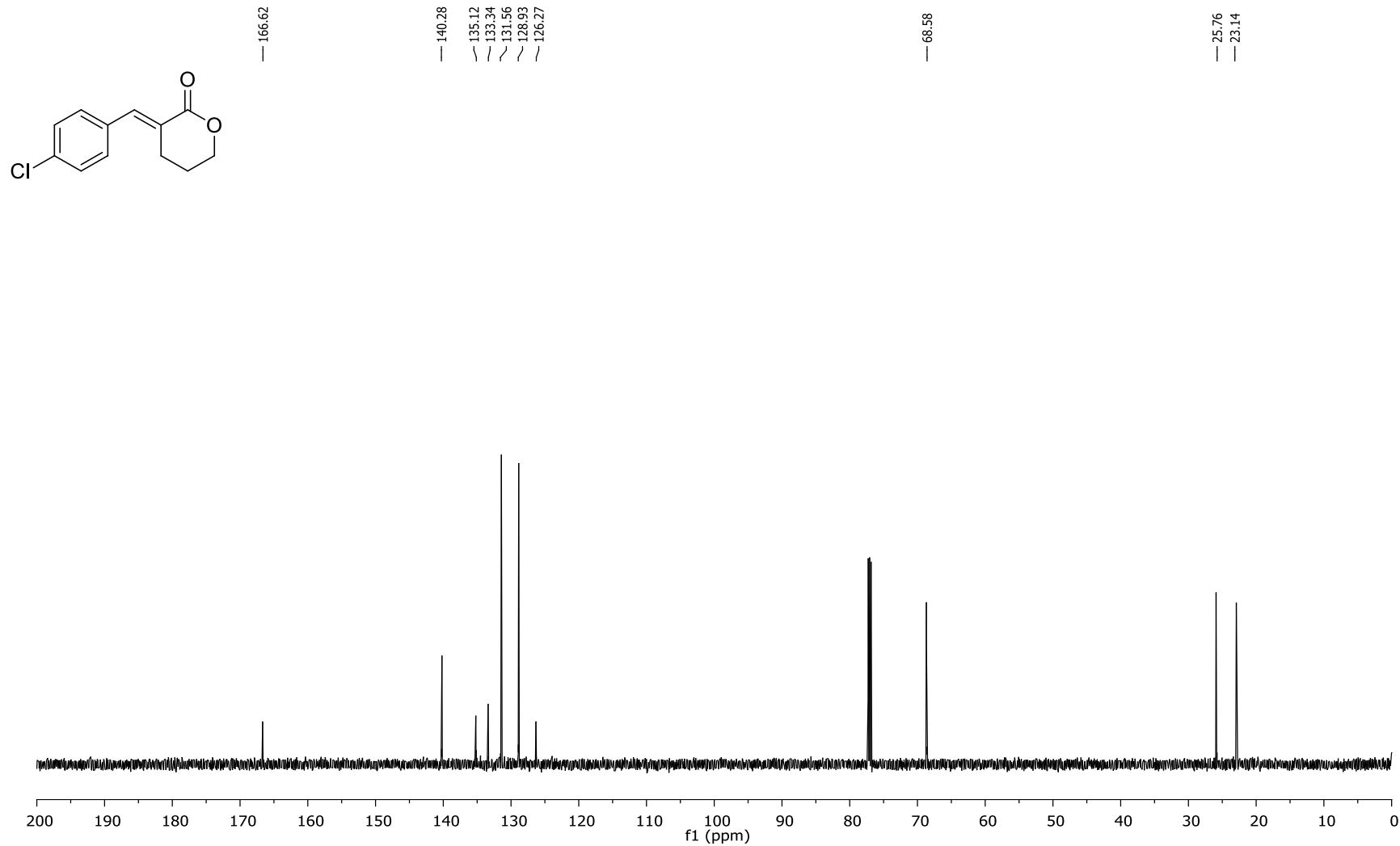
S2.40.  $^{13}\text{C}$  NMR (151 MHz) spectrum of **15E** in  $\text{CDCl}_3$ .



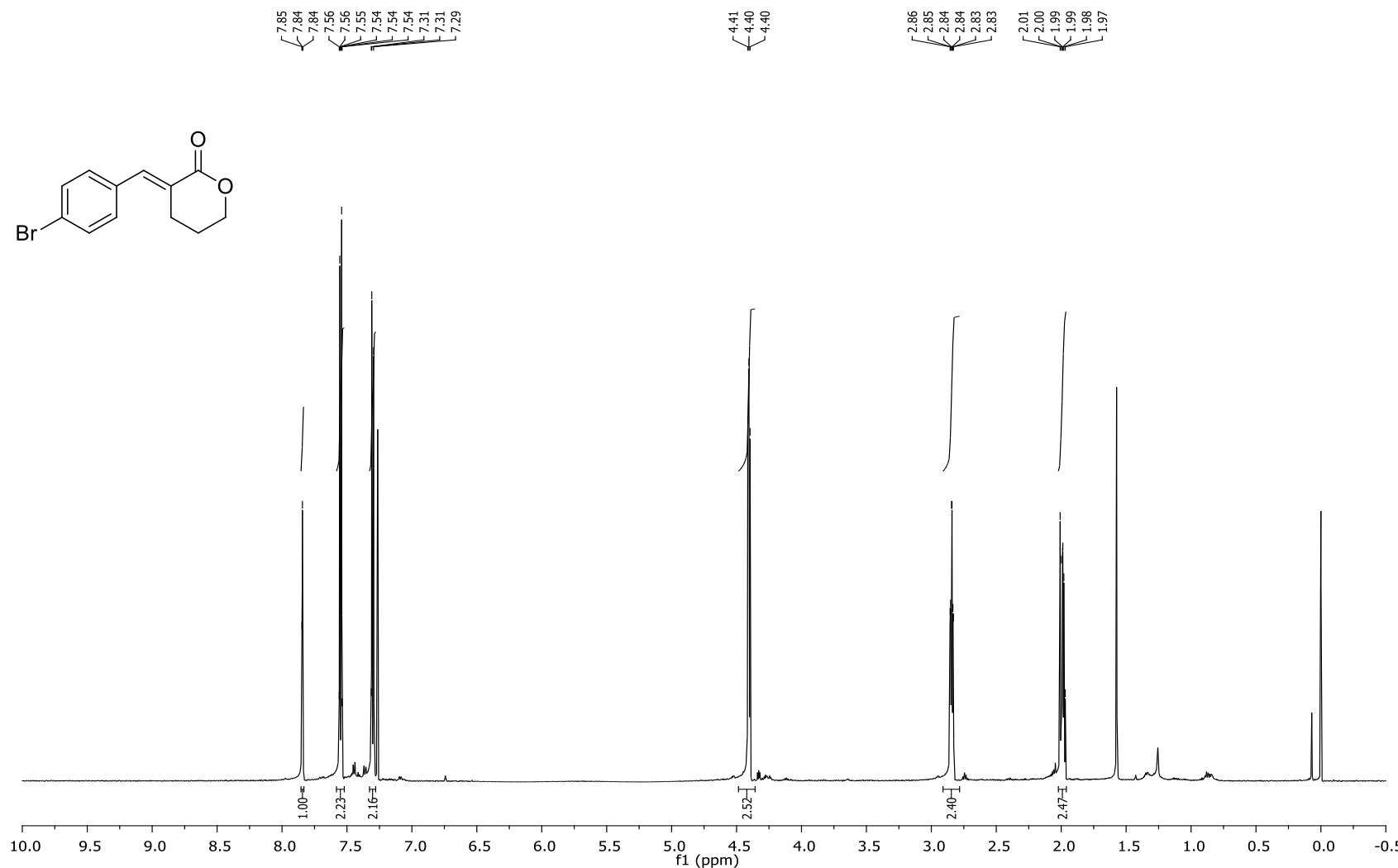
S2.41.  $^1\text{H}$  NMR (600 MHz) spectrum of **16E** in  $\text{CDCl}_3$  in  $\text{CDCl}_3$ .



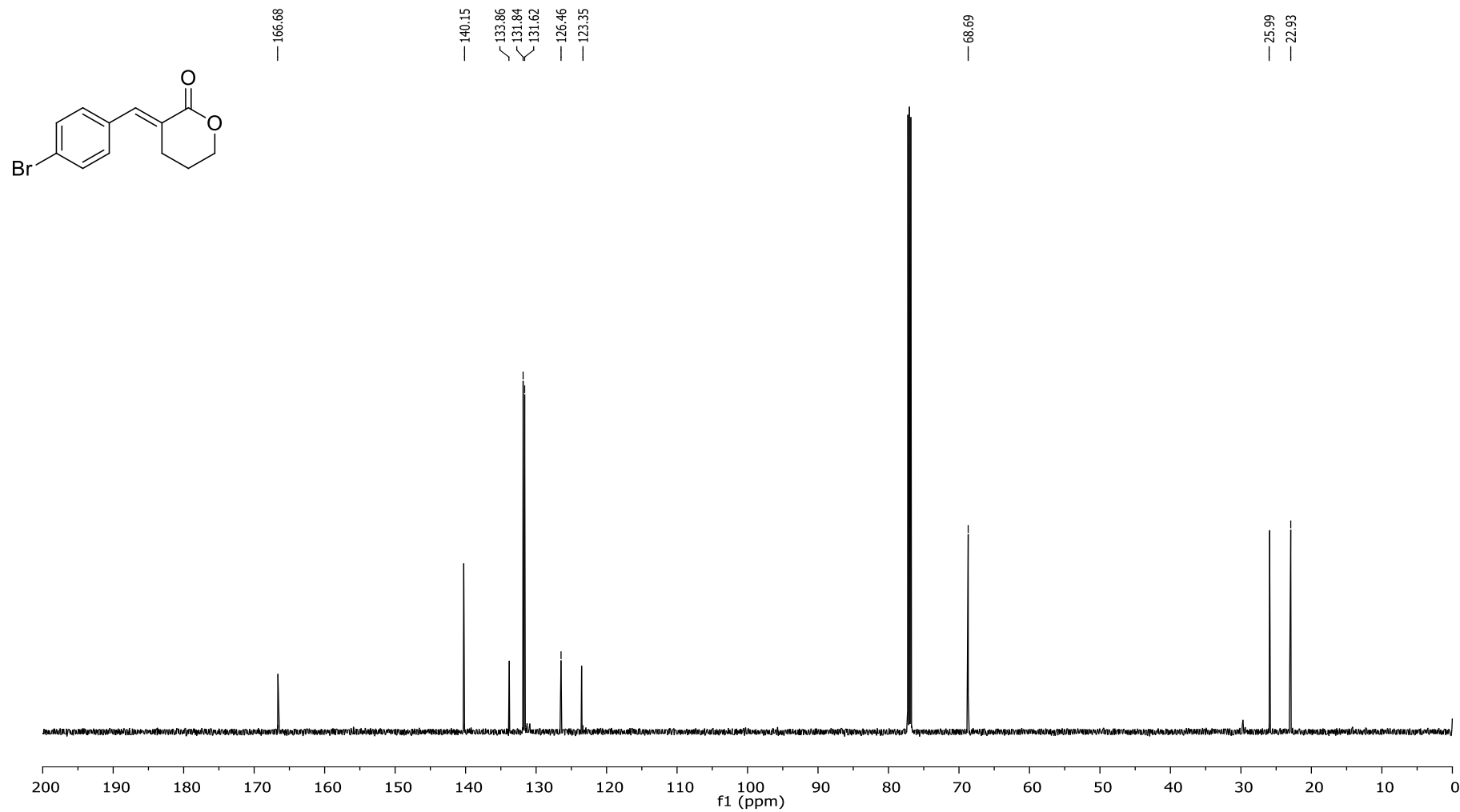
S2.42.  $^{13}\text{C}$  NMR (151 MHz) spectrum of **16E** in  $\text{CDCl}_3$ .



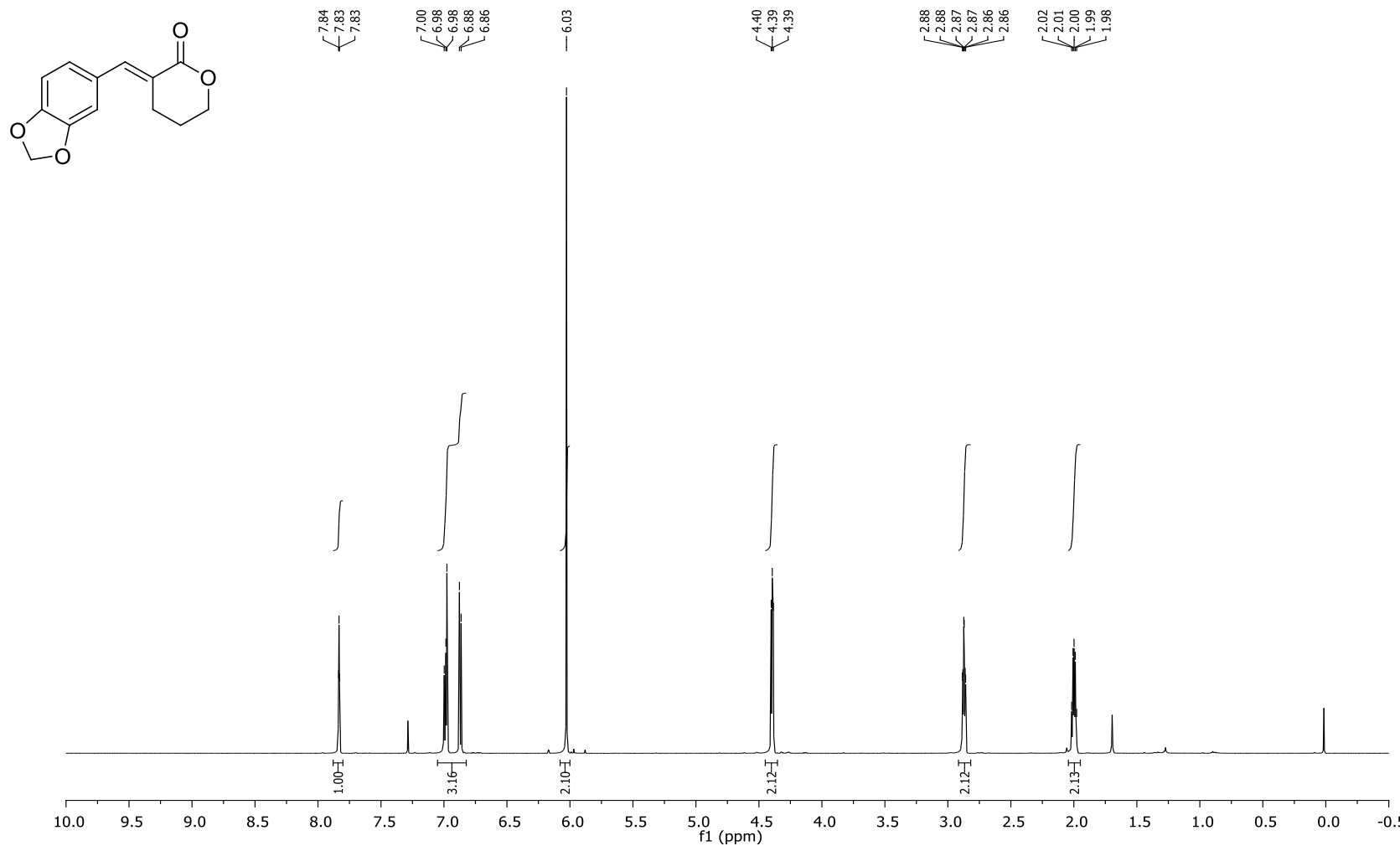
S2.43.  $^1\text{H}$  NMR (600 MHz) spectrum of **17E** in  $\text{CDCl}_3$  in  $\text{CDCl}_3$ .



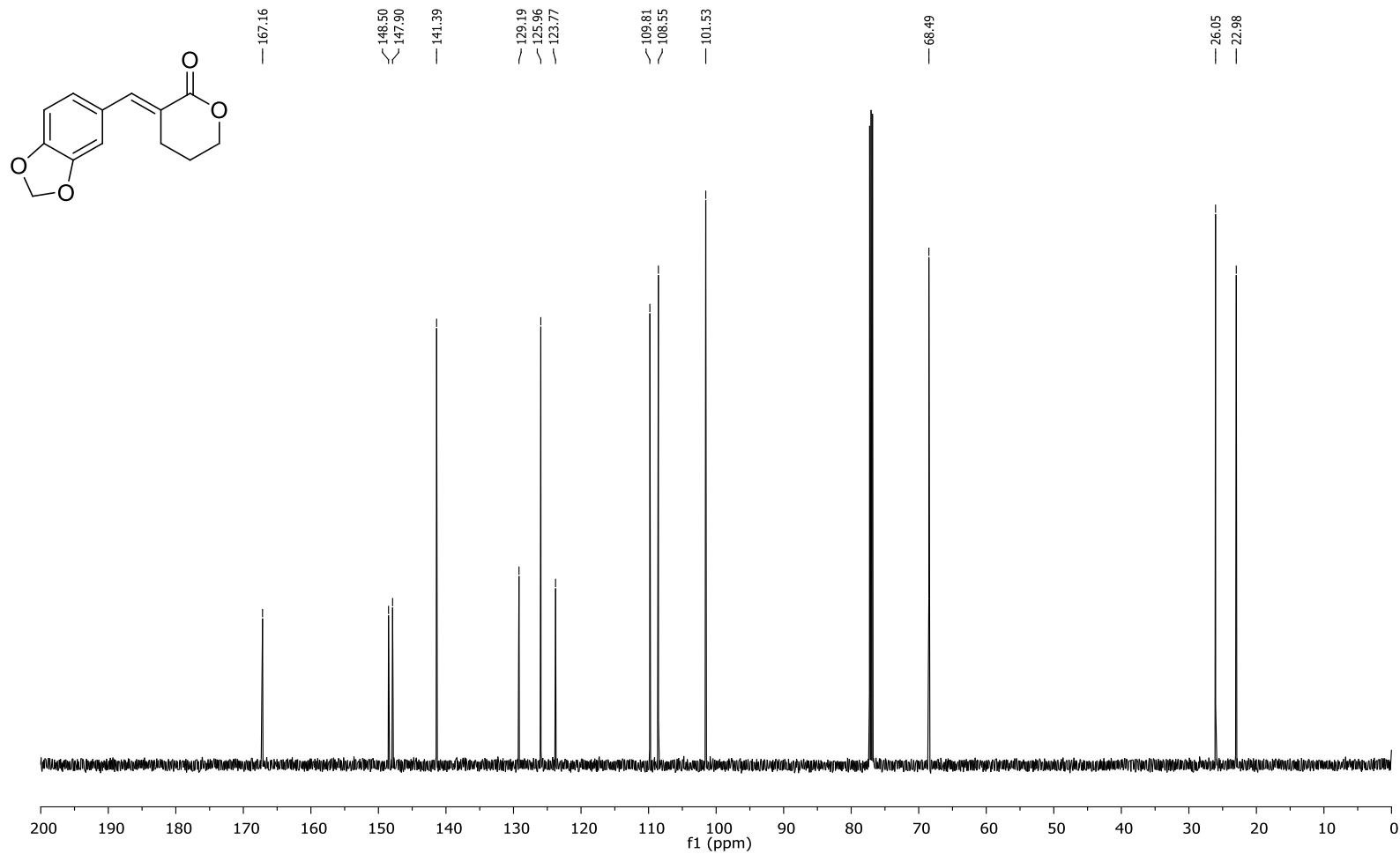
S2.44.  $^{13}\text{C}$  NMR (151 MHz) spectrum of **17E** in  $\text{CDCl}_3$ .



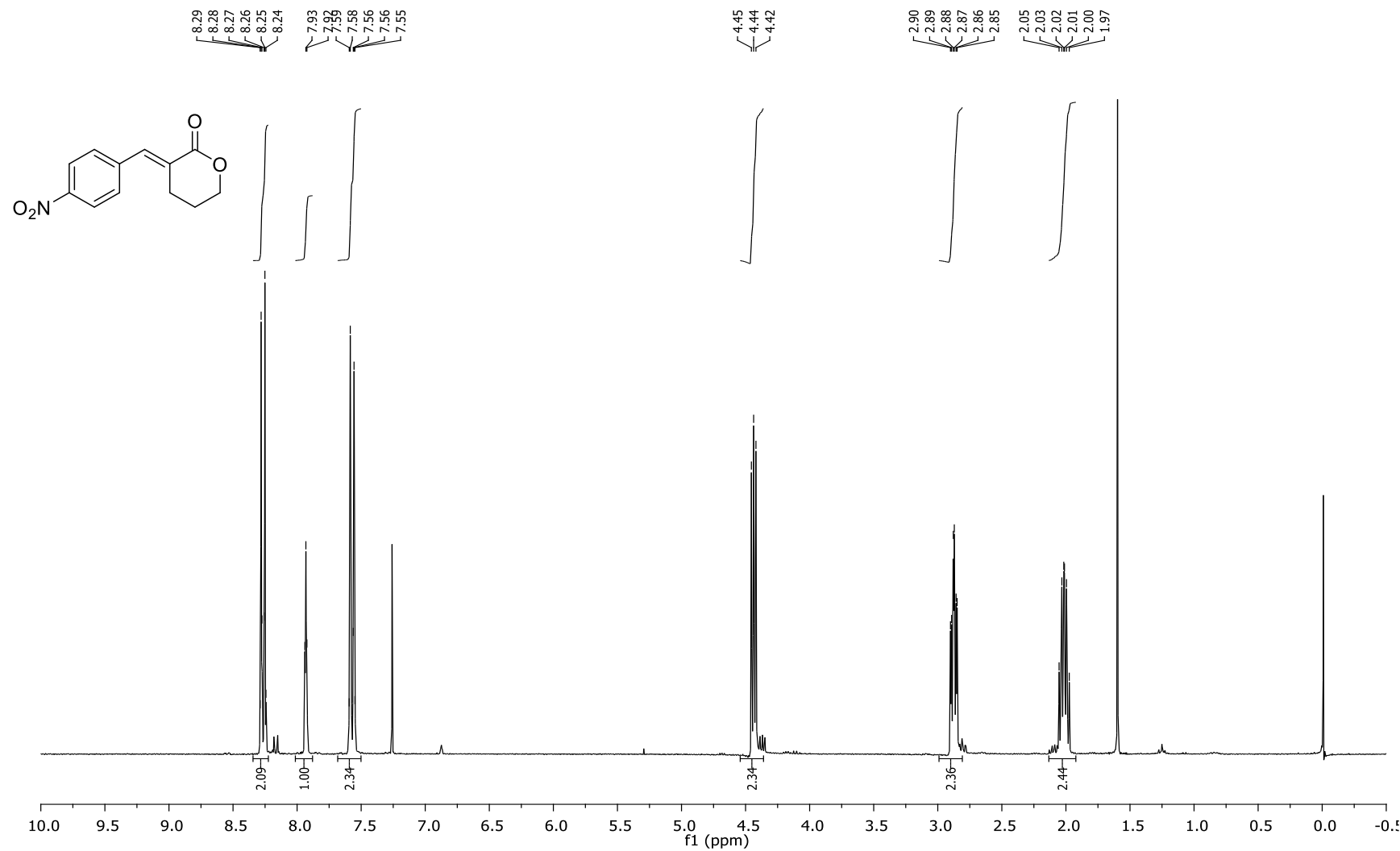
S2.45.  $^1\text{H}$  NMR (600 MHz) spectrum of **18E** in  $\text{CDCl}_3$ .



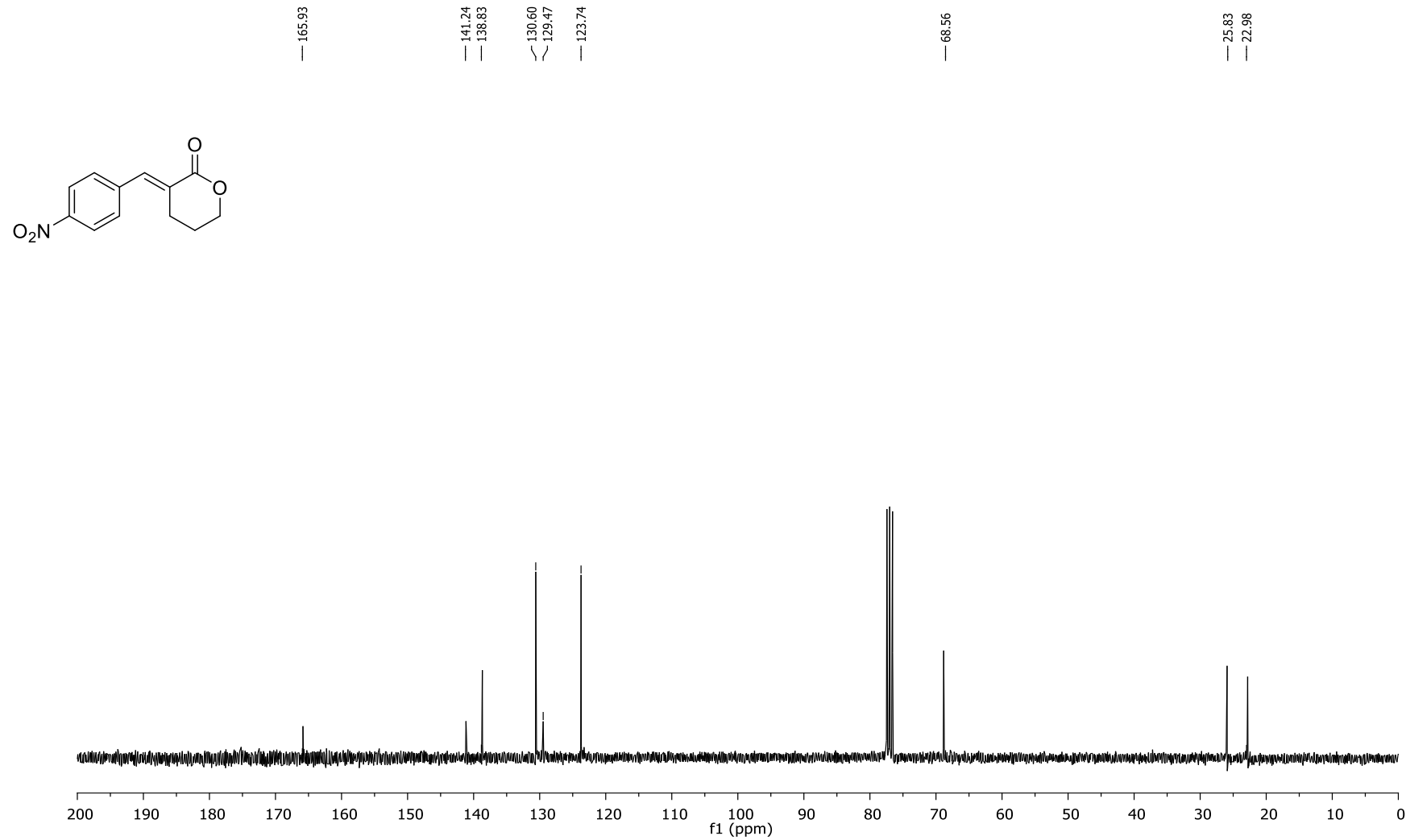
S2.46.  $^{13}\text{C}$  NMR (151 MHz) spectrum of **18E** in  $\text{CDCl}_3$ .



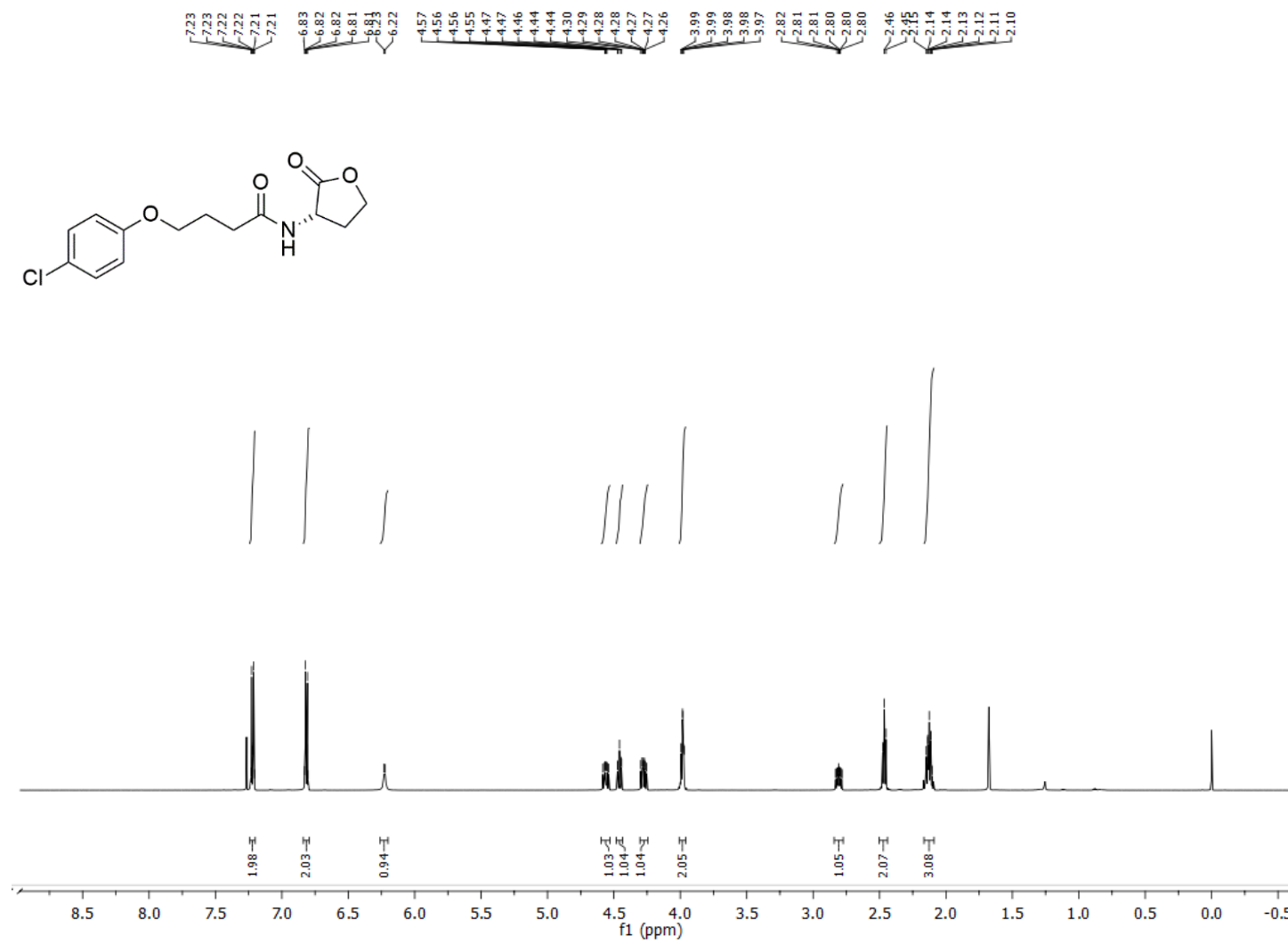
S2.47.  $^1\text{H}$  NMR (300 MHz) spectrum of **19E** in  $\text{CDCl}_3$ .



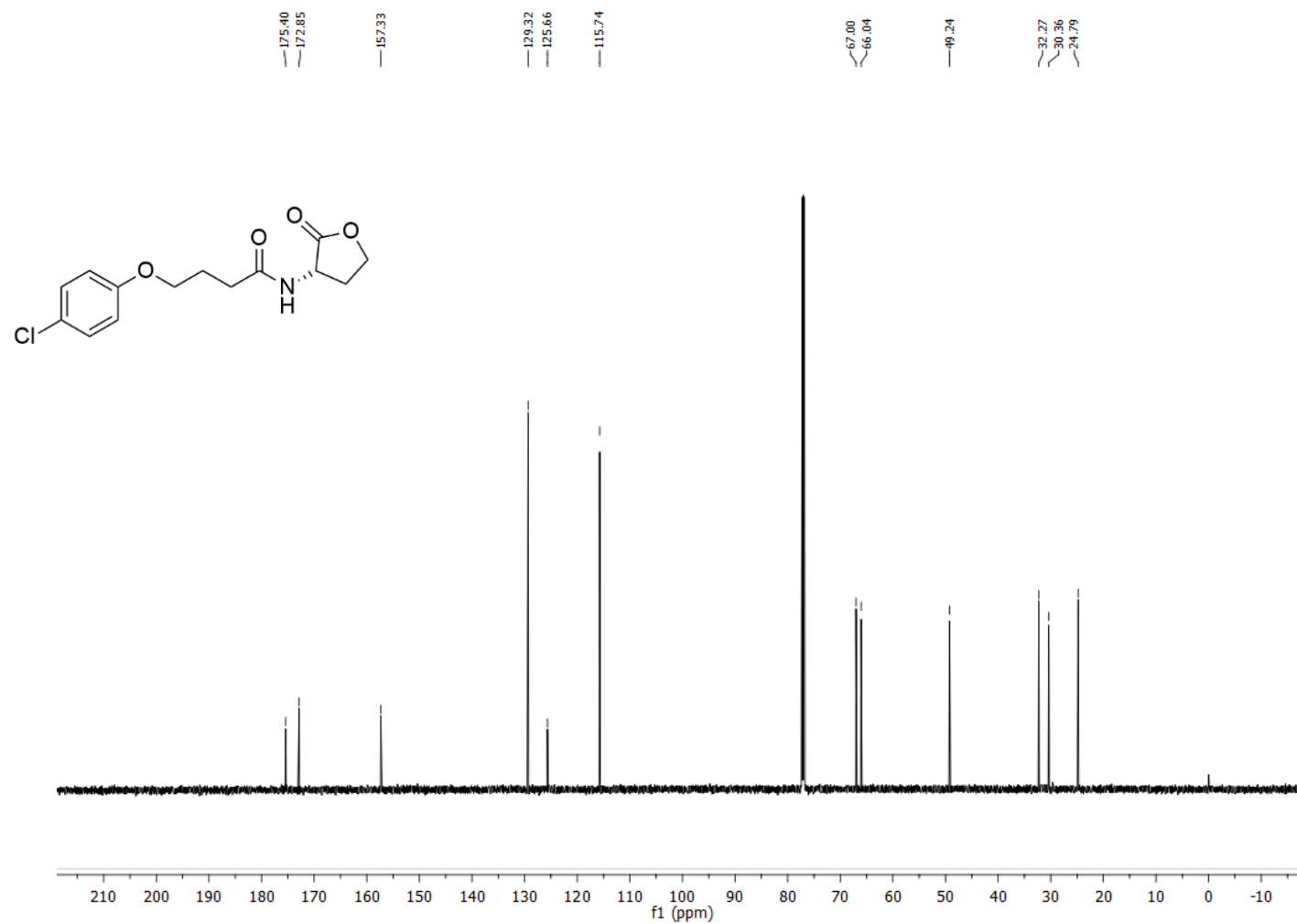
S2.48.  $^{13}\text{C}$  NMR (75 MHz) spectrum of **19E** in  $\text{CDCl}_3$ .



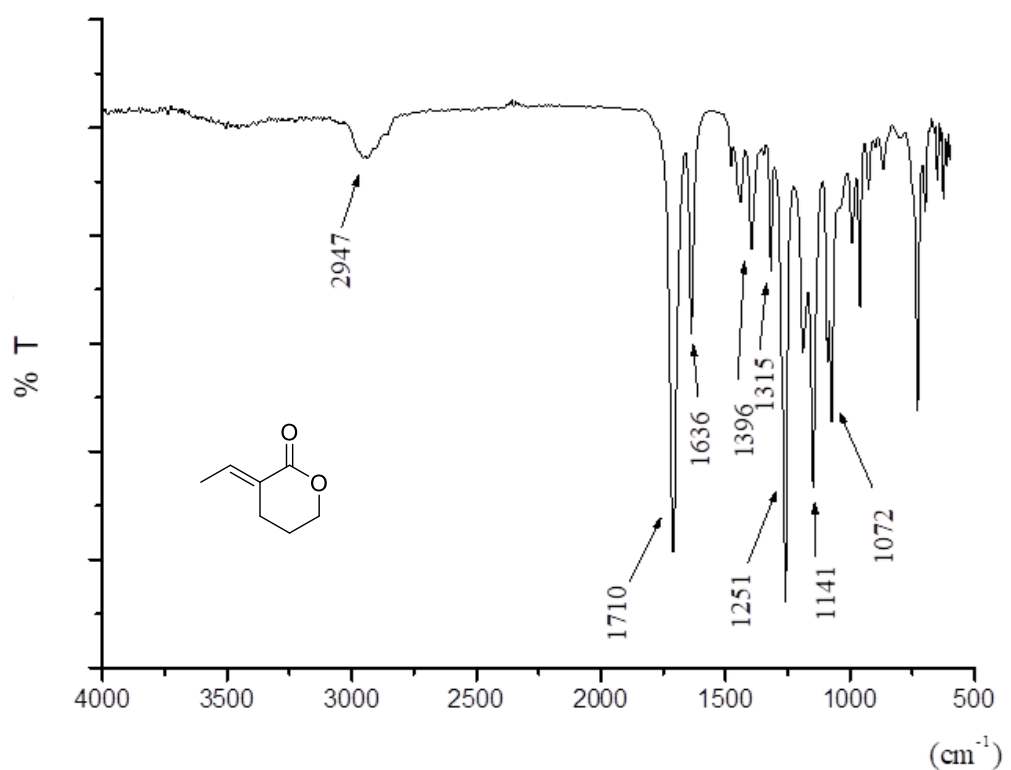
S2.49.  $^1\text{H}$  NMR spectrum of **20** in  $\text{CDCl}_3$ .



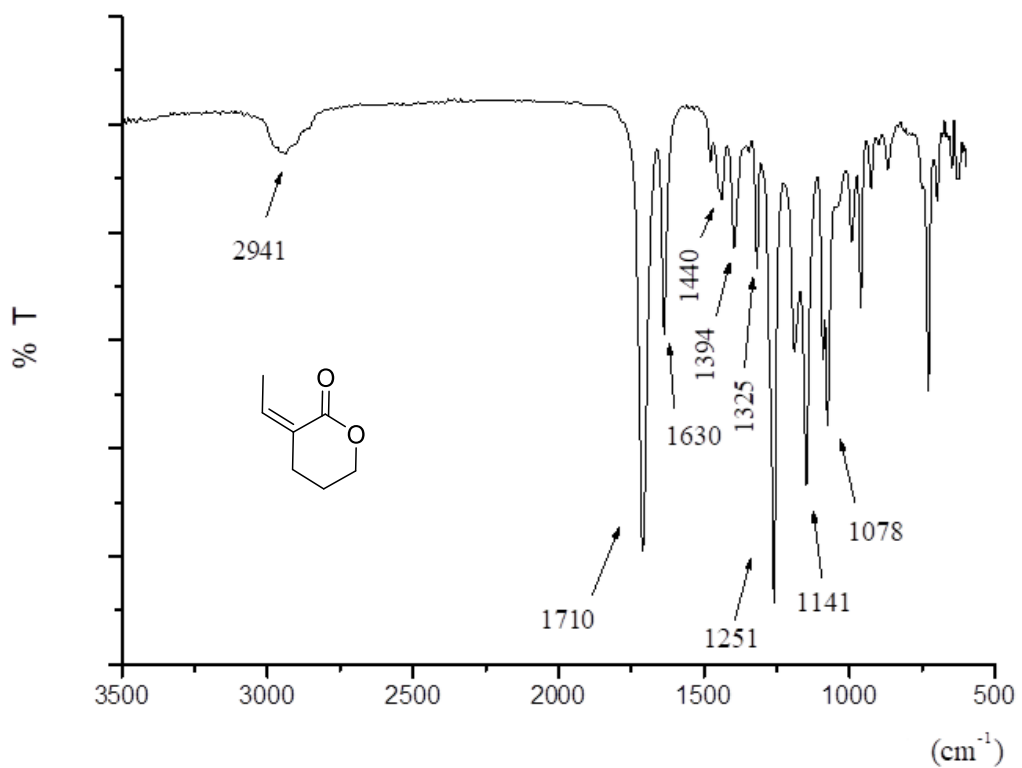
S2.50.  $^{13}\text{C}$  NMR spectrum of **20** in  $\text{CDCl}_3$ .



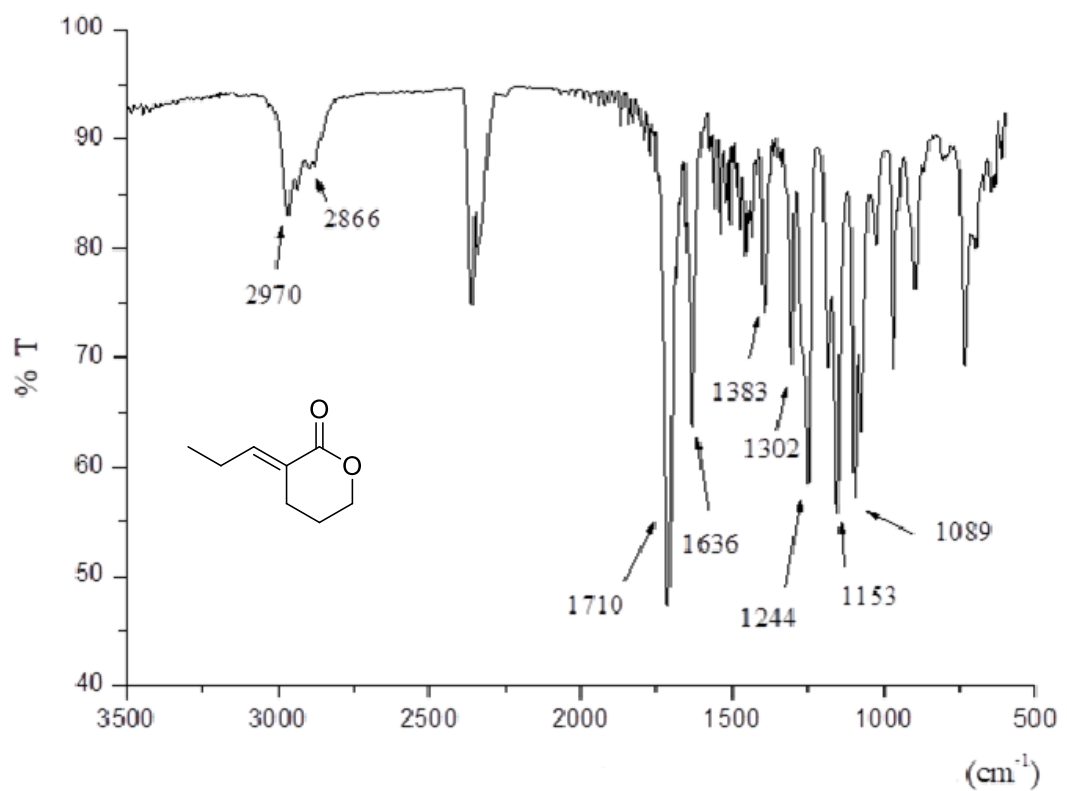
**S3.1. IR (ATR) spectrum of 10E.**



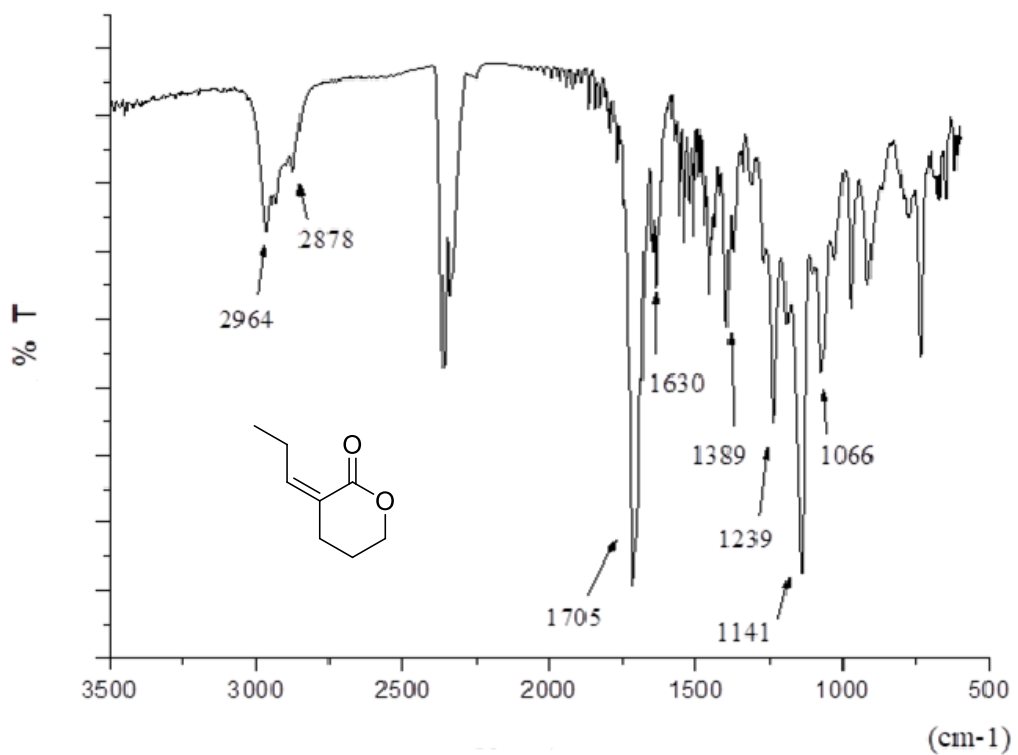
**S3.2. IR (ATR) spectrum of 10Z.**



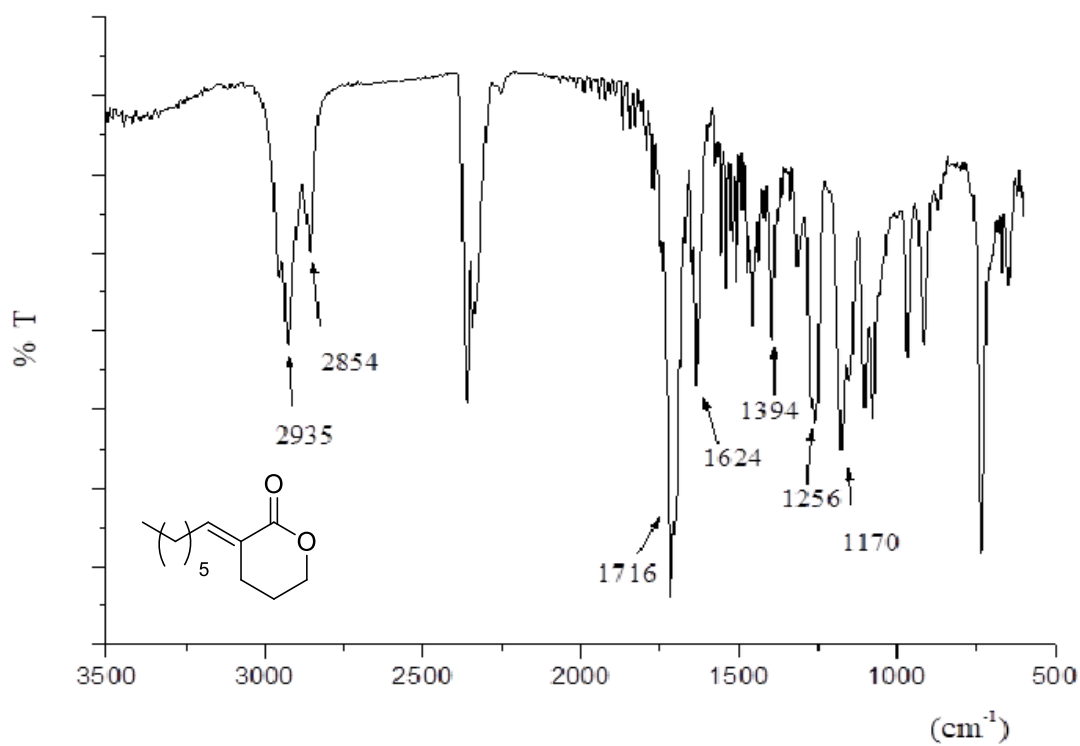
**S3.3. IR (ATR) spectrum of 11E.**



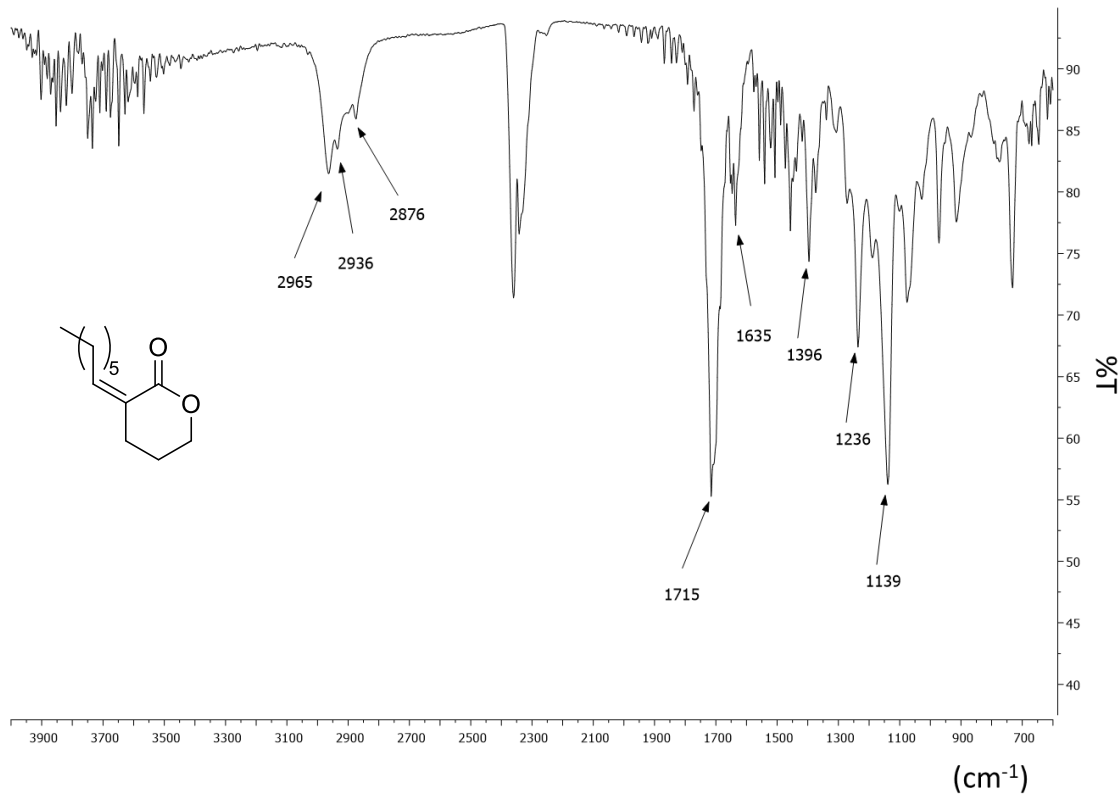
**S3.4. IR (ATR) spectrum of 11Z**



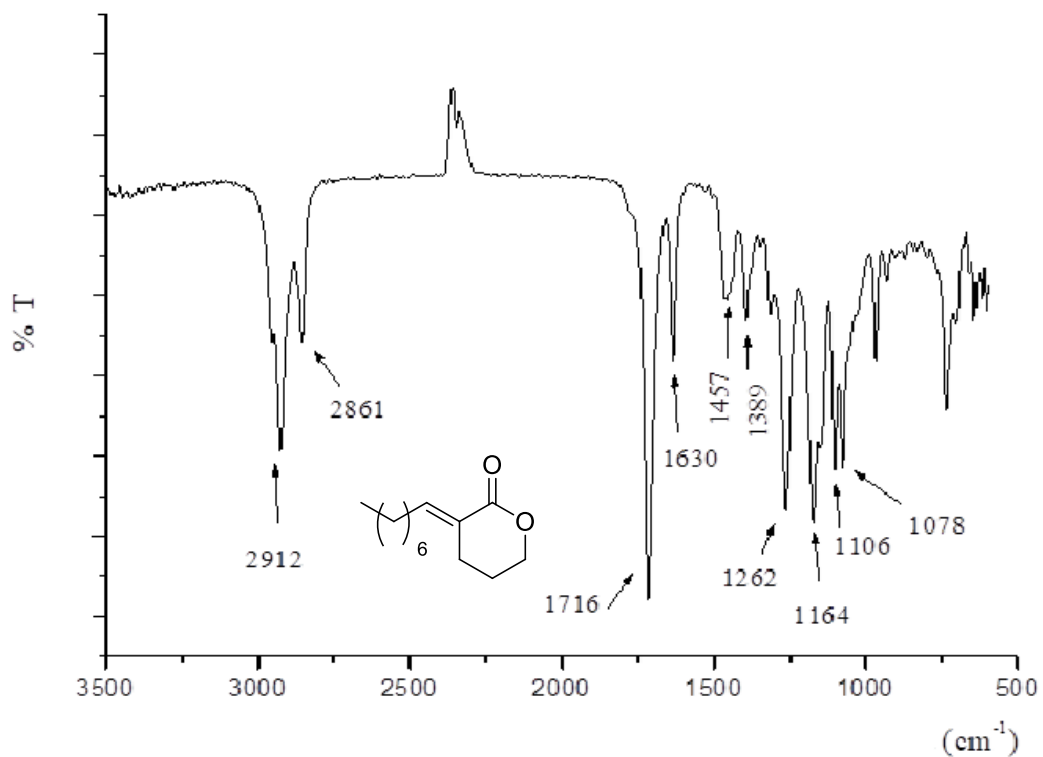
**S3.5. IR (ATR) spectrum of 12E.**



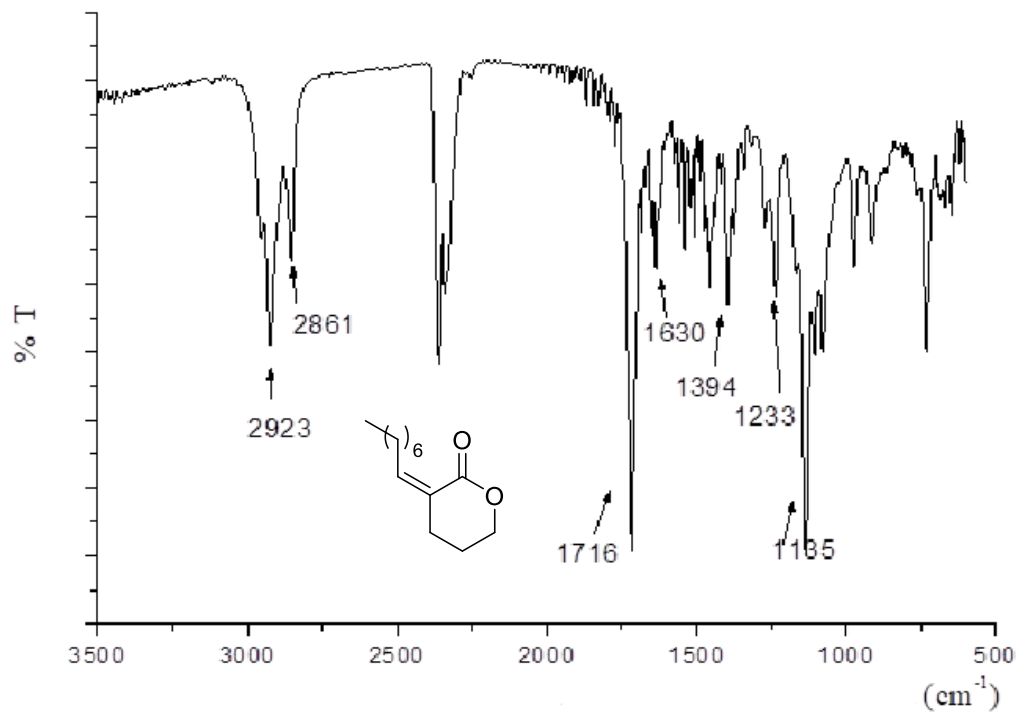
**S3.6. IR (ATR) spectrum of 12Z.**



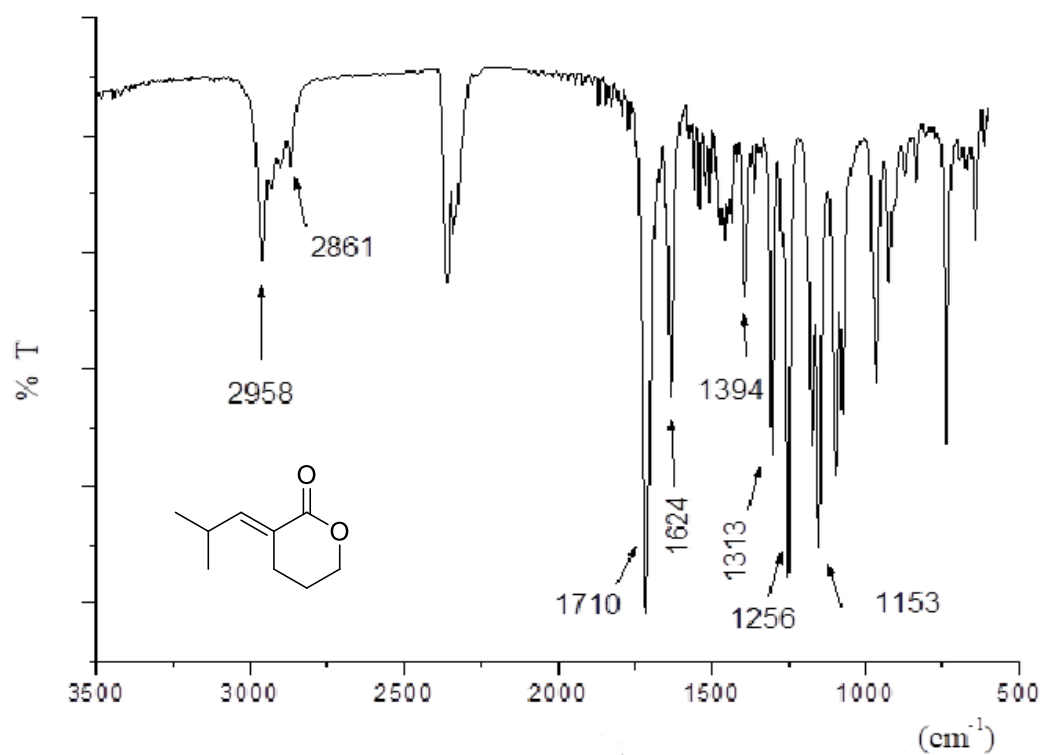
**S3.7. IR (ATR) spectrum of 13E.**



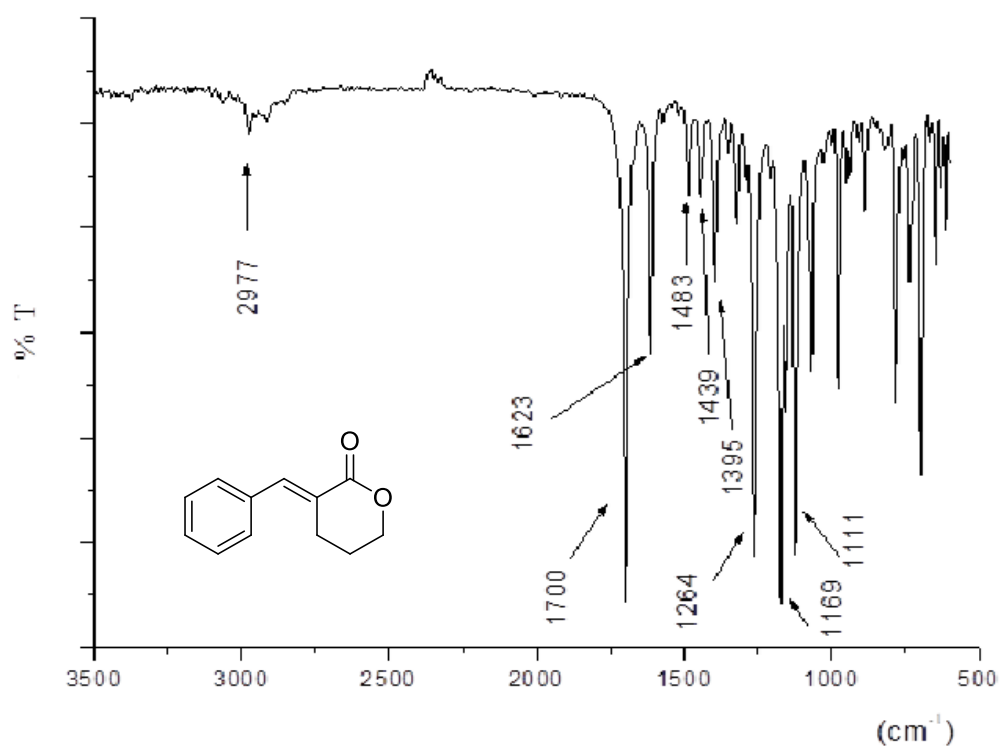
**S3.8. IR (ATR) spectrum of 13Z.**



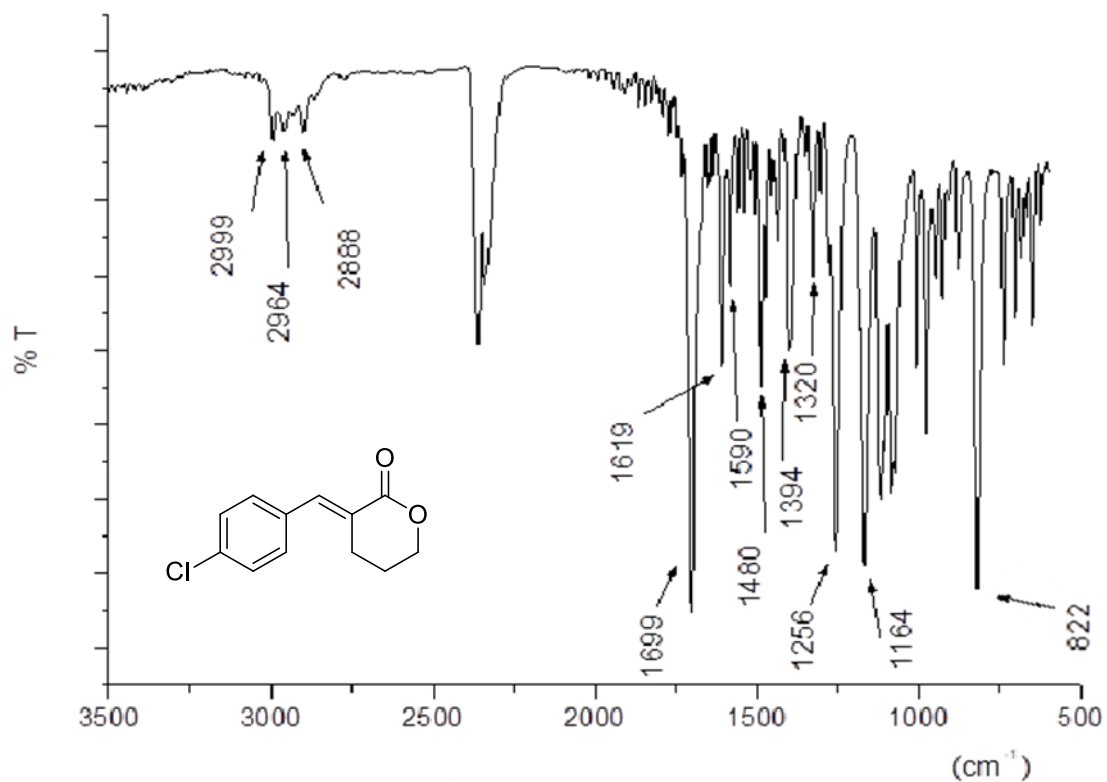
S3.9. IR (ATR) spectrum of 14E.



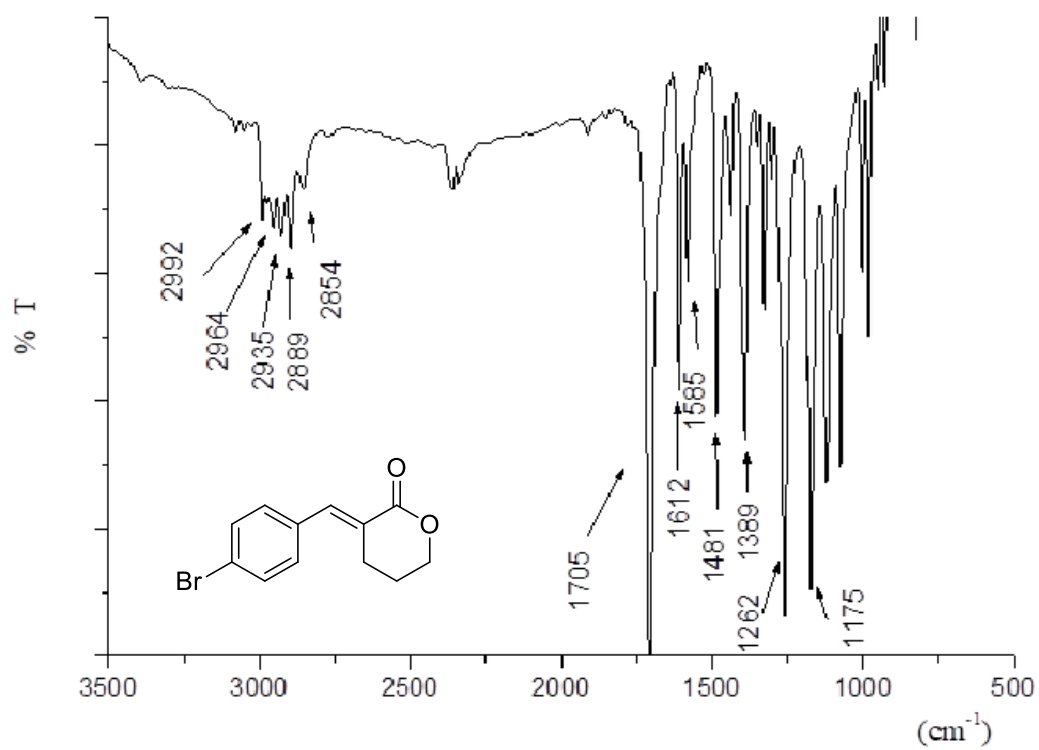
S3.10. IR (ATR) spectrum of 15E.



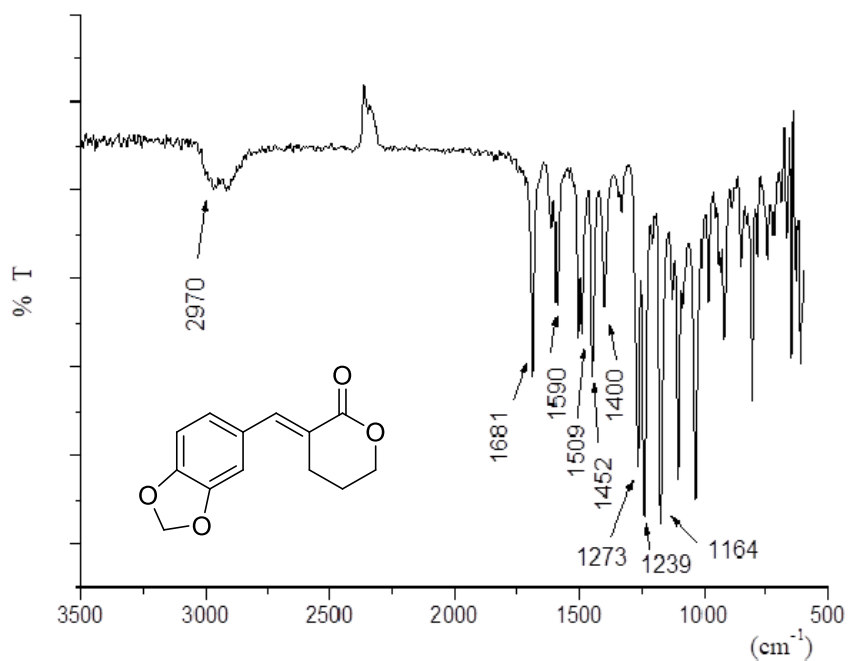
S3.11. IR (ATR) spectrum of 16E.



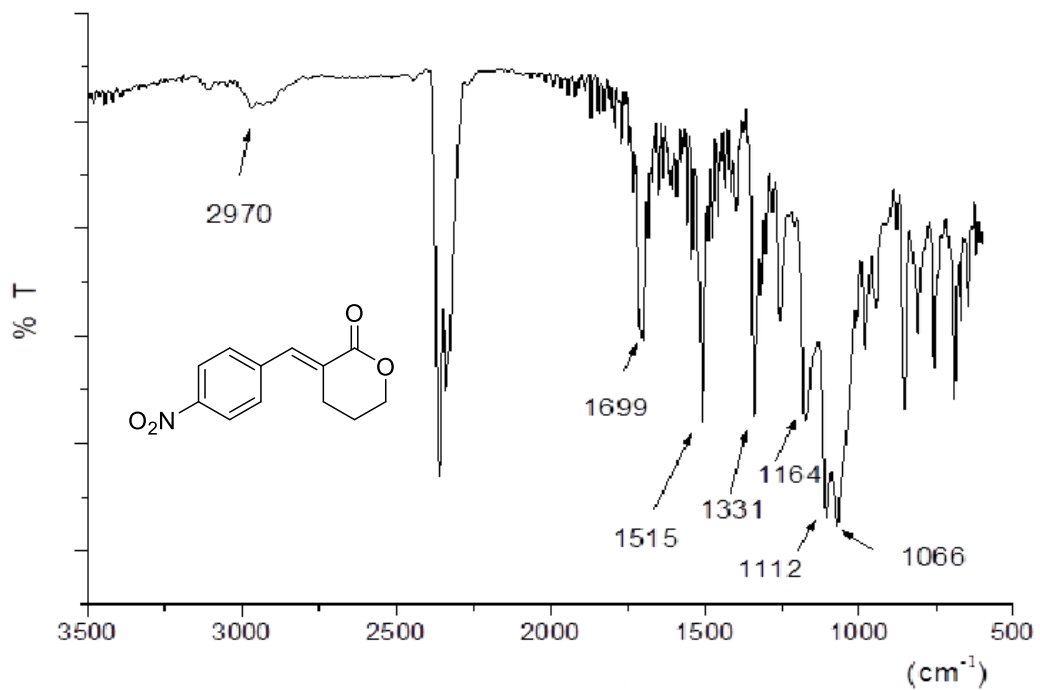
S3.12. IR (ATR) spectrum of 17E.



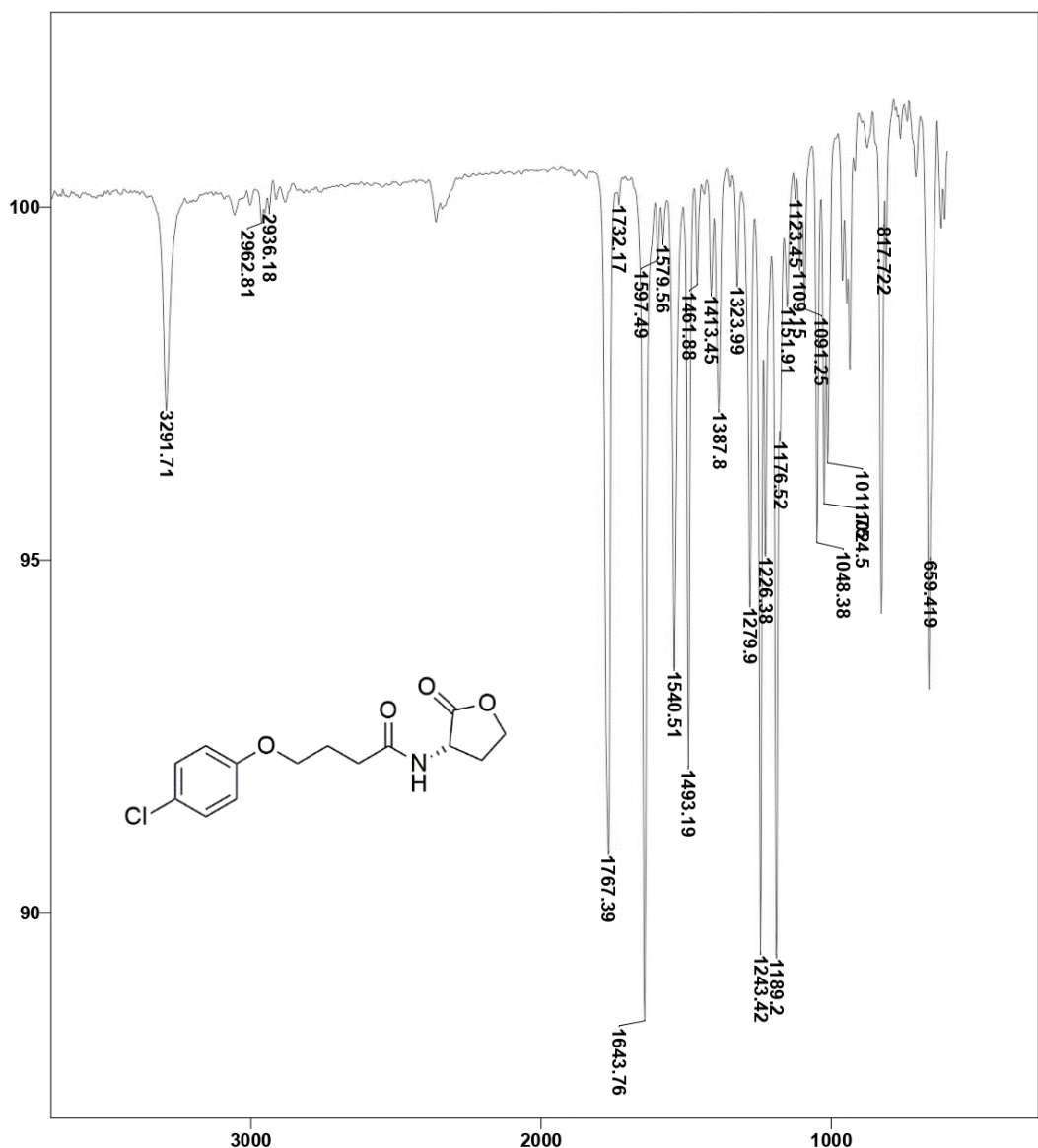
**S3.13. IR (ATR) spectrum of 18E.**



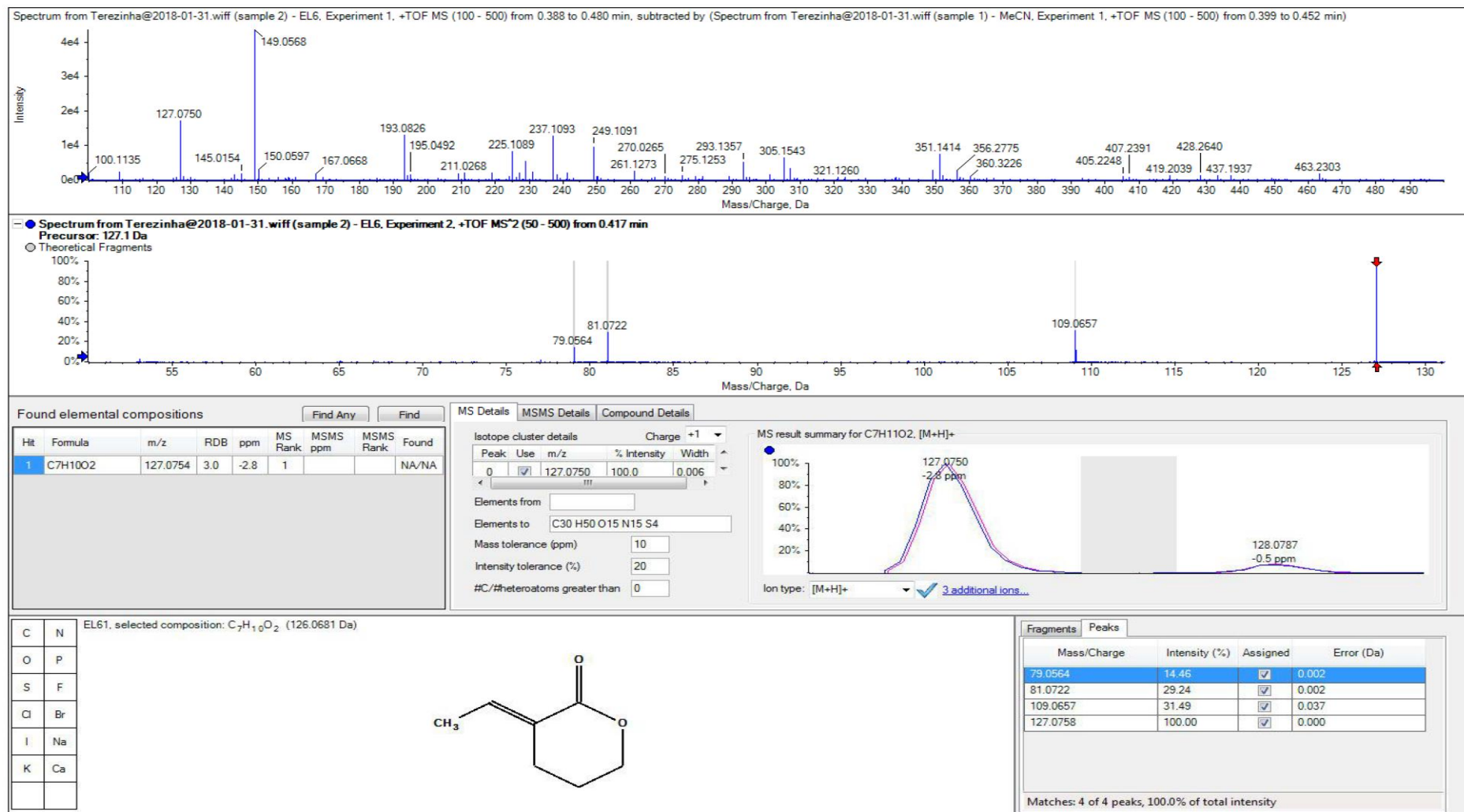
**S3.14. IR (ATR) spectrum of 19E.**



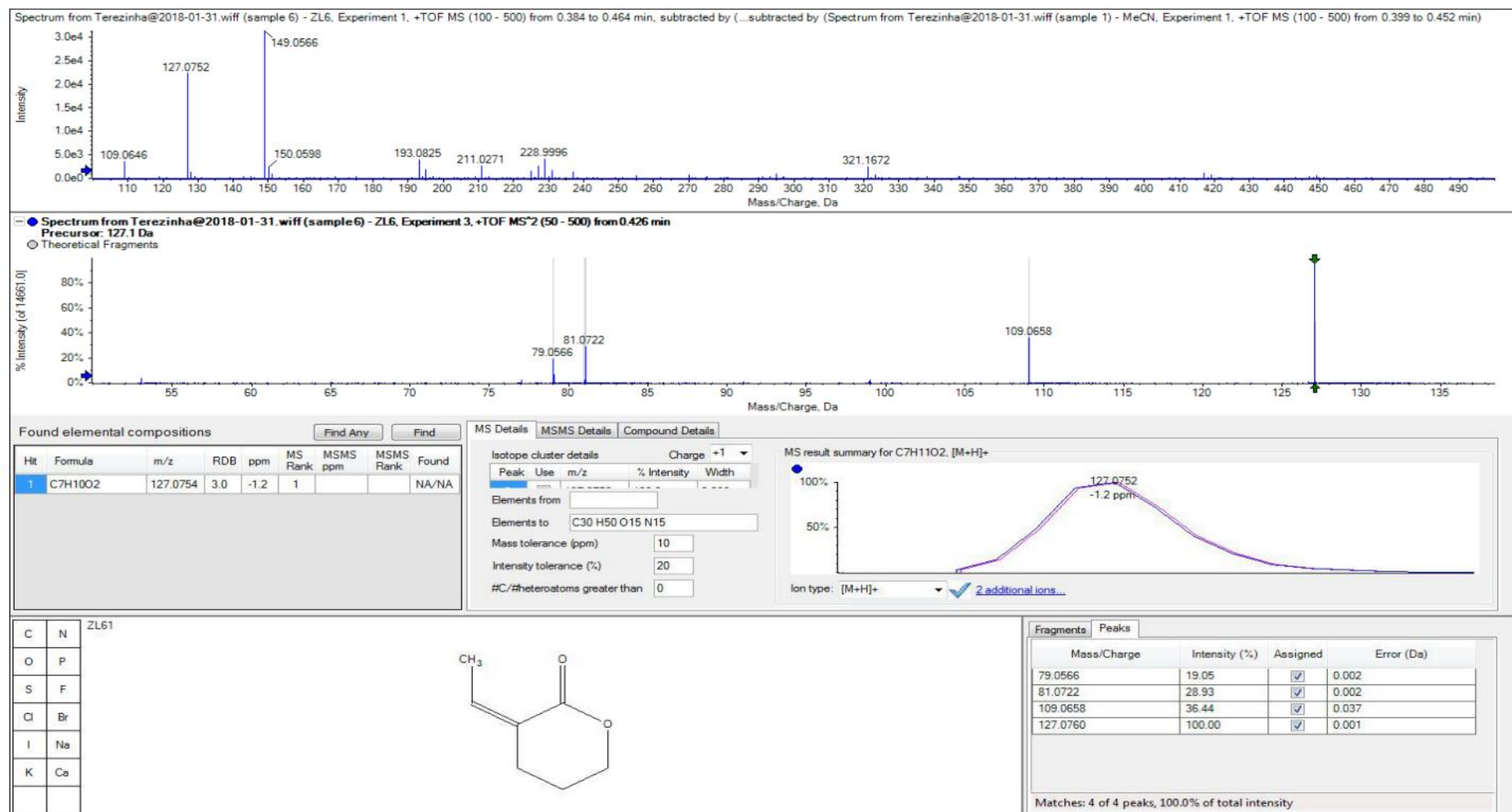
S3.15. IR (ATR) spectrum of 20.



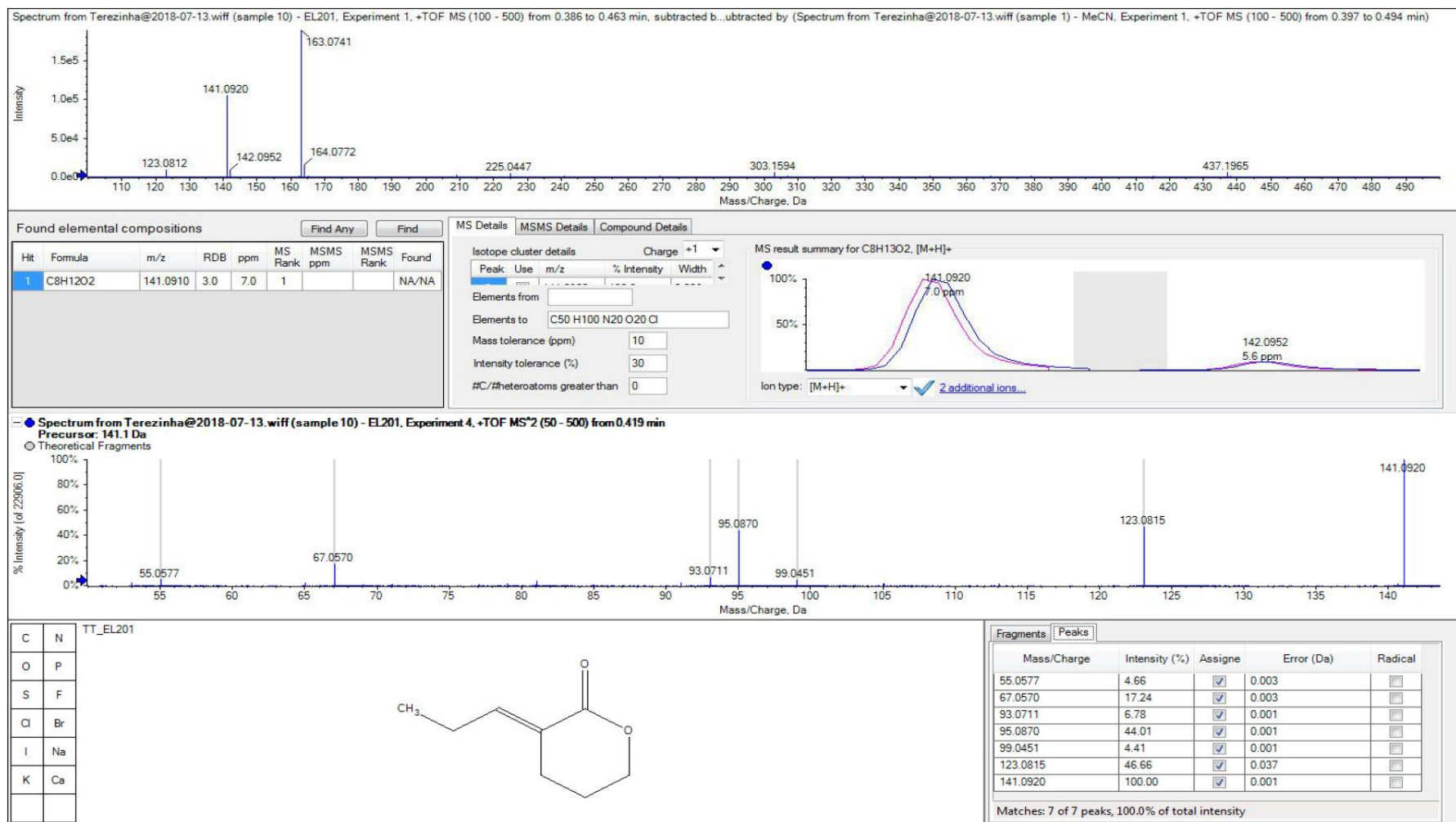
#### S4.1. HRMS data of 10E.



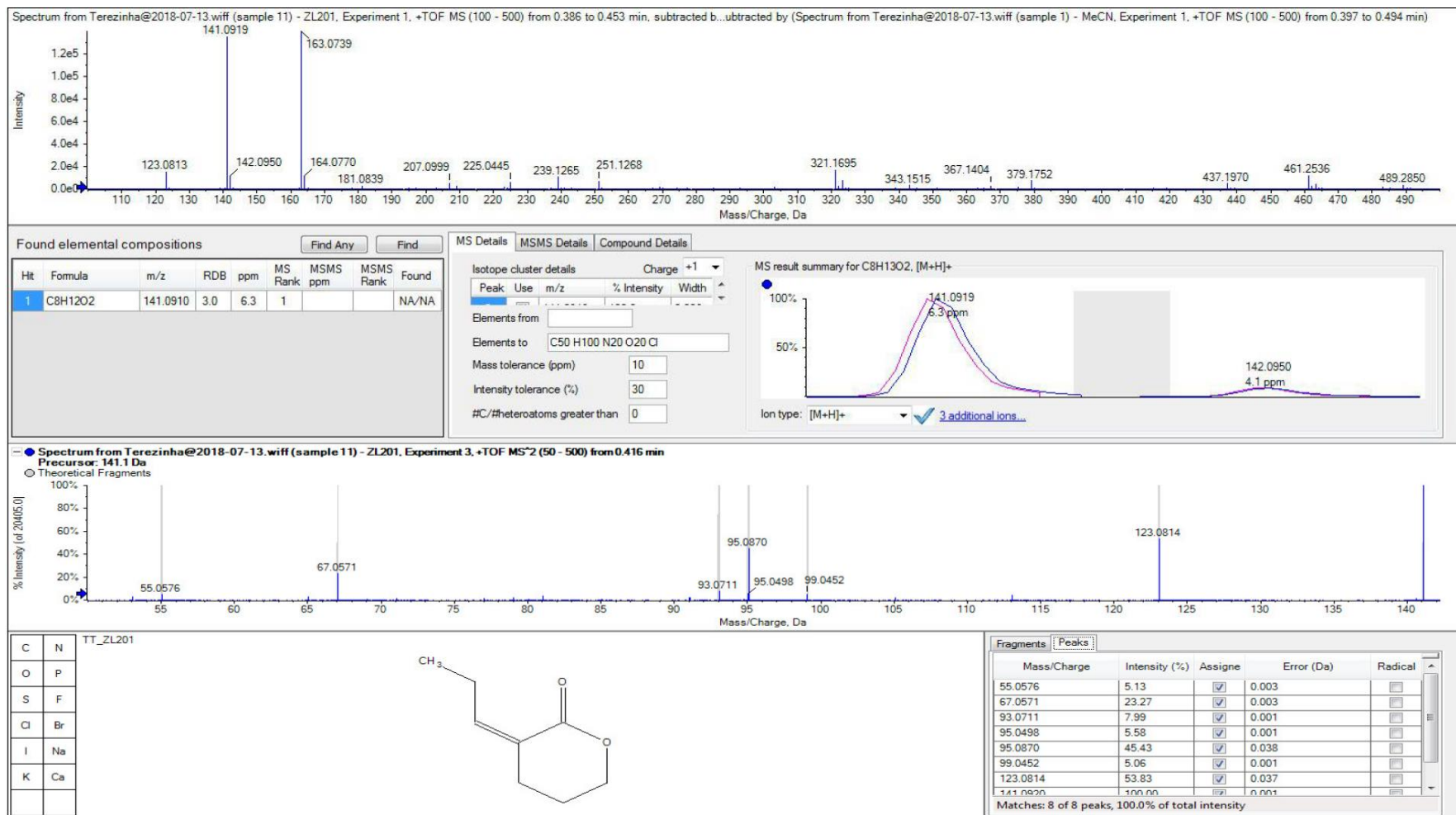
## S4.2. HRMS data of 10Z.



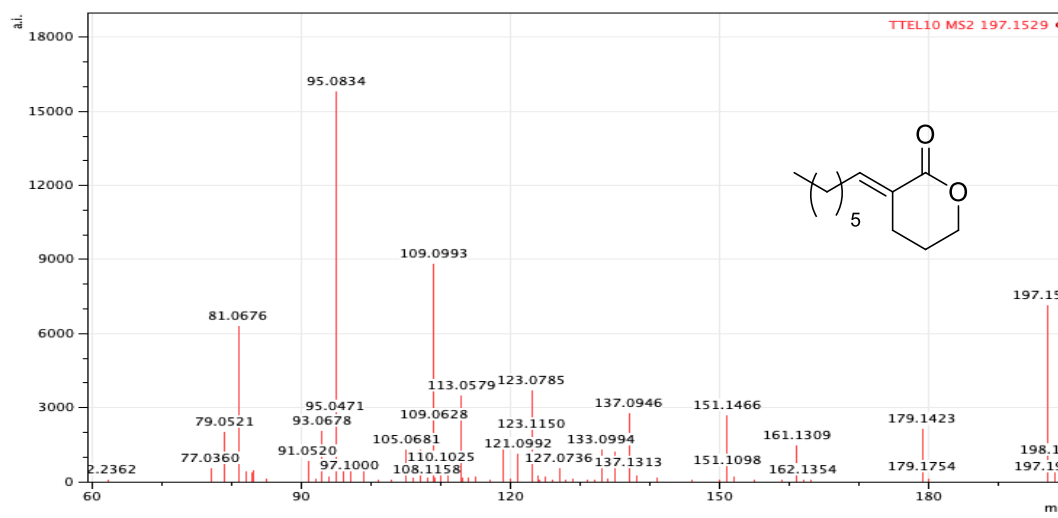
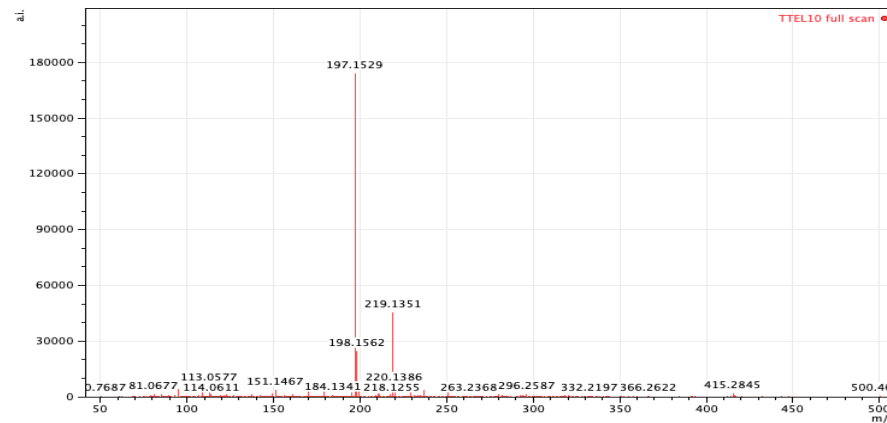
### S4.3. HRMS data of 11E.



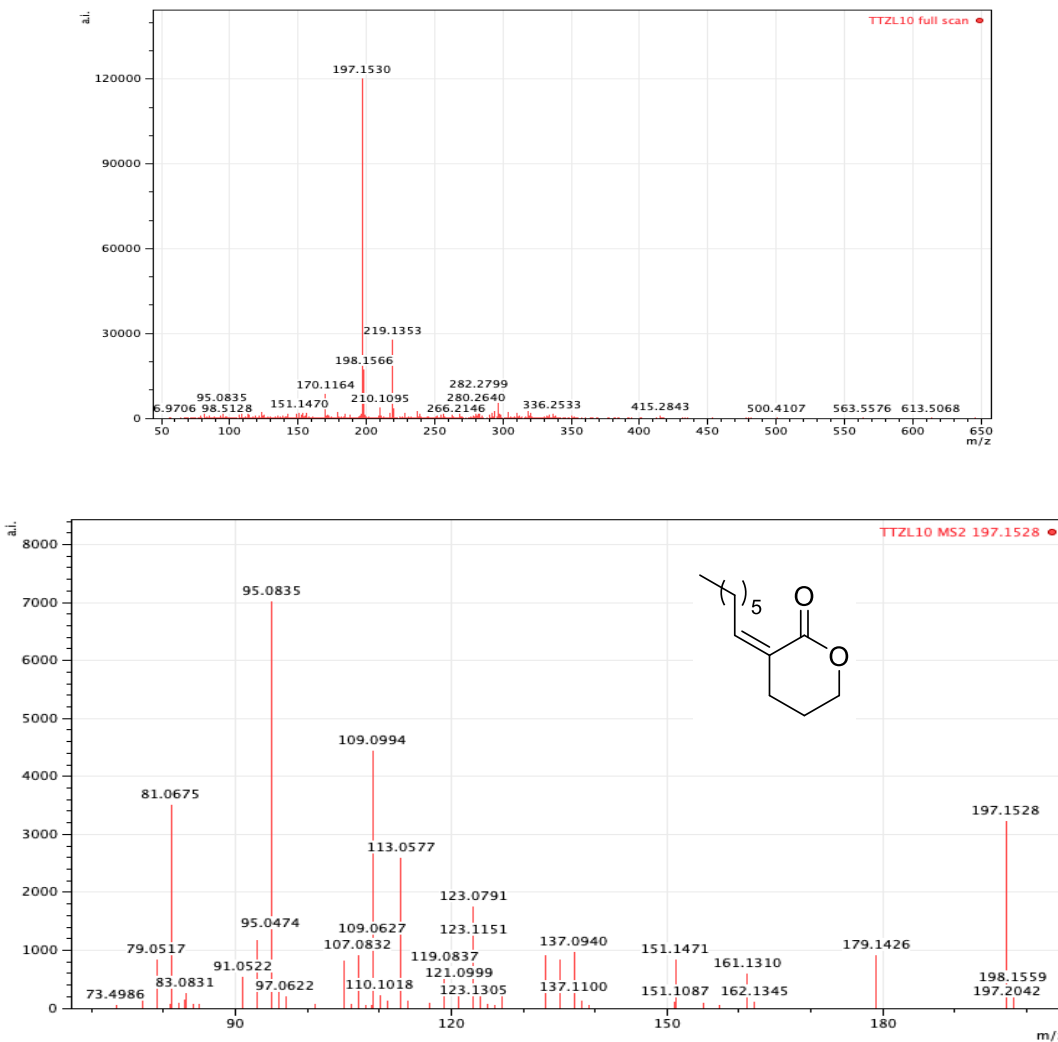
#### S4.4. HRMS data of 11Z.



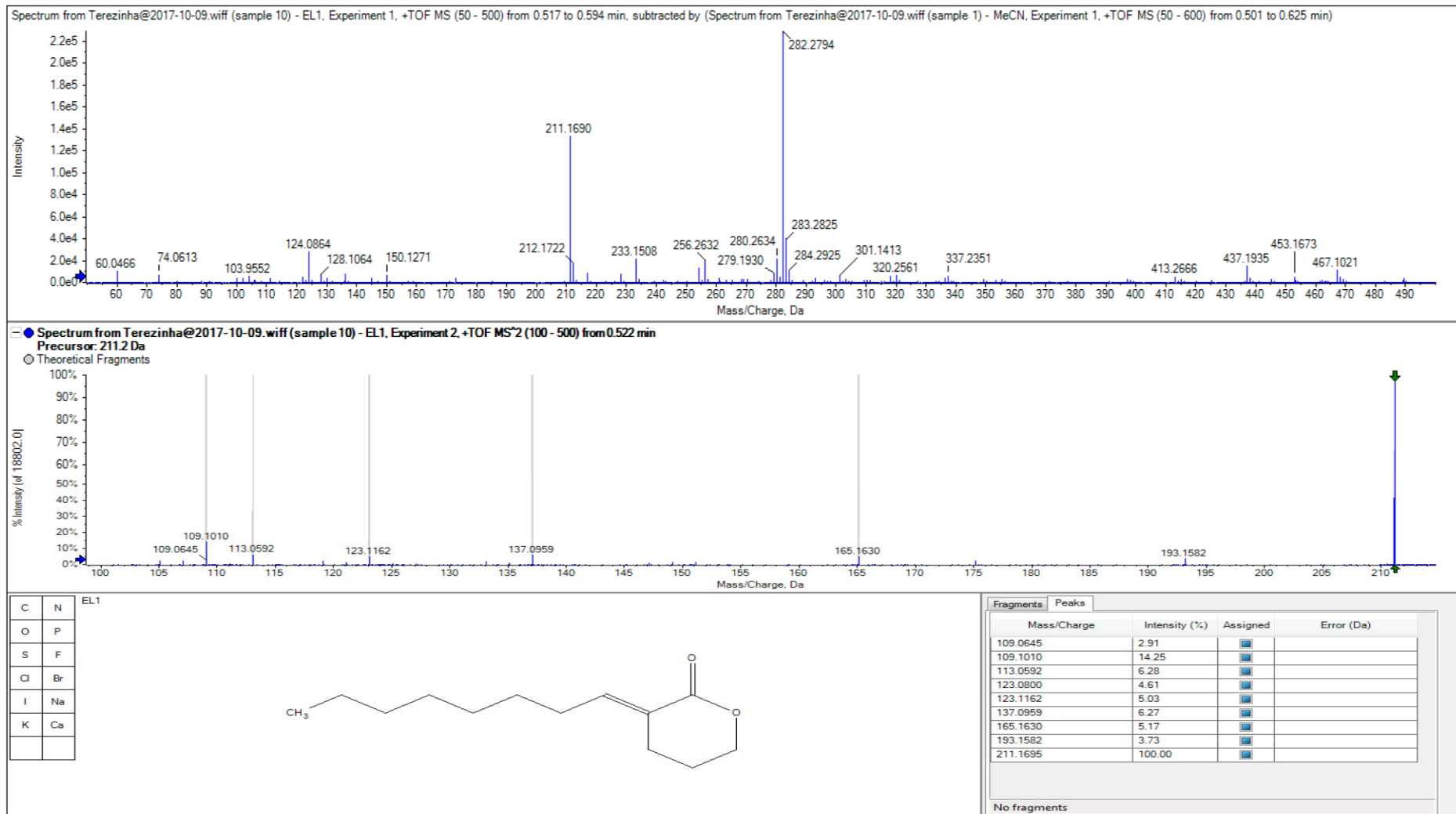
#### S4.5. HRMS data of 12E.



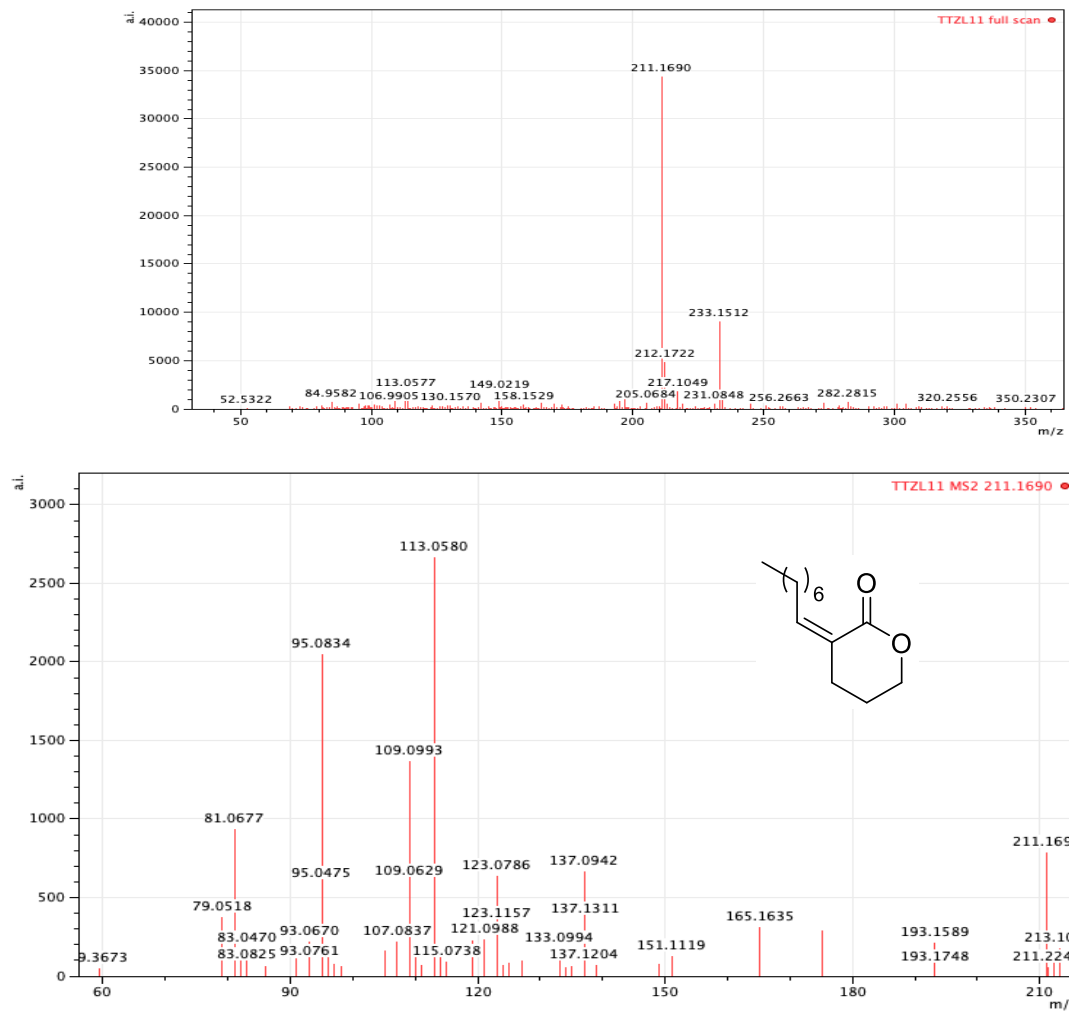
#### S4.6. HRMS data of 12Z.



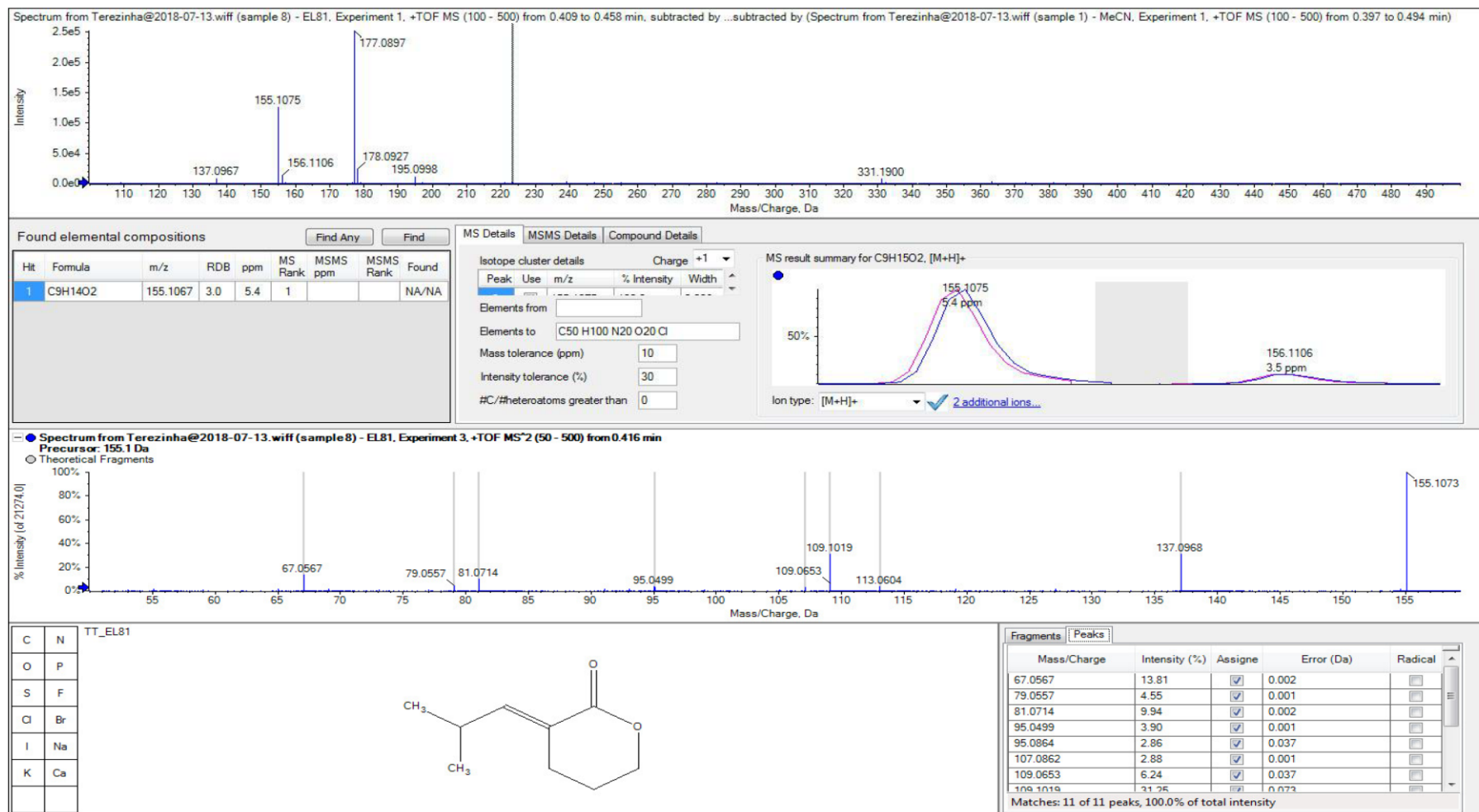
#### S4.7. HRMS data of 13E.



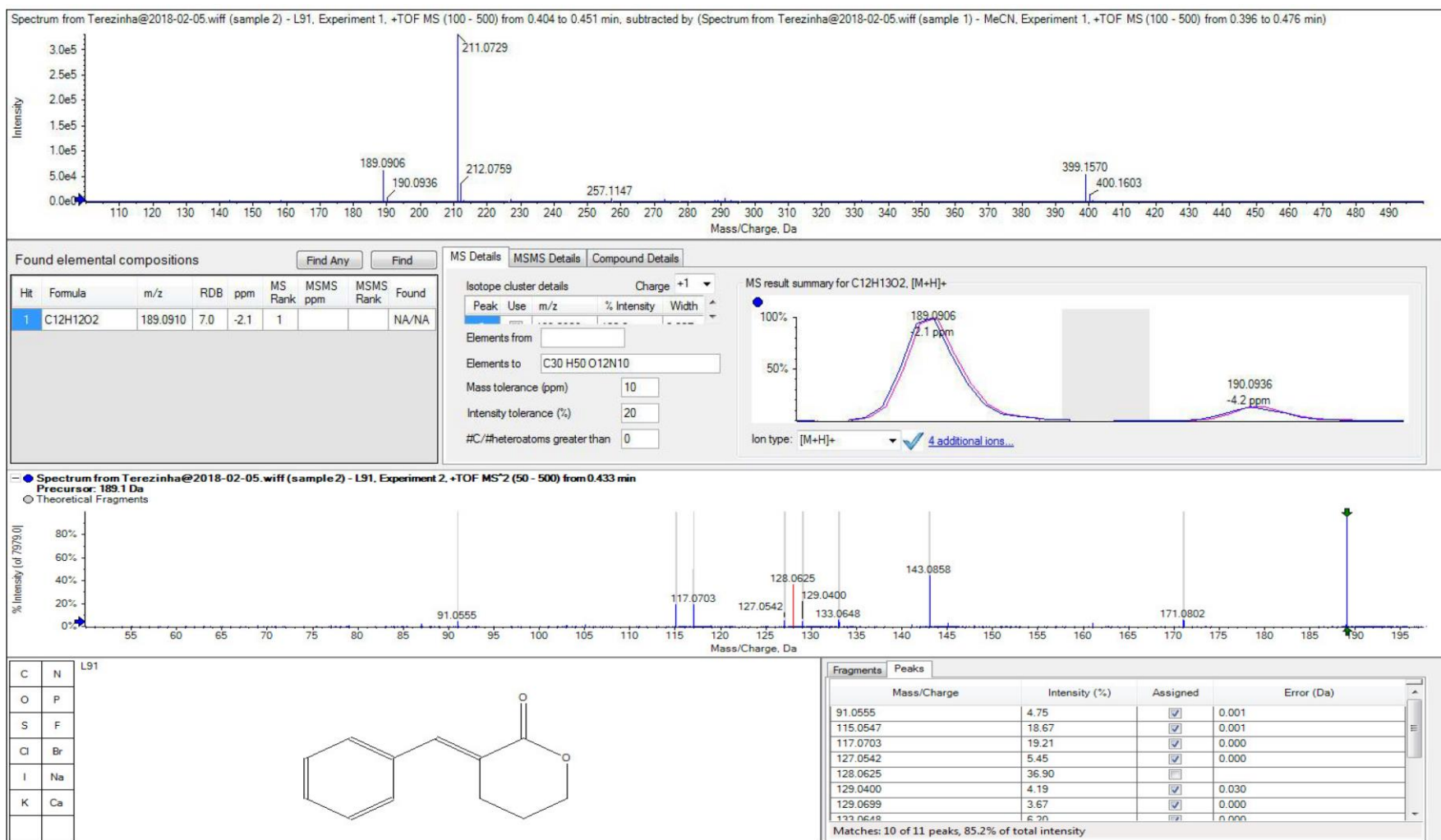
**S4.8. HRMS data of 13Z.**



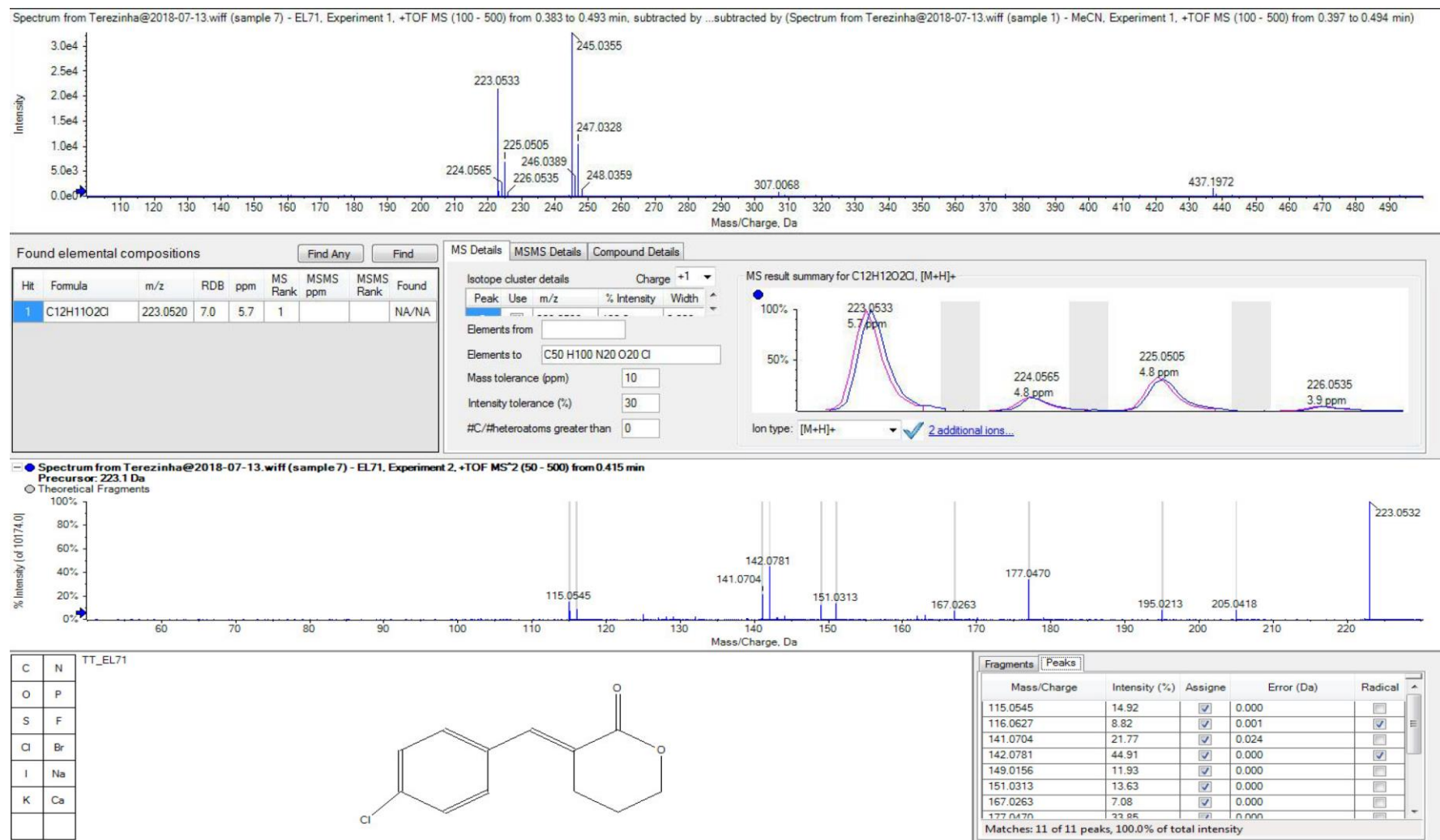
#### S4.9. HRMS data of 14E.



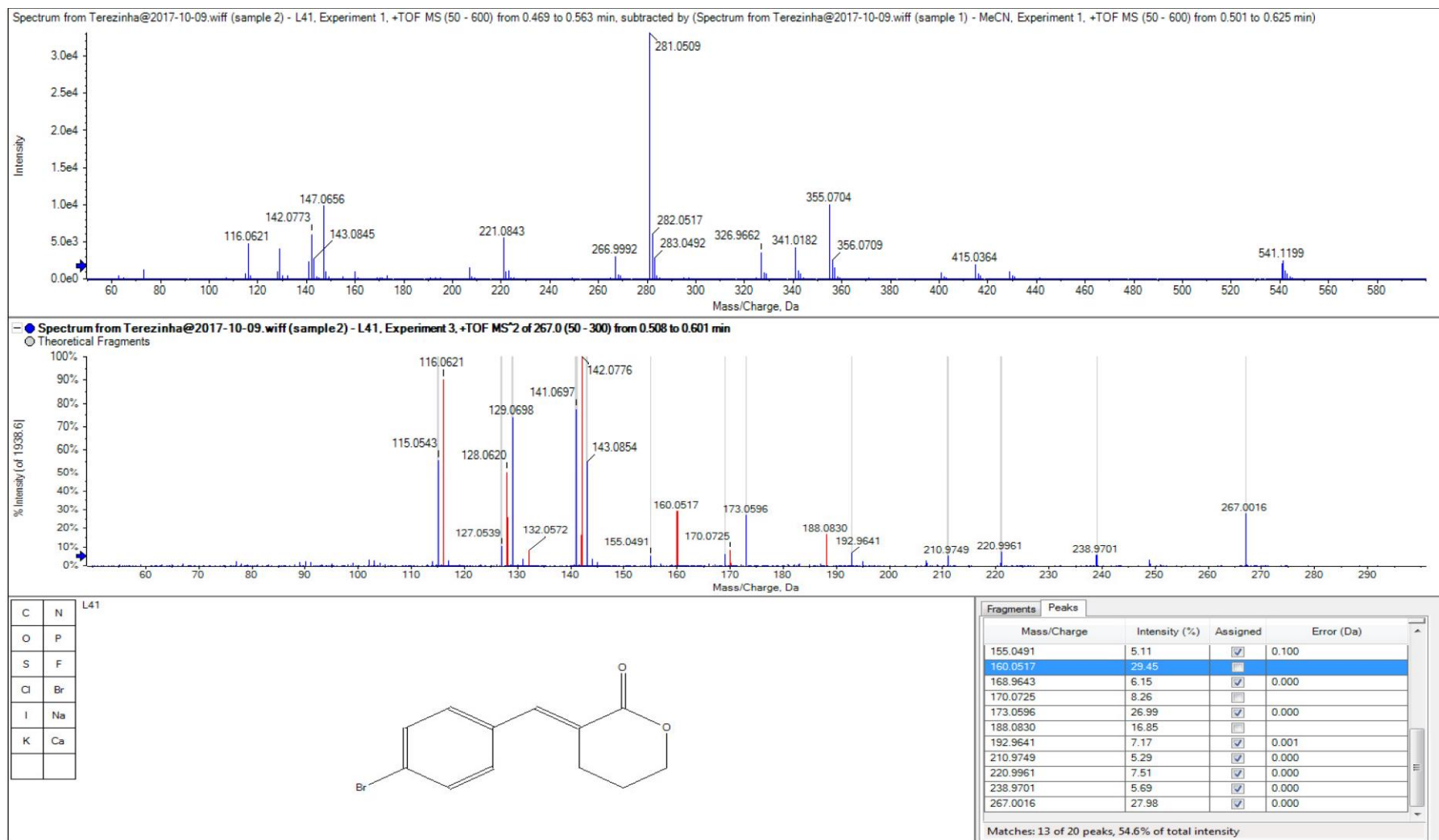
#### S4.10. HRMS data of 15E.



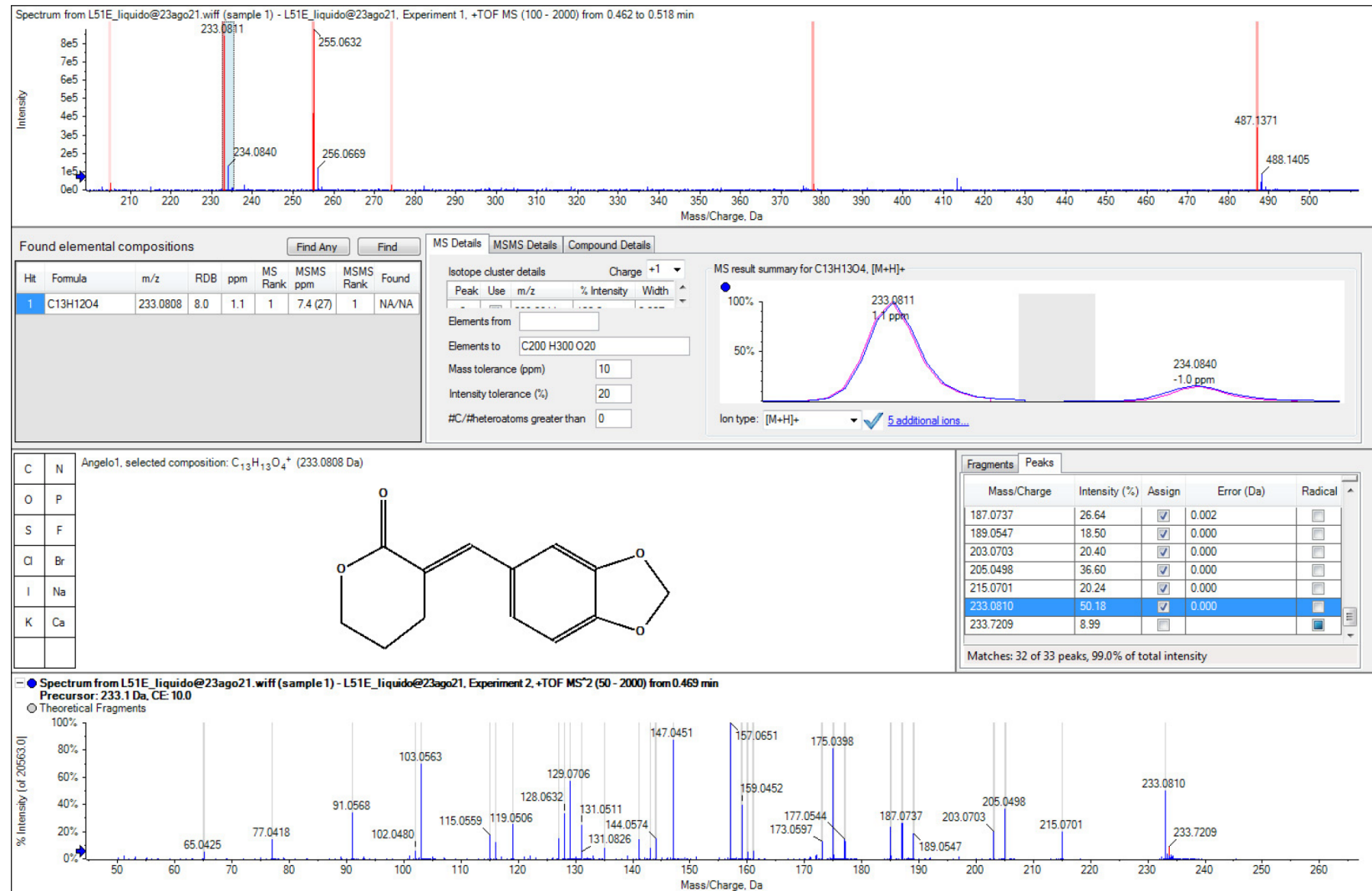
### S4.11. HRMS data of 16E.



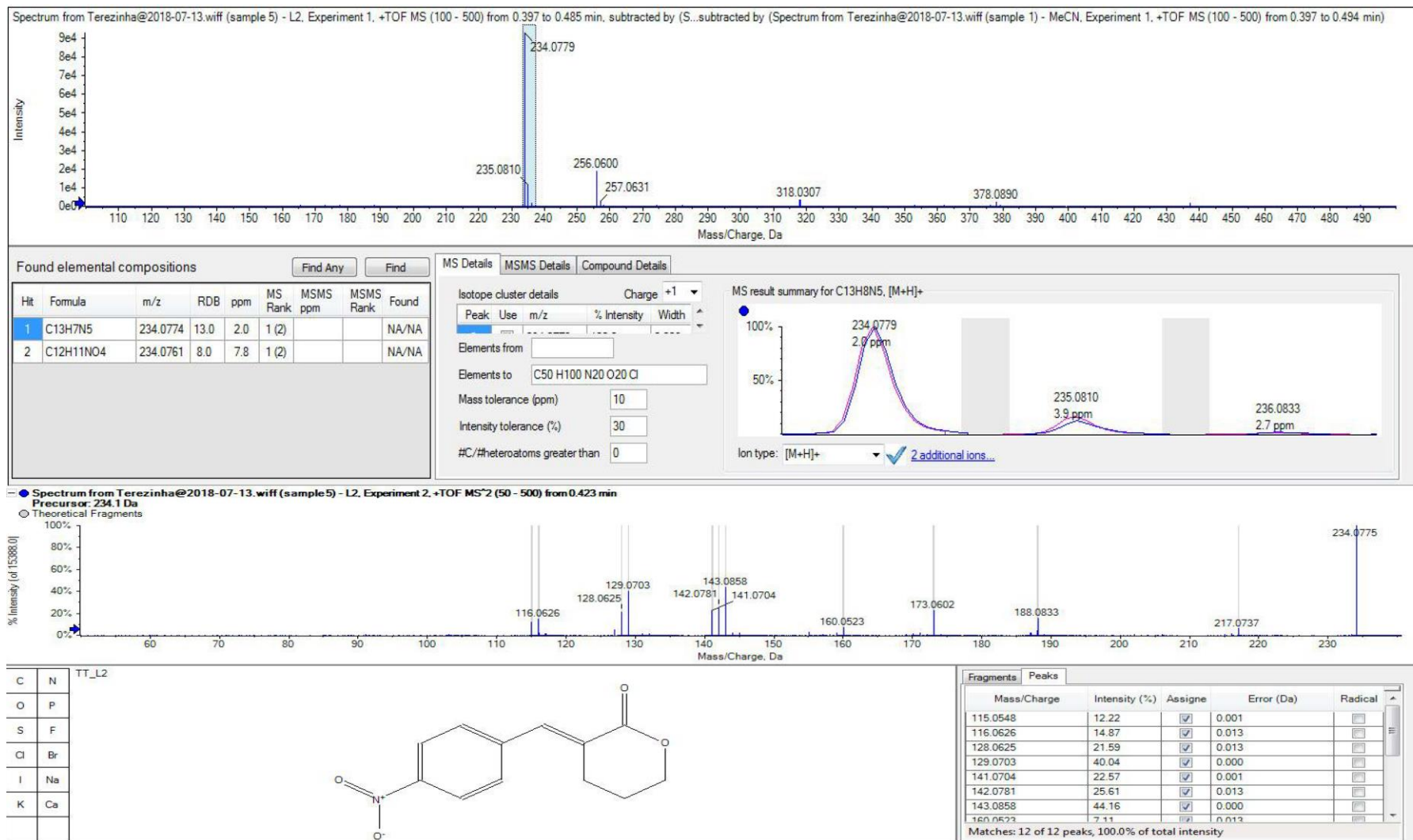
#### S4.12. HRMS data of 17E.



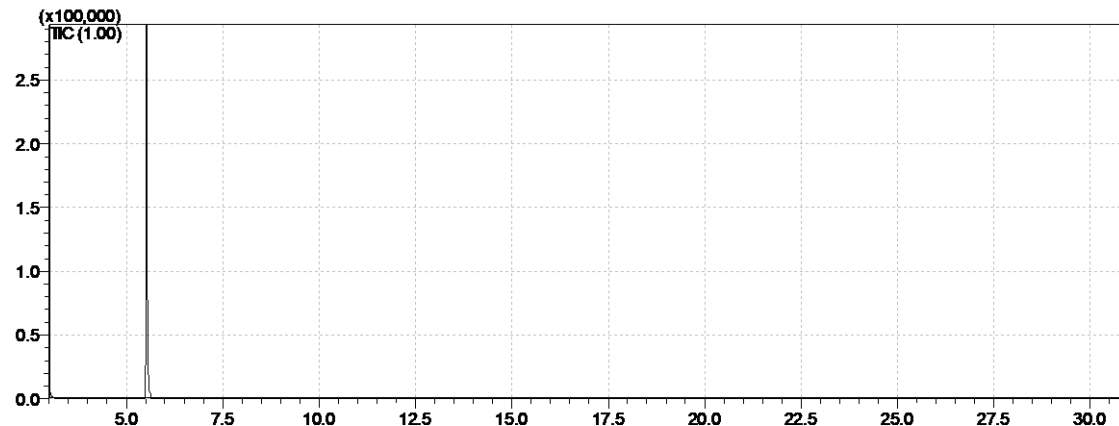
### S4.13. HRMS data of 18E



#### S4.14. HRMS data of 19E.

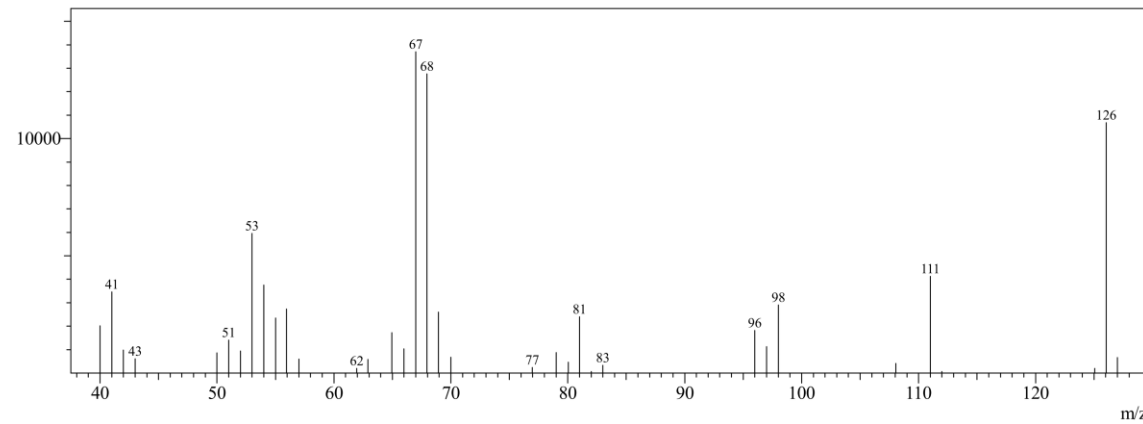


### S5.1. GC-MS data of 10E.

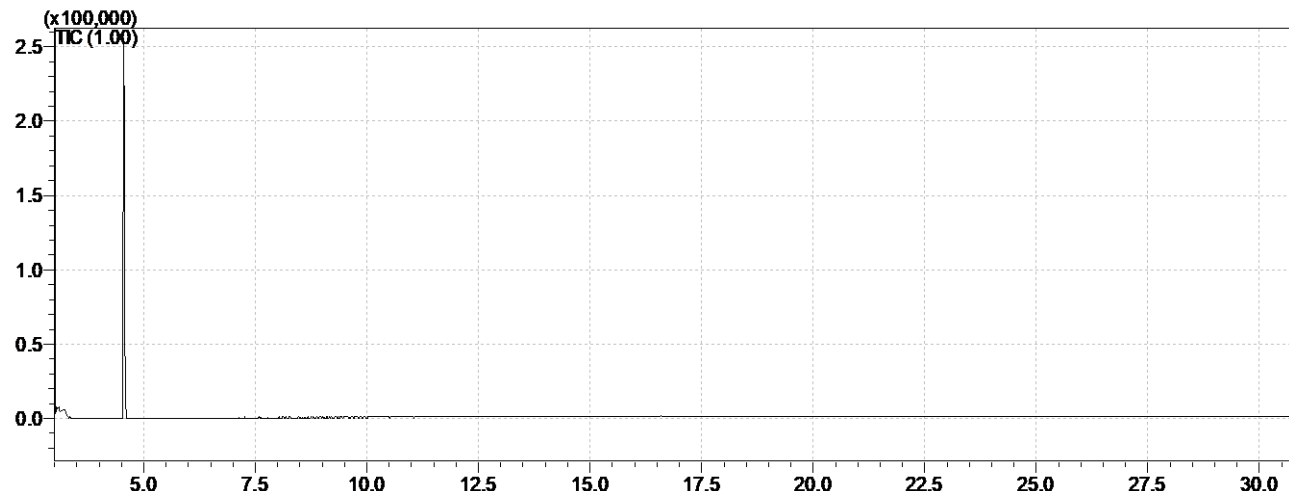


Purity: 98.1 %

Line#:1 R.Time:5.525(Scan#:304)  
MassPeaks:35  
RawMode:Averaged 5.492-5.625(300-316) BasePeak:67.00(13707)  
BG Mode:None Group 1 - Event 1 Scan

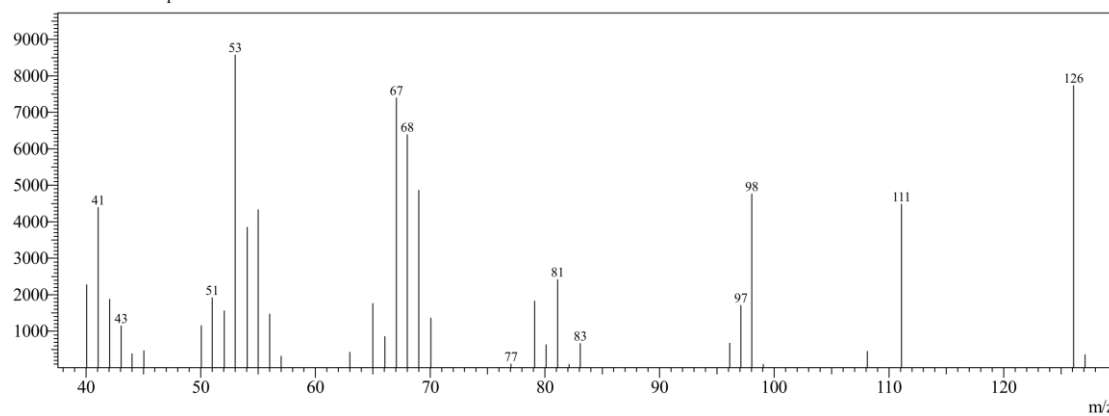


## S5.2. GC-MS data of 10Z.

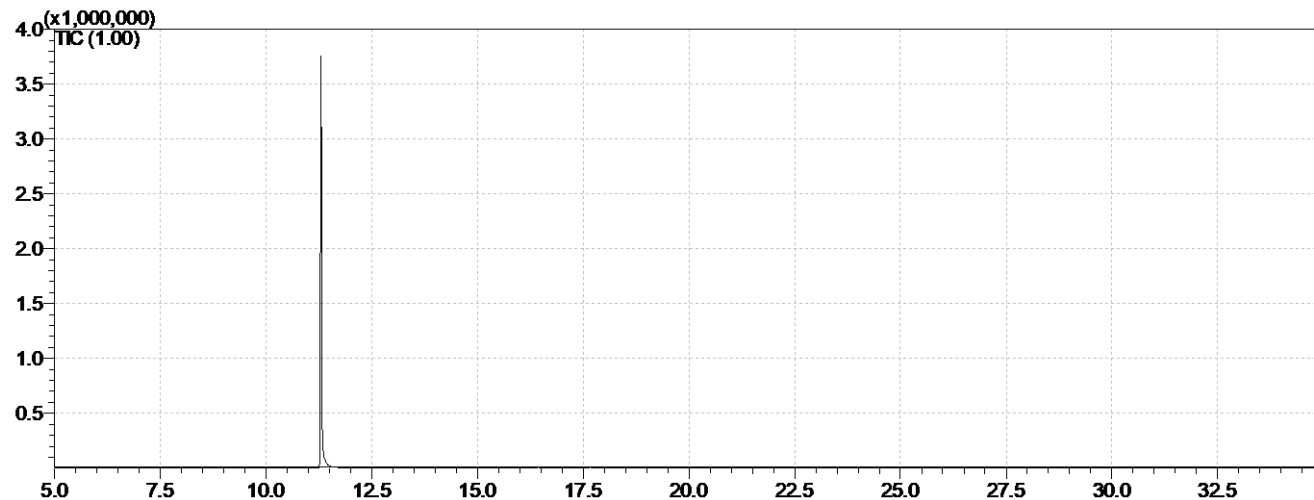


Purity: 96.9 %

Line#:1 R.Time:4.550(Scan#:187)  
MassPeaks:35  
RawMode:Averaged 4.517-4.608(183-194) BasePeak:53.00(8574)  
BG Mode:None Group 1 - Event 1 Scan

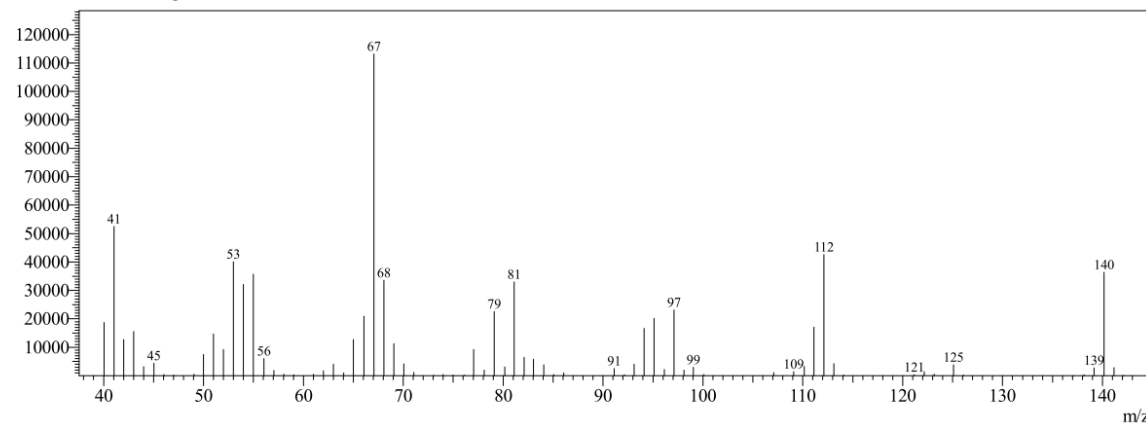


### S5.3. GC-MS data of 11E.

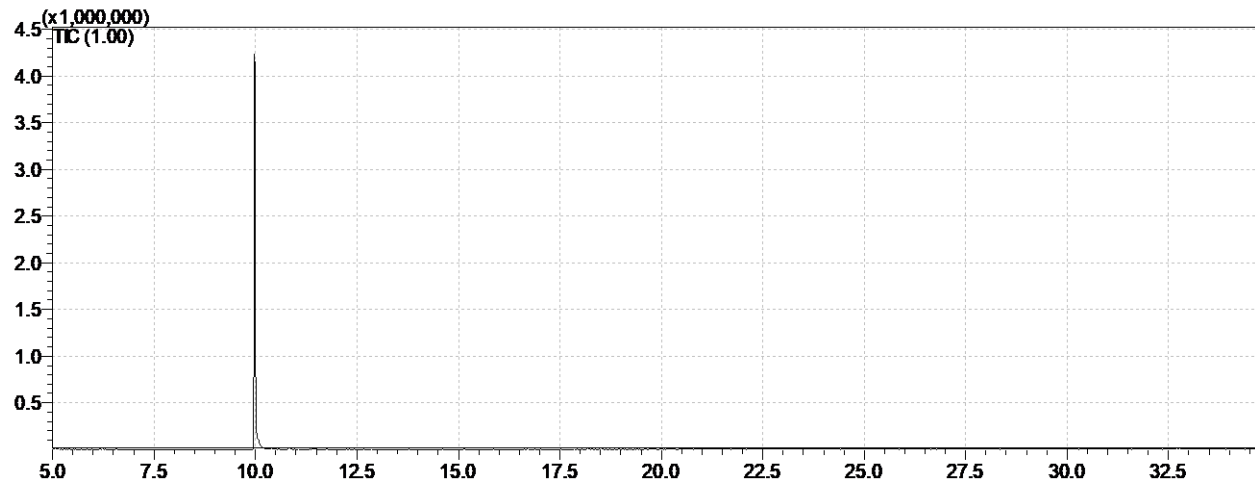


Purity: 99.6 %

Line#:1 R.Time:11.292(Scan#:756)  
MassPeaks:72  
RawMode:Averaged 11.258-11.433(752-773) BasePeak:67.05(113191)  
BG Mode:None Group 1 - Event 1 Scan

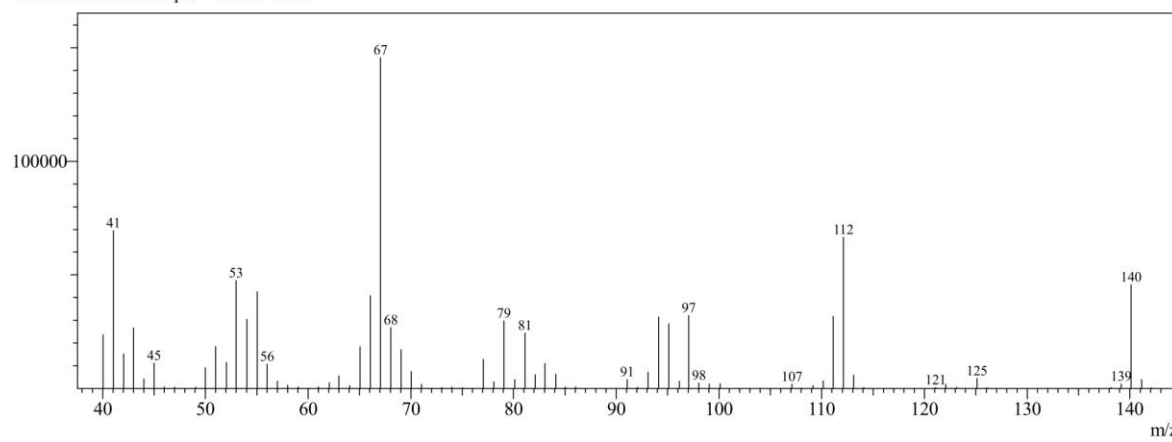


#### S5.4. GC-MS data of 11Z.

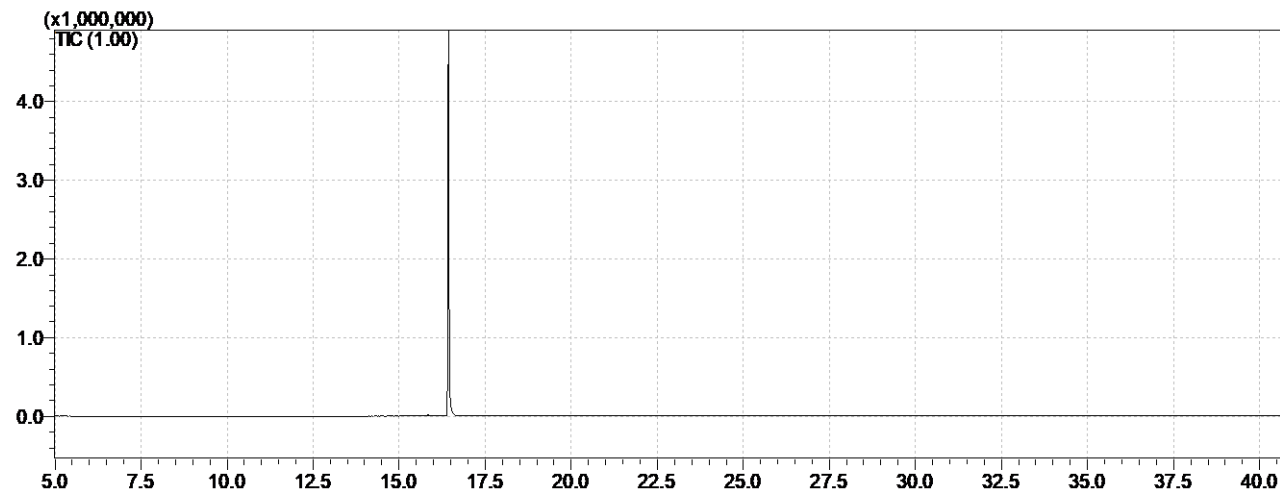


Purity: 98.9 %

Line#:1 R.Time:9.975(Scan#:598)  
MassPeaks:74  
RawMode:Averaged 9.942-10.083(594-611) BasePeak:67.05(145690)  
BG Mode:None Group 1 - Event 1 Scan

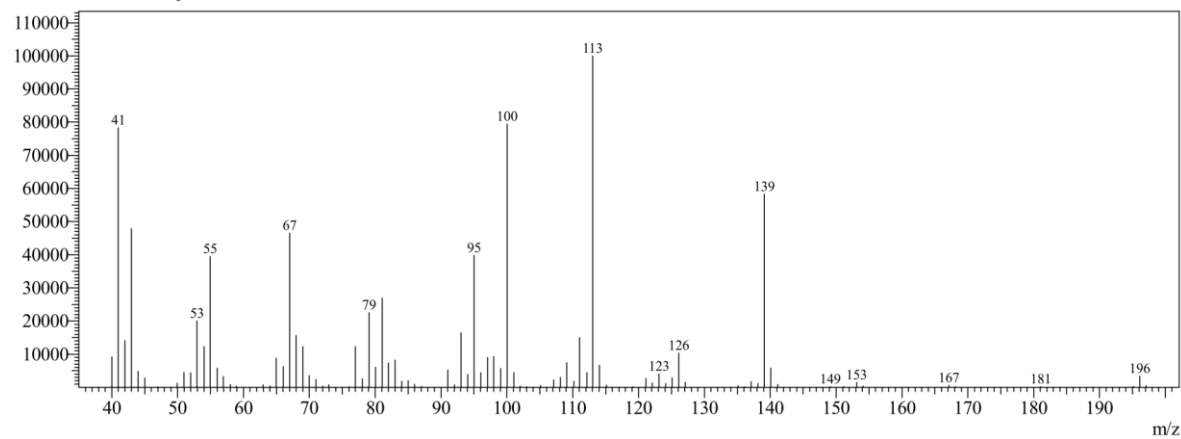


### S5.5. GC-MS data of 12E.

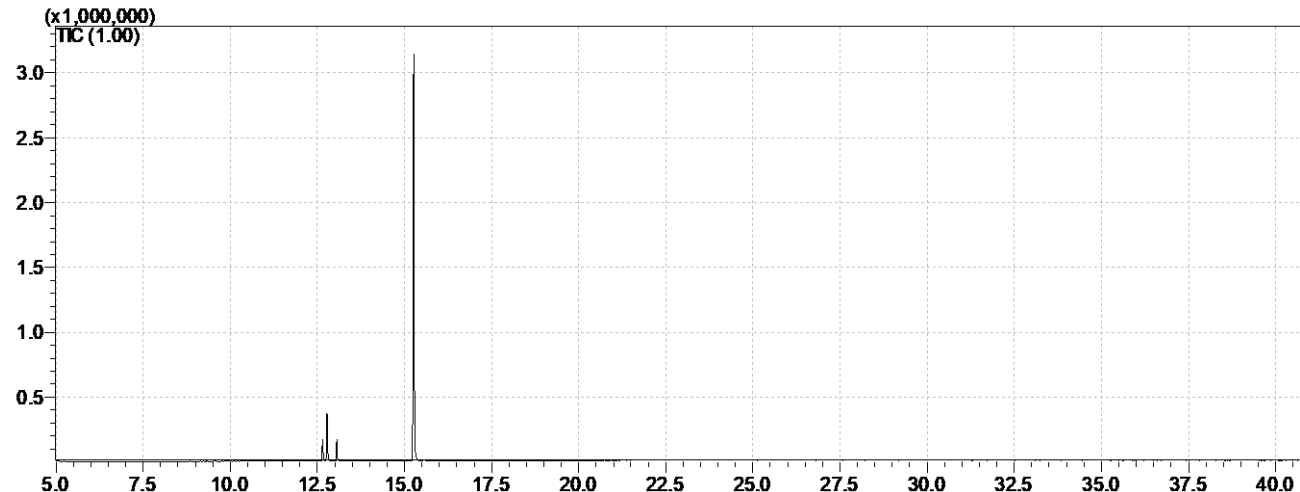


Purity: 98.8 %

Line#:1 R.Time:16.433(Scan#:1373)  
MassPeaks:91  
RawMode:Averaged 16.383-16.583(1367-1391) BasePeak:113.05(100004)  
BG Mode:None Group 1 - Event 1 Scan

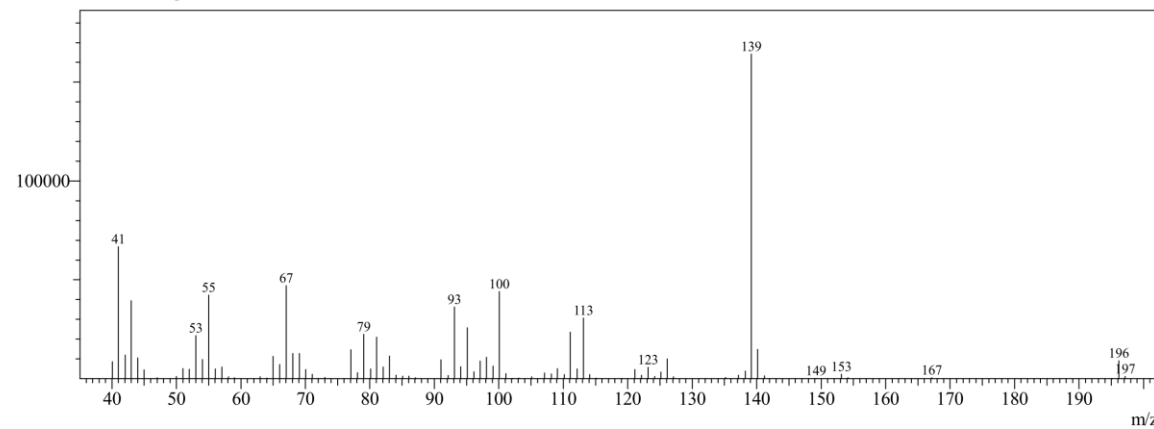


### S5.6. GC-MS data of 12Z.

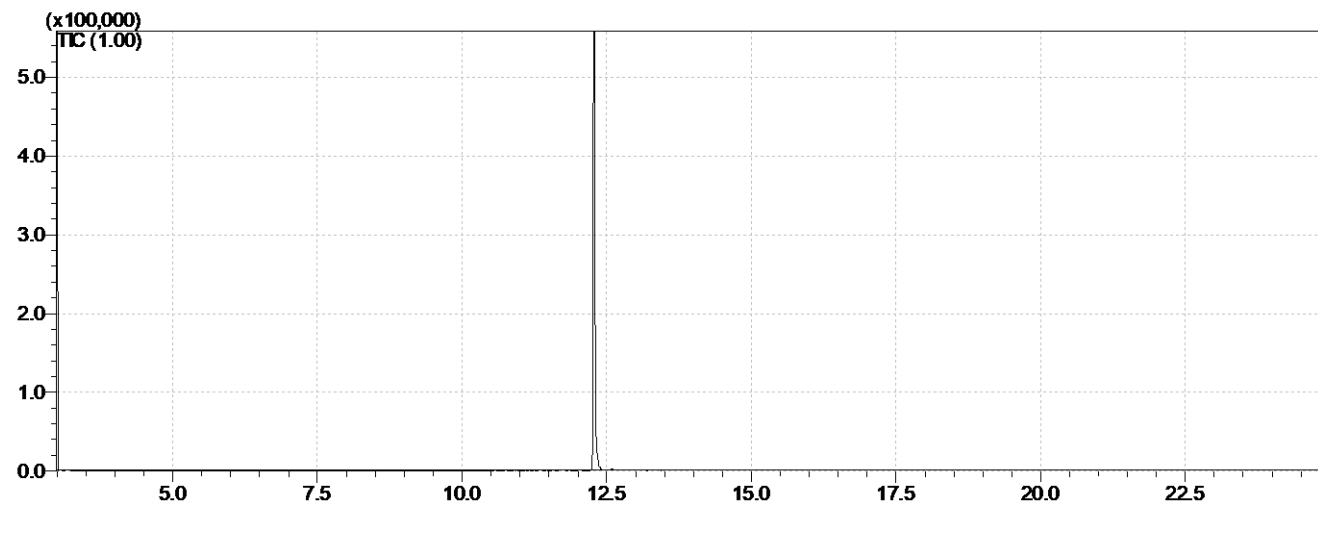


Purity: 82.3 %

Line#:1 R.Time:15.267(Scan#:1233)  
MassPeaks:84  
RawMode:Averaged 15.225-15.333(1228-1241) BasePeak:139.15(164241)  
BG Mode:None Group 1 - Event 1 Scan

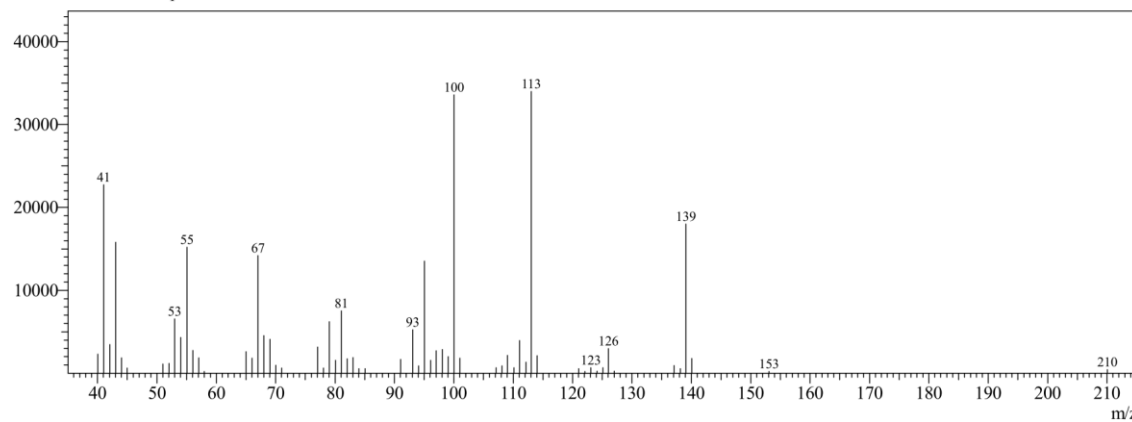


**S5.7. GC-MS data of 13E.**

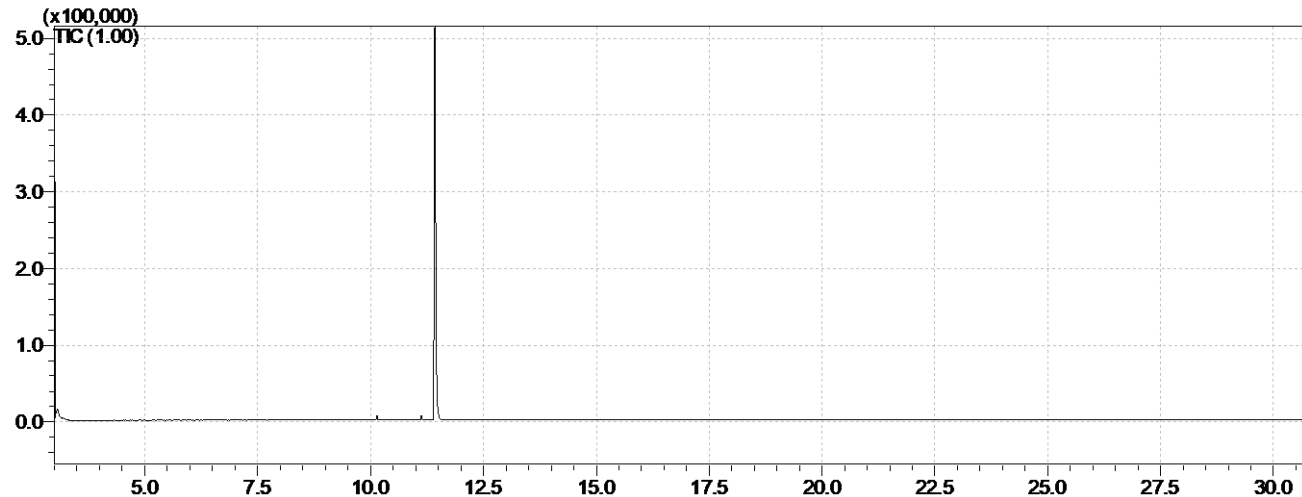


Purity: 99.7 %

Line#:1 R.Time:12.283(Scan#:1115)  
MassPeaks:61  
RawMode:Averaged 12.250-12.333(1111-1121) BasePeak:113.05(33980)  
BG Mode:None Group 1 - Event 1 Scan

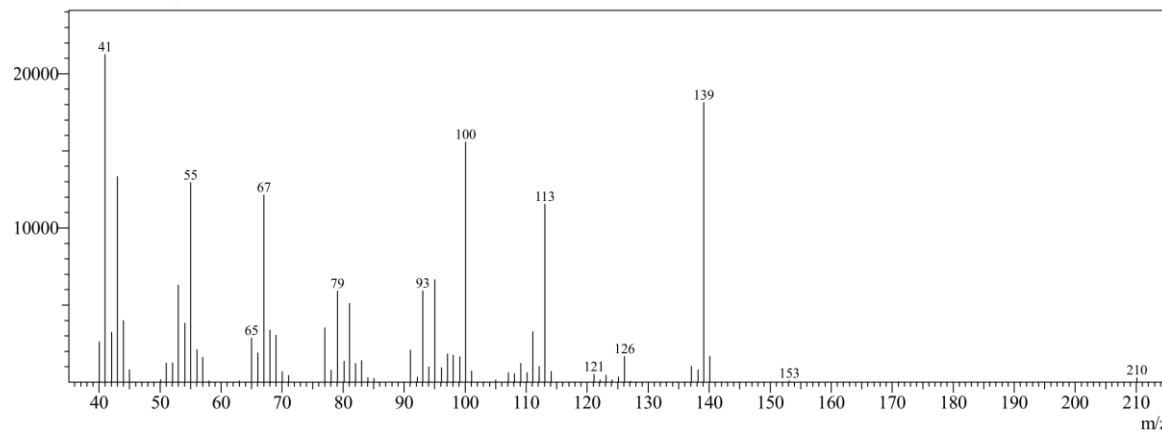


### S5.8. GC-MS data of 13Z.

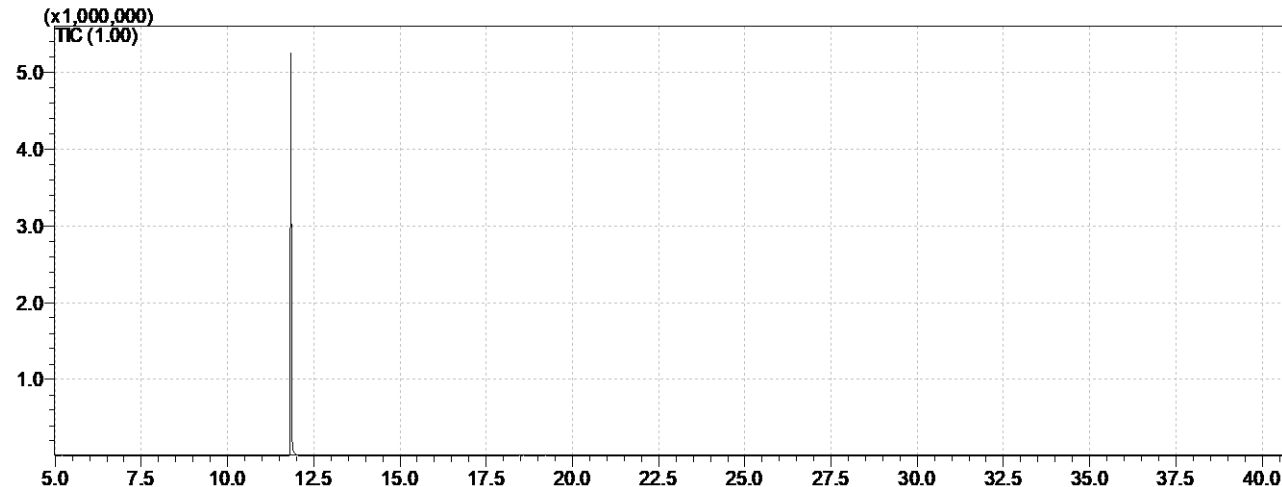


Purity: 98.8 %

Line#:1 R.Time:11.425(Scan#:1012)  
MassPeaks:65  
RawMode:Averaged 11.392-11.508(1008-1022) BasePeak:41.00(21255)  
BG Mode:None Group 1 - Event 1 Scan

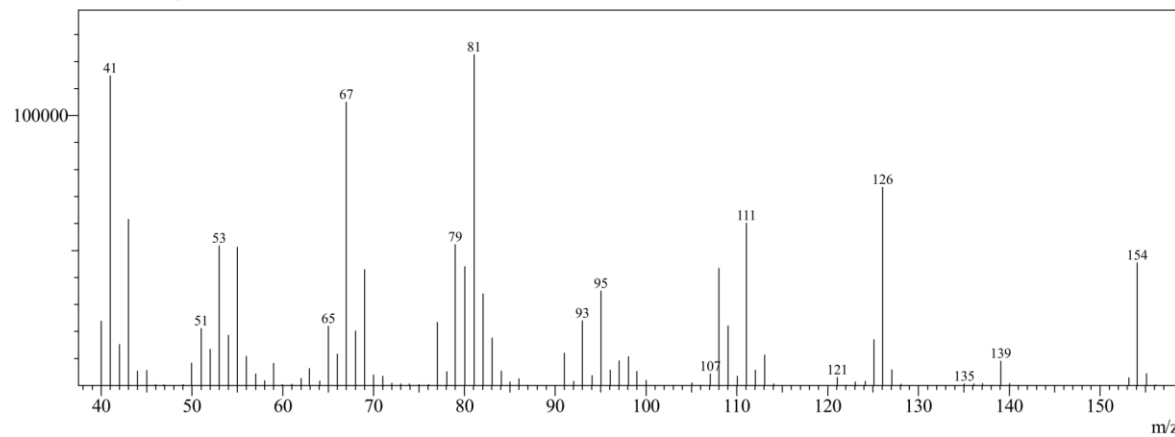


**S5.9. GC-MS data of 14E.**

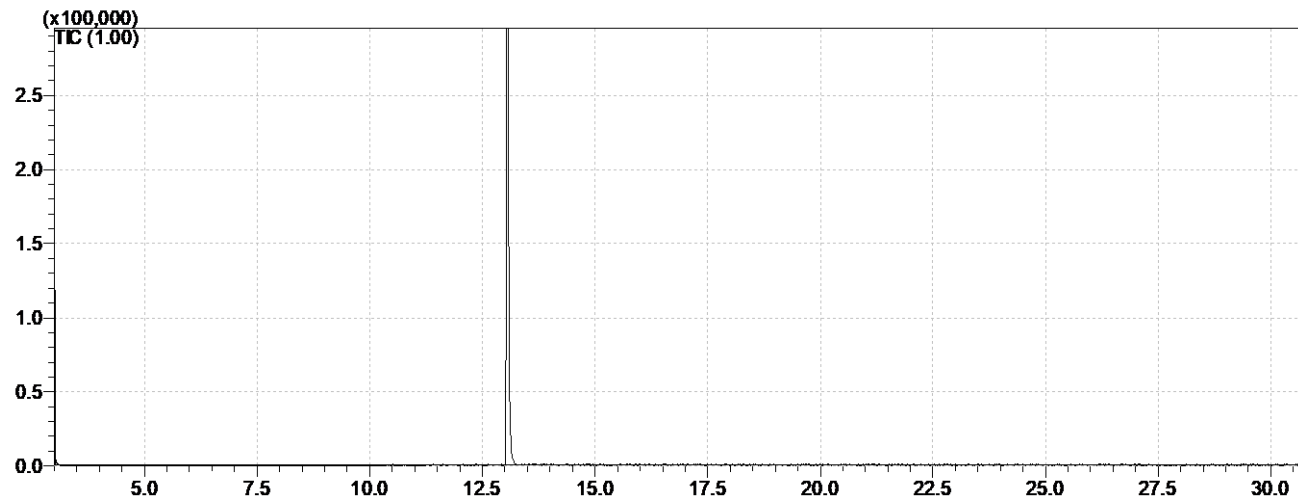


**Purity: 99.8 %**

Line#:1 R.Time:11.833(Scan#:821)  
MassPeaks:86  
RawMode:Averaged 11.792-11.908(816-830) BasePeak:81.05(122579)  
BG Mode:None Group 1 - Event 1 Scan

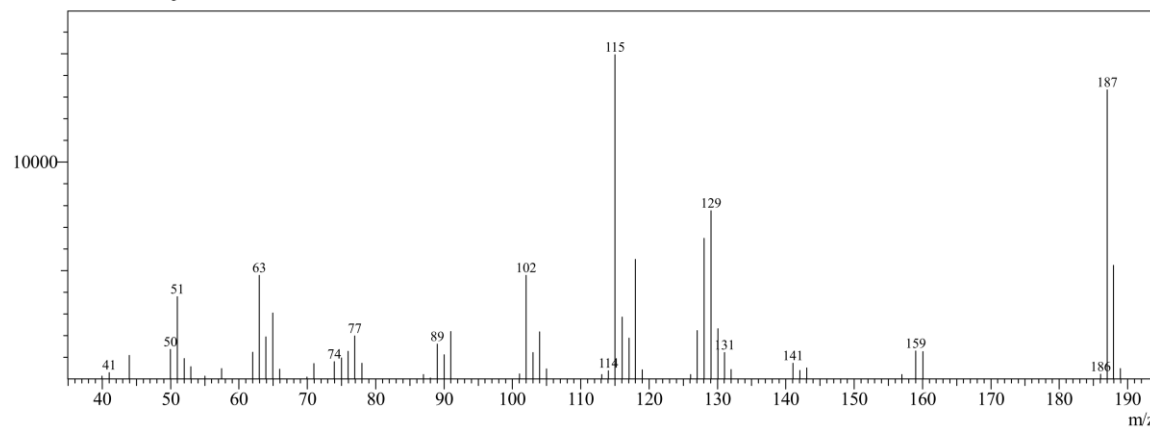


**S5.10. GC-MS data of 15E.**

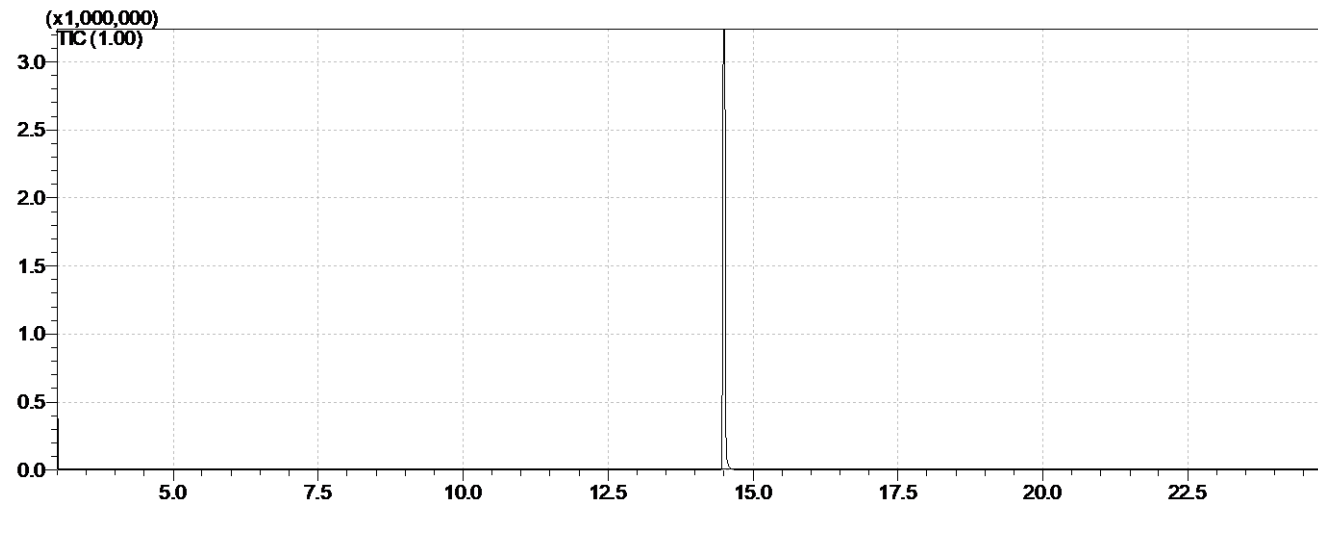


Purity: 99.9 %

Line#:1 R.Time:13.058(Scan#:1208)  
MassPeaks:55  
RawMode:Averaged 13.000-13.200(1201-1225) BasePeak:115.00(14962)  
BG Mode:None Group 1 - Event 1 Scan

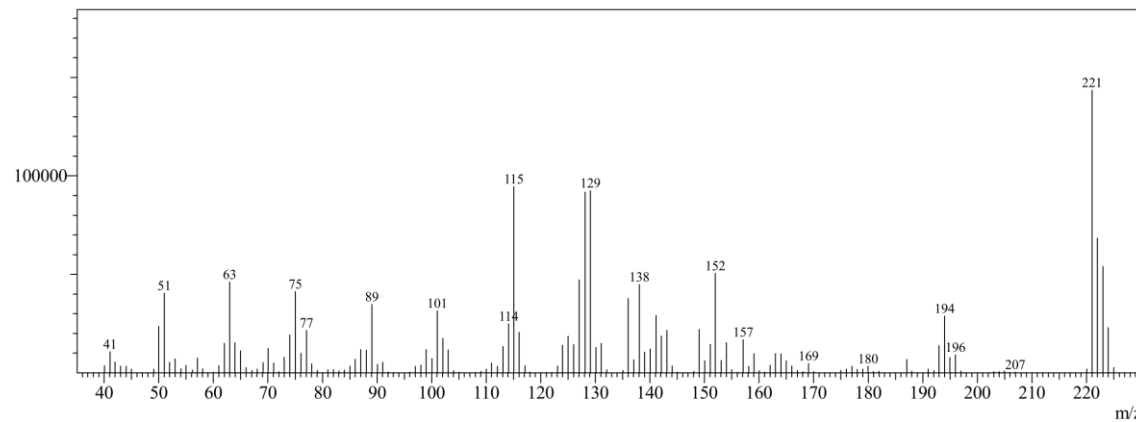


**S5.11. GC-MS data of 16E.**

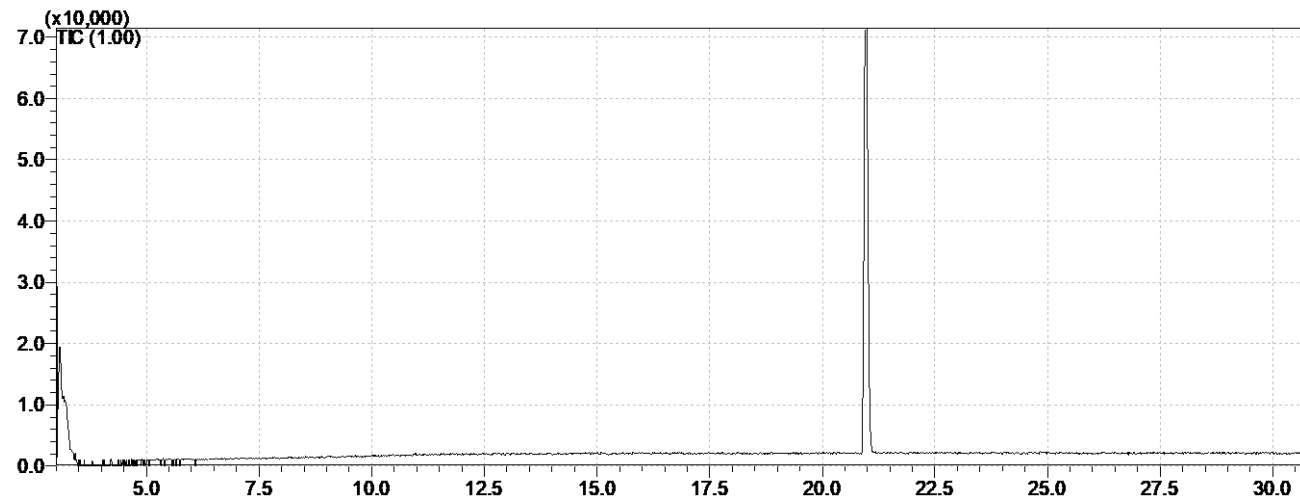


Purity: 99.9 %

Line#:1 R.Time:14.500(Scan#:1381)  
MassPeaks:146  
RawMode:Averaged 14.450-14.567(1375-1389) BasePeak:221.00(143438)  
BG Mode:None Group 1 - Event 1 Scan

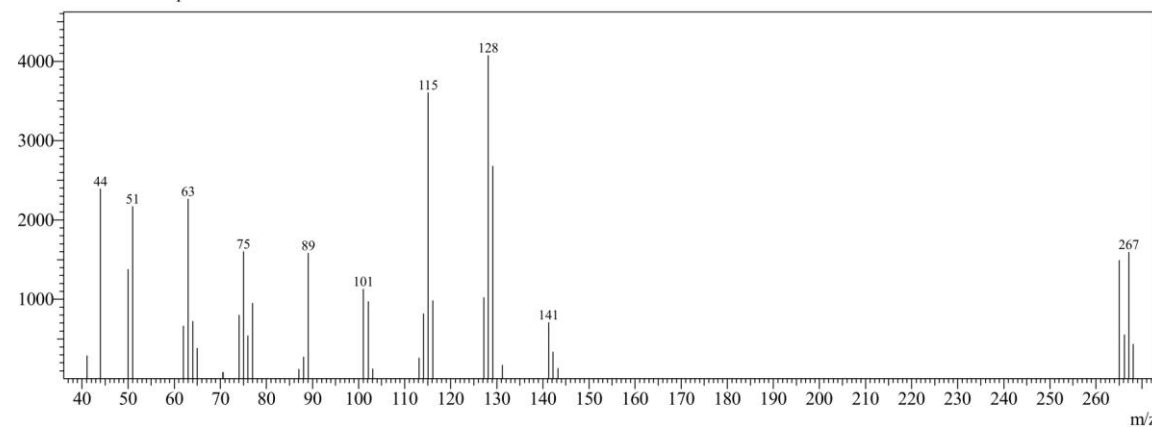


**S5.12. GC-MS data of 17E.**

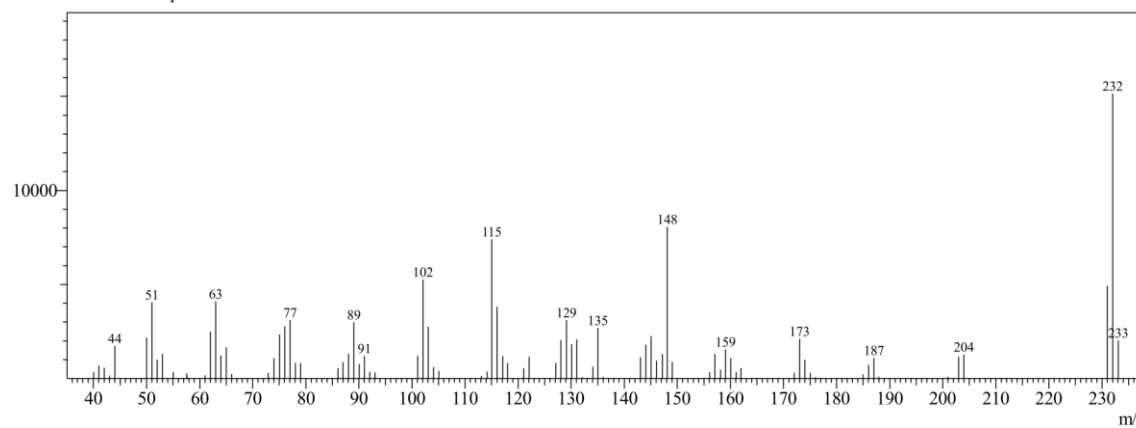
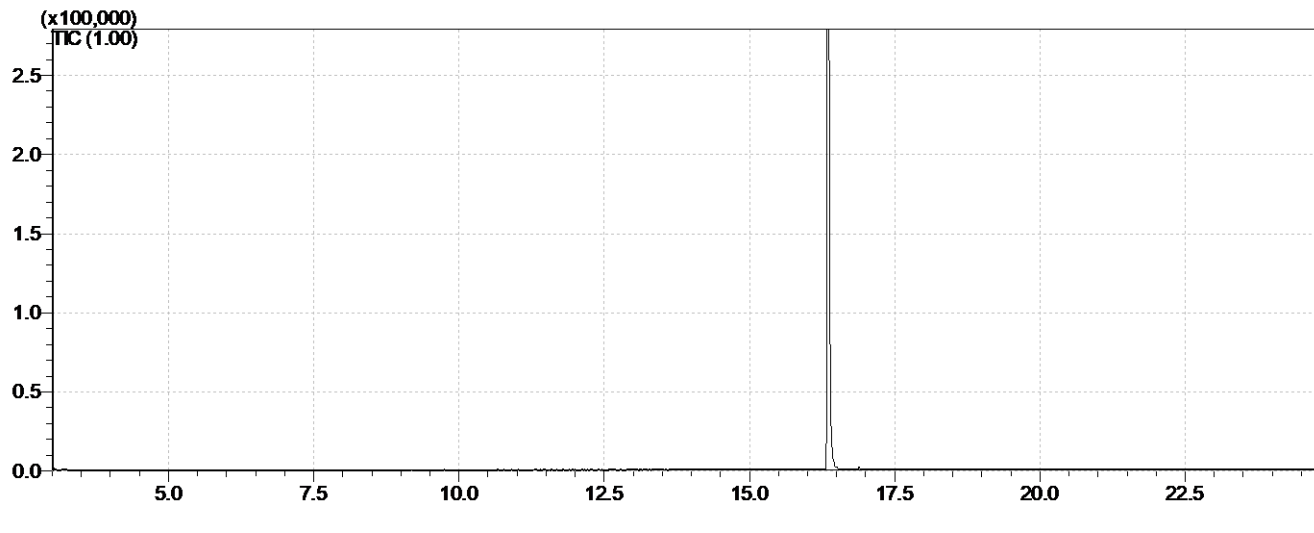


Purity: 99.9 %

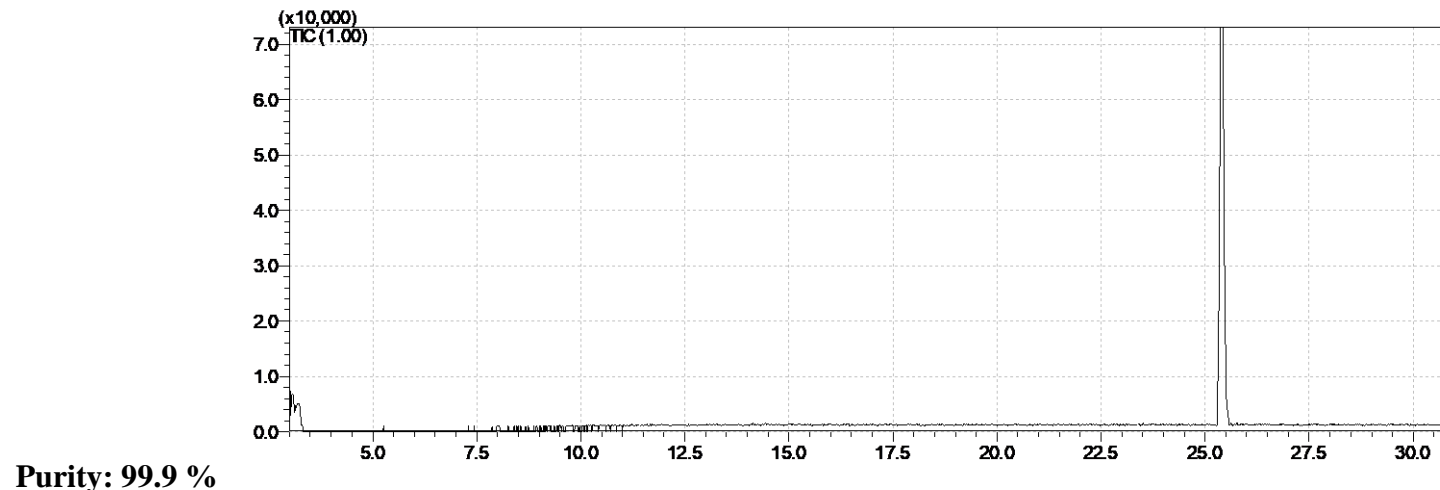
Line#:1 R.Time:20.967(Scan#:2157)  
MassPeaks:35  
RawMode:Averaged 20.875-21.083(2146-2171) BasePeak:128.15(4074)  
BG Mode:None Group 1 - Event 1 Scan



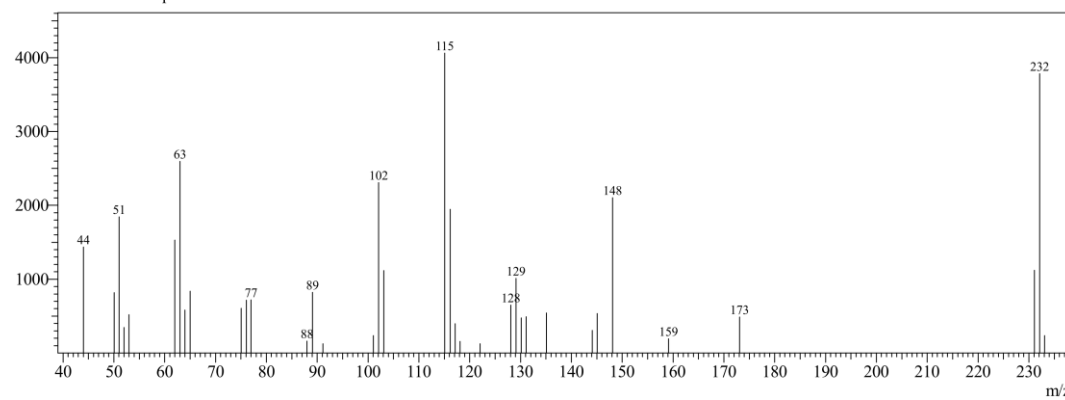
**S5.13. GC-MS data of 18E.**



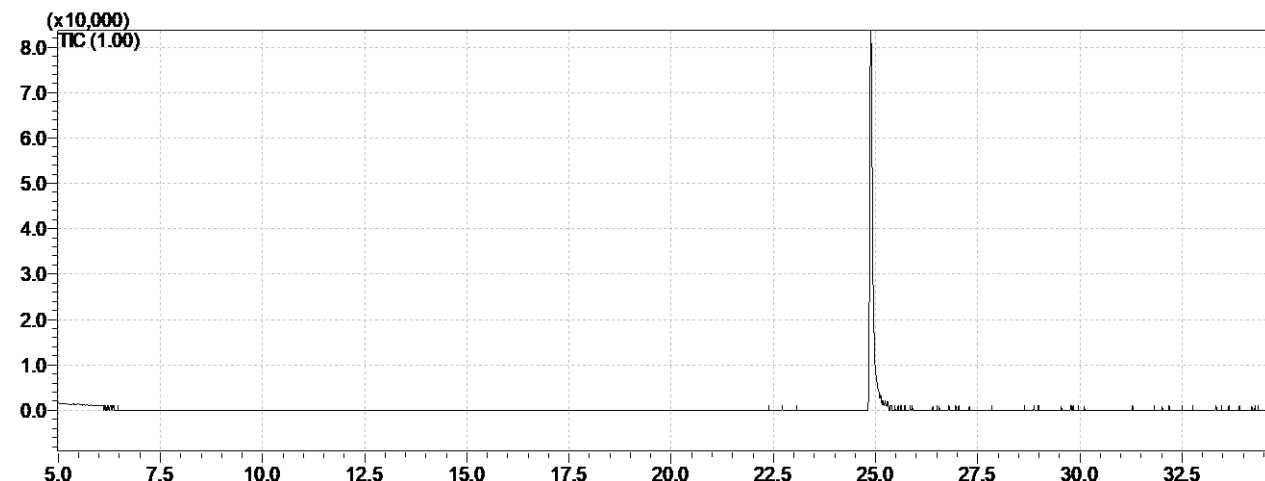
**S5.14. GC-MS data of 19E.**



Line#:1 R.Time:25.400(Scan#:2689)  
MassPeaks:36  
RawMode:Averaged 25.283-25.558(2675-2708) BasePeak:115.10(4064)  
BG Mode:None Group 1 - Event 1 Scan



**S5.14. GC-MS data of 20.**



Putiry: > 99.9 %

Line#:1 R.Time:24.883(Scan#:2387)  
MassPeaks:25  
RawMode:Averaged 24.692-25.417(2364-2451) BasePeak:170.10(2830)  
BG Mode:None Group 1 - Event 1 Scan

